Structure and spectroscopy of candidates for an electron electric dipole moment experiment

by

Edmund R. Meyer

B.Sc., University of Washington, 2004 (Physics)

B.Sc., University of Washington, 2004 (Astronomy)

A thesis submitted to the

Faculty of the Graduate School of the

University of Colorado in partial fulfillment

of the requirements for the degree of

Doctor of Philosophy

Department of Physics

2010

This thesis entitled:
Structure and spectroscopy of candidates for an electron electric dipole moment experiment
written by Edmund R. Meyer
has been approved for the Department of Physics

John L. Bohn

Chris H. Greene

Date

The final copy of this thesis has been examined by the signatories, and we find that both the content and the form meet acceptable presentation standards of scholarly work in the above mentioned discipline.

Meyer, Edmund R. (Ph.D., Physics)

Structure and spectroscopy of candidates for an electron electric dipole moment experiment

Thesis directed by Prof. John L. Bohn

The identification of suitable diatomic molecules as candidates for an electron electric dipole moment (eEDM) experiment is presented. A model is derived and developed in order to efficiently and accurately identify possible diatomic molecules. This model gives the magnitude of the effective electric field experienced by an electron at the site of one of the nuclei in the molecule. In particular, this thesis identifies several $^3\Delta$ molecules as viable candidates for the eEDM search. In addition, the relevant tools for doing precision spectroscopy on these molecules are developed. For molecular ions in rotating trapping fields, a description of geometric phases is presented that reduces to the common result in the adiabatic limit, but allows for a description of the effect of atomic and molecular structure on these phases.

Dedication

For my family

Acknowledgements

First, I should acknowldege all those people who kept me motivated to stay in graduate school by going out and doing things outside of physics. I then want to thank my parents Bob and Diana as well as my siblings Joe, Dave, and Michelle for always being supportive.

The many members of the Bohn group with whom I have had many useful discussions on science and non-science alike are C. Ticknor, D.C.E. Bortolloti, M. Lara, R.M. Wilson, S. Ronen, and G. Quéméner.

I have had the pleasure of discussing at length with many experimentalists and theorists in my time at JILA, all of whom have enhanced my knowledge of physics. They are B. Peden, S. Rittenhouse, R. Pepino, Z. Walters, R. Stutz, L. Sinclair, B. Stuhl, B.C. Sawyer, J. Schlaerth, D. Meiser, B.L. Lev, A.E. Leanhardt, H. Lewandowski, J. Ye, and E.A. Cornell.

Lastly, I owe a big heap of gratitude to my advisor, J.L. Bohn, for his boundless enthusiasm for science which is more than a little catching.

Contents

Chapter

Tables

Table

Figures

Figure

Chapter 1

In the Beginning...

The universe is asymmetric and I am persuaded that life, as it is known to us, is a direct result of the asymmetry of the universe or of its indirect consequences.

–Louis Pasteur

The remarks of Pasteur seem rather full of foresight. However, it must be taken into account that these remarks were made long before the discovery of quantum mechanics and the Standard Model (SM) of particle physics. While the asymmetry alluded to by Pasteur is a requisite step in the formation of life — the clumping of matter into ever larger aggregations — the asymmetry is a result of the fact that there is even matter with which to start the aggregating. The inhomogeneous distribution of matter is a direct result of the asymmetry between matter and anti-matter, and therefore life an indirect consequence of this asymmetry. What do you know, Pasteur was right, in a way.

1.1 Origin of an electron electric dipole moment

A long, long time ago, before galaxies were even a twinkle in the universe's eye, a raging battle was taking place. Particles and anti-particles were created and destroyed with reckless abandon in a variety of interactions. Their creation and annihilation was in balance as neither matter nor anti-matter could win favor. Then, at a certain energy

scale, a symmetry broke, and the preservation of balance between particle and its anti-particle nemesis was forever shattered. Inside this broken symmetry lies a peculiar oddity, matter particles such as the electron are more likely to be produced. Matter now takes the upper hand in the interactions amongst the various particles in nature, and this is what matters for us; for we are here and not the anti-us.

It appears that the matter-anti-matter asymmetry is connected to charge-conjugation (C). From experimental measurements on the decay of the Kaon (see Ref [1]) only the combination charge-conjugation plus parity (CP) violation has been measured. In addition, CP-violation has been measured in the B-meson system [2]. A CP operation reverses all the additive quantum numbers as well as the direction, i.e. an electron moving to the right ($+x$-direction) would become a positron moving to the left (but still in the $+x$-direction in this parity swapped universe). Now, a violation of CP causes one to expect a violation of time-reversal (T). This is because of the expectation that the product of CPT should always be invariant. This is akin to saying there is no preferred direction in space, that no matter the mass of the particle at hand its anti-partner has the same mass, and that all internal quantum numbers are opposite for each. Schwinger showed (implicitly) that this invariance is implied by having invariance under Lorentz transformations [3], transformations at the heart of relativity.

Using the requisite knowledge of the amount of CP violation in the Kaon and B-meson sectors, one can ask whether it is enough to explain the matter to anti-matter asymmetry in the observed universe. If one looked out into the universe and measured the amount of matter and compared this to the prediction that ensues from the Kaon and B-meson CP violation, she would find that there is still more matter than can be explained [1]. Thus, one is prompted to search for different forms of CP or T violation. A natural place to look begins by asking whether fundamental particles have a permanent electric dipole moment (EDM), or a linear shift in energy with applied electric fields of arbitrarily small magnitude. Ramsey began searching for the neutron EDM (see

Ref. [4] for a review on neutron EDMs) and soon the race was on to measure it in electrons, atoms, muons, neutrinos, and various other composite particles like the Λ^0 and molecules.

Why do EDMs violate T-reversal, and thus CP? The answer lies in the interaction. Imagine an electron with two spin-axes, one electric and one magnetic. If these axes were independent, there would be an introduction of a new quantum number, the projection of electric spin onto the electric spin-axis. However, given the stability of the periodic table, i.e. there is no element with 4 electrons in the $1s^2$ state, and the Pauli exclusion principle, it seems fairly safe to proclaim that there is only one spin-axis: the magnetic spin axis. Therefore, if there is a EDM, it must lie along (or against) this axis. Thus, an interaction of the form

$$H_{\rm EDM} = -d_e \sigma \cdot \mathcal{E}, \tag{1.1}$$

would violate T and P symmetries. This is easy to see given that under P, $\mathcal{E}$ reverses sign while under T, σ reverses sign. Thus, $P\ H_{\rm EDM} = T\ H_{\rm EDM} = -H_{\rm EDM}$. Therefore, a measurement of a permanent EDM is evidence for CP violation above and beyond what is already measured; because CPT is assumed invariant.

Because the electron is of so much interest in this thesis, it is where the search will begin. Now, the Standard Model (SM) prediction for electron EDM (eEDM) is extremely small; expected to be about [5, 6]

$$|d_e| \lesssim 10^{-40}\ {\rm e-cm}, \tag{1.2}$$

a number beyond ridiculously small. Ridiculously small is here defined as being 10^{10} times smaller than an avid experimenter can measure. An example of a diagram which contributes to this effect is in Fig. 1.1. The entailed calculation is one that is beyond my paygrade. Note that wherever the W boson couples to the electron (solid, thick black line) or quark loop (red triangle) there is a phase associated with the coupling. This is the phase that leads to parity violation. In order to yield an eEDM, the phase

needs to not vanish at some order in the diagram. It takes four loops in order for the parity violating phase associated with the weak force to not cancel out. Even though parity violation exists, near cancellations occur in the calculation which yield a very small value for the eEDM. In fact, if the u_i and d_j (up and down quarks) were of the same mass, then the eEDM would cancel even to this order [6].

To get a feel for the type of energy shifts this eEDM would produce, it is useful to see that an atomic unit of electric field ($\sim 10^9$ V/cm) would produce an energy shift of 10^{-31} eV. There is no hope to measure something like this in today's modern lab. Fields reachable in the lab (about 4 orders of magnitude less than one atomic unit) would produce a shift a four orders of magnitude smaller. Thus, why bother to search for the eEDM?

The fact is that there are many theories which go beyond the SM. Surprisingly (or not so) many of these theories involve interactions with heretofore unseen, massive particles which do not necessarily obey the rules of CP conservation. These as yet unobserved particles can give rise to ever larger values of the eEDM because these particles may not have the fortuitous cancellation of a parity violating phase that occurs in the W-boson, quark-loop diagram in Fig. 1.1.

The current experimental limit on the eEDM ($d_e \leq 1.6 \times 10^{-27}$ e cm) is given by the experiment on the thallium atom [7]. This is a bit shy of the SM prediction. There exists a large gap, and it is this gap that theories of physics beyond the SM aim to fill; let them be called the Theories of the Gap[1] . 12 or so orders of magnitude is a lot with which to work in a new theory. However, there seems to be a whole smorgasbord of various theories which seem to predict eEDMs in a similar range, a range at or just below today's experimental limits. These new theories are constructed such that the new particles have masses that are larger than any particle mass yet measured, for otherwise the community would likely have already observed them. Let one of these

[1] Term coined by J. Schlaerth during beer and billiards

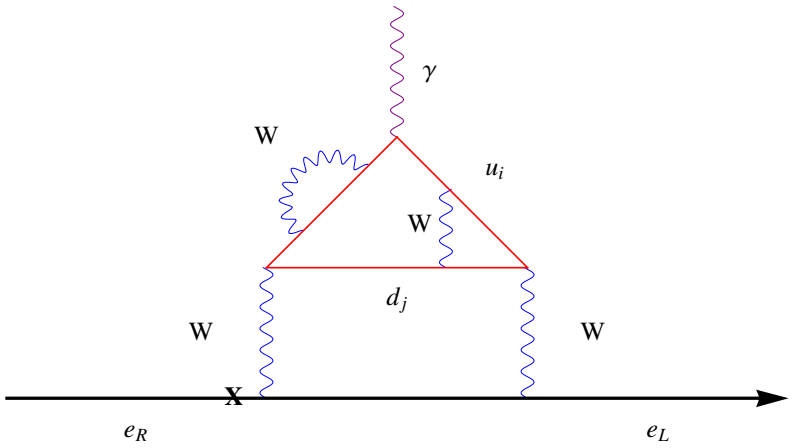

Figure 1.1: One of many contributions to the eEDM in the SM. The cross denotes a mass insertion, a technical way to treat the mass of the particle perturbatively. A right-handed electron, through the many subsequent interactions becomes left-handed. d (u) denote an up (down) quark while W denotes a weak boson. γ is a photon. Figure adapted from Ref. [6].

new particles be called Y (because, why not) and have a mass m_Y.

Instead of trying to write out expressions for the various theories beyond the SM, it is more instructive to just gain a feel for the size of the eEDM that these theories will predict. Given the plethora of adjustments to the SM, it seems rather surprising that many of these theories give rise to an eEDM that is in the range of 10^{-28}–10^{-30} e cm. To understand why, in a qualitative sense, it will be beneficial to recall the electron $g-2$ diagram. This is the electron vertex function. Evaluation can be found in Ref. [8]. This is presented in the bottom panel of Fig. 1.2.

The electron $g-2$ diagram is well understood, and it can be used to qualitatively understand the emission and absorption of a large mass, parity violating particle from the electron. Fig. 1.2 gives an example of a one loop correction (top panel, (a)) that would lead to an eEDM. The phase ϕ is a CP violating phase associated with the coupling of an electron to this new particle, the coupling strength of which is f. In the SM, where the exchange of a W-boson does contribute to the electron one-loop diagram, it does not lead to an eEDM at this order due to the cancellation of the phase. Thus, an interaction of the sort presented in Fig. 1.2 is assumed to couple with a different phase to left and right-handed electrons denoted e_L and e_R.

Bickman and DeMille have presented a simple relationship for the size of an eEDM that particle Y can induce in the electron as compared to the Bohr magneton μ_B and $g-2$ from such a loop [9, 10]. The heavy particle introduces a propagator $\sim 1/m_Y^2$. Because m_e is the only other mass scale in the problem one argues on dimensional grounds the diagrams in (a) and (b) of Fig. 1.2 lead to a dimensionless ratio

$$\frac{d_e}{(g-2)\mu_B} \propto \left(\frac{m_e}{m_Y}\right)^2, \tag{1.3}$$

where m_e is the electron mass. In Gaussian based atomic units it is thus that (noting $\mu_B = \alpha/2$)

$$d_e \approx \sin(\phi)\left(\frac{f}{c}\right)^2\left(\frac{m_e}{m_Y}\right)^2\left(\frac{\alpha^2}{2\pi}\right), \tag{1.4}$$

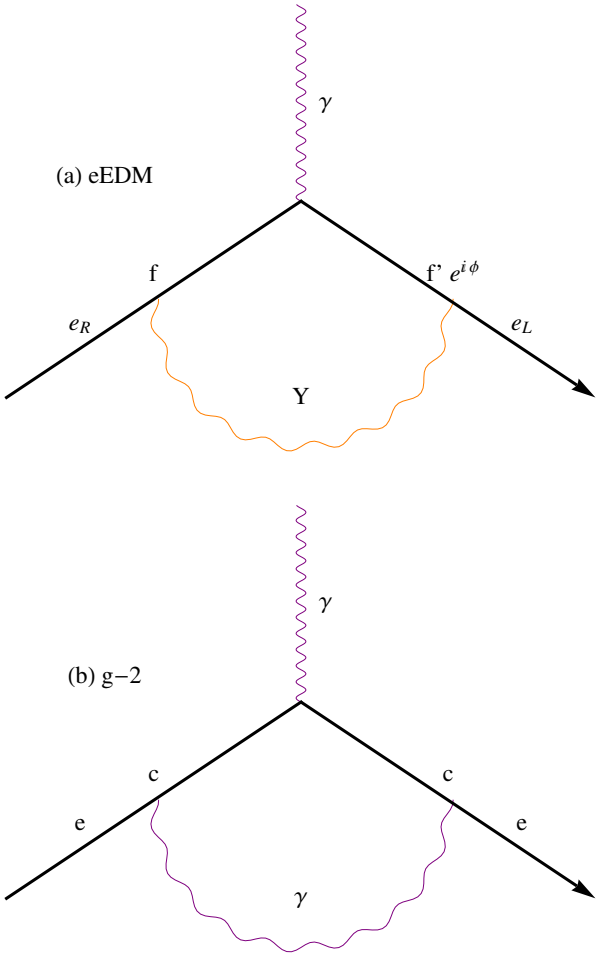

Figure 1.2: In theories beyond the SM, an eEDM may be generated by a yet unobserved particle Y. This unobserved particle couples to the different handedness states of the electron with a phase that is not quite equal, and thus does not completely cancel. This phase is labeled ϕ. The top panel (a) is the eEDM inducing interaction with the yet unseen particle Y. The bottom panel (b) is the electron $g-2$ diagram. This diagram is well known and understood by the physics community. By drawing analogies, it is possible to express the top panel in terms of known quantities in the bottom panel.

where $(g-2) = \alpha/\pi$ has been used. The reason that many theories predict an eEDM that is just around the 10^{-28}–10^{-30} e cm mark is because from this point forward certain assumptions will lead to similar estimates. It is often assumed that coupling constants to the electron will have a similar order of magnitude and thus $f/c \sim 1$. The CKM quark mixing matrix in the SM gives a value of $\sin(\phi) \approx 1$ [11] and one may expect a similar result to hold in theories beyond the SM. Granted, these are merely assumptions about the theories, and some do introduce new phases and coupling strengths which can vary due to suppression of CP-violating phases and coupling strengths; this is just to get a feel of the order of magnitude that the eEDM can take. Using these assumptions and that the mass of the new particle Y is expected to be in the range of m_Y ~100 GeV/c^2–1 TeV/c^2, many theories beyond the SM predict eEDMs around 10^{-27}–10^{-30} e cm, where m_Y, the coupling strength ratio f/c, and $sin(\phi)$ may each vary by an order of magnitude to yield this range. Higher order loops can also contribute, but each loop is generally reduced in magnitude by a factor α/π and therefore is 10^{-3} times smaller than a one-loop correction.

Thus, there is reason for experimentalists to pursue measurements of the eEDM; if not just to rule out theories beyond the SM. High energy experiments naturally aim to reach scales comparable to the mass scale of the supposed new particles while table-top AMO experiments aim to use precision measurements to finagle the eEDM to reveal itself through tiny shifts in energy. It is the latter which is of concern here.

Sandars showed long ago that an atom can have an electric dipole moment many times larger than in the electron itself; an enhancement factor makes the applied field effectively larger [12, 13]. An electron bearing an EDM will give to the atom an EDM many times larger. Only the unpaired electron will contribute. The reason is that an electron that is paired up with another, as in the ground state of the He atom, will have its spin lie against that of its paired partner thereby negating any effect of a eEDM. This relies on arguments presented earlier above Eq. (1.1). This enhancement

is the advantage of which the Tl experiment took. In Tl, the enhancement is around $|\frac{\mathcal{E}_{\rm eff}}{\mathcal{E}_{\rm app}}| \approx 585$, a rather large number [5].

Of course, new bounds must always be set and current work on YbF molecules by the group of Ed Hinds looks to set the new standard [14]. The reason to switch from atoms to molecules becomes evident when one considers the size of the field required to go beyond the measurement in Tl. In that experiment the applied field was about 10^5 V/cm making the effective field roughly 60 MV/cm. In order to go beyond this, one either needs to increase the applied field, find another atom with a larger enhancement factor, or move onto molecules. Since the enhancement scales very favorably with the atomic number Z (see Chap. 2 of this thesis and Ref. [5]), Tl is a front runner for atomic searches. Not many elements are heavier; at least none that are not on restricted lists and possibly cause bad things to an experimenter's graduate student(s). Applying larger fields introduces difficulties with which, being a theorist, I am less familiar. Though, I can imagine that getting into the many 10s–100s of kV/cm with precision control is a daunting task.

Therefore one moves to molecules. Molecules can have quite large internal fields. In fact, given the charge transfers and typical molecular sizes, electric fields within molecules can be on the order of an atomic unit, or 5 GV/cm. This is a high electric field laboratory. It is this lab that the Hinds group is using to find the eEDM. In order to take advantage of such a system one must understand the system. How can one calculate the size of the effective electric field? Will it really be on the order of an atomic unit of field? Does bringing in more than one atom complicate the problem? These questions and so many more are extremely important to answer.

In this thesis I will address the use of molecules as high electric field laboratories for searching for the eEDM. The motivation to pursue the study of these candidates is driven by the experimental work in JILA in the group of Eric Cornell [15]. Certain experimental constraints limit the type of molecules that would be useful. Some of these

constraints include the ability to easily polarize the molecule. This immediately rules out homonuclear diatomics. In addition, one wants either small rotation constants or small Λ-doublets (see Chap. 3 and Ref. [16]). This further limits the search to molecules that have large reduced masses or are of a certain class of Hund's case. Thus, the 10^4 possible combination of diatomics to search through has been greatly reduced to about 10^2. Further reduction must come from ingenuity, or an understanding gained from a few years in graduate school studying molecular systems. It is these years that will be presented in the next few chapters.

Firstly, one must know whether molecules possess large effective electric fields. Chapter 2 will address the understanding of the estimation of this quantity. I will use a standard approach that has been modified to include requisite physics to calculate the effective fields. Some basics of relativistic quantum mechanics will be reviewed. Then a recap of Schiff's theorem [17] will lead into calculating the effective electric field. Comparisons will be made to more elaborate calculations.

Chapter 3 will deal with the structure and spectroscopy of diatomic eEDM candidates. A review of the computational methods used will be presented first. The remaining part of the chapter is broken up into two camps: $^2\Sigma$ and $^3\Delta$ molecules. Each section will deal with the structure and then the spectroscopy of each type of molecule. Because some of the proposed molecules are to be held in ion traps, Chapter 4 will deal with the additional phase that is introduced by a rotating field. A simple dressed state formalism will be developed that encapsulates all of the aspects of uniform rotation of a field interacting with a dipole moment, electric with electric and magnetic with magnetic. The results reduce to that of Berry [18] in the limit of adiabatic rotation. In addition, non-adiabatic corrections as well as the effects of structure will be addressed in simple examples. The complications that arise for an eEDM experiment in $^3\Delta_1$ molecules will be addressed last.

Chapter 5 will sum up what you are about to read. In addition, some minor

improvements that can be made as well as future work with molecules for addressing physics beyond the SM will be discussed.

Chapter 2

Let's Get Relative

Although this may seem a paradox, all exact science is dominated by the idea of approximation. When a man tells you that he knows the exact truth about anything, you can be safe in inferring that he is an inexact man.

–Bertrand Russell

Now, let me tell you exactly what I know. As learned in Chap. 1, there is every reason to expect the electron electric dipole moment (eEDM) to be extremely small; vanishingly so in the case of the Standard Model (SM). Therefore, it is a great approximation to use perturbation theory ideas to establish the size of the energy shift induced by an interaction of an eEDM with the internal electric field in the atom. This chapter will introduce Schiff's theorem which states that an electron in an atom will experience zero total electric field even when a laboratory electric is implied, understand its evasion, understand the size of the effective electric field that interacts with the electron, and which molecular candidates are best suited for searching out the eEDM in today's experiments. But first, a mini-review of the Dirac equation.

2.1 Dirac equation: A mini-review

The Dirac Hamiltonian for an electron in an electromagnetic field can be simply written

$$H_{\text{Dirac}} = \beta mc^2 - e\phi + c\vec{\alpha} \cdot (\vec{p} - e\vec{A}), \tag{2.1}$$

where m is the electron mass, $-e$ its charge, $\vec{p}$ its momentum vector and ϕ and $\vec{A}$ the scalar and vector potential. As usual, $\vec{\mathcal{E}} = -\vec{\nabla}\phi$ and $\vec{\mathcal{B}} = \vec{\nabla} \times \vec{A}$ The remaining terms are matrices

$$\begin{aligned} \beta &= \begin{pmatrix} \mathbf{1} & 0 \\ 0 & -\mathbf{1} \end{pmatrix}, \\ \vec{\alpha} &= \begin{pmatrix} 0 & \vec{\sigma} \\ \vec{\sigma} & 0 \end{pmatrix}, \\ \vec{\mathbf{\Sigma}} &= \begin{pmatrix} \vec{\sigma} & 0 \\ 0 & -\vec{\sigma} \end{pmatrix}. \end{aligned} \tag{2.2}$$

$\vec{\sigma}$ are the Pauli matrices and $\mathbf{1}$ is the identity matrix. Now, Foldy and Wouthuysen showed how to transform the odd terms (terms containing $\vec{\alpha}$), which connect positive and negative energy states, into even terms through a series of transformations [19]. For a complete description of all the terms arising in an atom and molecule using such techniques, the interested reader is referred to Chap. 3 of Ref. [16].

Hydrogen-like atoms satisfy the following Dirac equation (think of the outermost electron only)

$$H_0\psi = (c\vec{\alpha} \cdot \vec{p} + \beta mc^2 - \frac{Ze^2}{r})\psi = E\psi. \tag{2.3}$$

Here, there is only a scalar potential that depends on the magnitude of the separation of the electron from the nucleus. This equation can be solved using methods in Refs. [20, 21]. For purposes here, one is interested in the form of this solution close to the nucleus. In a many electron atom, "close to the nucleus" means close enough that the electron sees the unscreened charge [1] of the nucleus, or roughly given by $r \ll a_0/Z^{1/3}$, where a_0 is the Bohr length. The solution can be written in terms of a radial and angular piece

$$|njlm\rangle = \begin{pmatrix} \phi_{njl}(r)\Omega_{jlm} \\ \xi_{njl}(r)\,(-\imath\vec{\sigma} \cdot \hat{r})\,\Omega_{jlm} \end{pmatrix}, \tag{2.4}$$

[1] otherwise known as the Full Monty experience

where ϕ and ξ are the large and small parts of the radial wave function, respectively. The Ω terms are the usual angular functions from angular momentum addition of spin and orbit. They are eigenfunctions of l^2, l_z, s^2, and s_z.

In this regime the radial wave functions can be expanded in terms of Bessel functions that are both regular as $r \to 0$ via

$$\begin{aligned} \phi_{njl}(r) &= \frac{c_{njl}}{r}\left[(\gamma_j + \kappa)J_{2\gamma_j}(x) - \frac{x}{2}J_{2\gamma_j - 1}(x)\right] \quad (2.5) \\ \xi_{njl}(r) &= \frac{c_{njl}}{r} Z\alpha J_{2\gamma_j}(x), \quad (2.6) \end{aligned}$$

where

$$\begin{aligned} x &= \left(\frac{8Zr}{a}\right)^2, \\ \gamma_j &= \sqrt{(j+1/2)^2 - Z^2\alpha^2}, \quad (2.7) \\ \kappa &= (l-j)(2j+1). \end{aligned}$$

The value of c_{njl} is determined by requiring that the large component of the radial wave function should go over to the semi-classical, non-relativistic solution - this is because the large component is the dominant term when relativity is weak, or when $r \gg a/Z$ and the electron is well screened from the bare nucleus.

The ordinary, non-relativistic semi-classical solution to the Schrödinger equation is

$$R_{nl}(r) = \frac{b_{nl}}{r\sqrt{k(r)}} \sin\left(\int_{r_1}^{r} dr' k(r') + \delta\right). \quad (2.8)$$

The value of $k(r)$ is given by the difference of the energy and the modified potential (the potential including the centrifugal barrier) such that

$$k^2(r) = 2m_e\left(E_{nl} - U(r) - \frac{(l+1/2)^2}{2m_e r^2}\right), \quad (2.9)$$

where $U(r)$ is the electronic potential experienced by the electron. $U(r) \approx -\frac{Ze^2}{r} + \sum_{i<j}\frac{e^2}{r_{ij}}$, where r_{ij} is the separation between two electrons. r_1 is the turning point while δ is a constant phase. Between the two turning points inside the potential, r_1

and r_2, is the dominant contribution to the integral because of the potentials depth. Ignoring terms beyond the turning point and setting the square of the integral to unity (normalization condition) it is then seen that

$$b_{nl}^2 \int_{r_1}^{r_2} \frac{dr}{k(r)} \sin^2\left(\int_{r_1}^{r} dr' k(r') + \delta\right) \approx \frac{b_{nl}^2}{2} \int_{r_1}^{r_2} \frac{dr}{k(r)} = 1, \tag{2.10}$$

where $\sin^2()$ has been replaced by $1/2$.

Recall the Bohr quantization rule for radial motion which states

$$\int_{r_1}^{r_2} dr k(r) = \pi(n_r + \beta), \tag{2.11}$$

where β is a constant. Differentiating this with respect to n_r, using $k(r)$ from Eq. (2.9) and remembering that $k(r_{1,2}) = 0$, yields

$$m_e \frac{dE_{nl}}{dn_r} \int_{r_1}^{r_2} \frac{dr}{k(r)} = \pi, \tag{2.12}$$

and therefore a quick substitution into Eq. (2.10) gives

$$b_{nl}^2 = \frac{2m_e}{\pi} \frac{dE_{nl}}{dn_r} = \frac{2}{\pi a_0^2 \nu^3}, \tag{2.13}$$

where the outer electron energy has been approximated by

$$E_{nl} = -\frac{Z_{\text{eff}}^2}{2\nu^2}, \tag{2.14}$$

where $\nu = n_r + l + 1 - \sigma_l$. σ_l is a quantum defect which accounts for the effects of $U(r)$ on the energy E_{nl}; thus it accounts for the outer electron whizzing through a cloud of other electrons as well as the nucleus. It effectively diminishes the principal quantum number $n = n_r + l + 1$, because the electron when far away sees a charge of unity, but up close sees the complete nuclear charge. The energy is shifted by the interaction of this electron with the remaining cloud around the nucleus.

Z_{eff} takes the value of 1 (2) in neutral (singly ionized) atoms while in a molecule one can assign a value based on the molecular structure (see Sec. 2.4). The coefficient c_{njl} can be found by comparing Eq. (2.5) with Eq. (2.8) at distances $a_0/Z \ll r \ll a_0/Z^{1/3}$

$$c_{njl} = sign(\kappa) \left(\frac{\pi a_0}{2Z}\right)^{1/2} b_{nl} = sign(\kappa) \left(\frac{1}{Z a_0 \nu_l^3}\right)^{1/2} Z_{\text{eff}}. \tag{2.15}$$

Quantum Defect Theory is a rich field and the interested reader should look in Ref. [22]. ν_l is a parameter gained from experimental data on the atom of interest.

The take away message is we can write a form of the radial wave functions at short distances $r \ll a/Z^{1/3}$ in terms of the nuclear charge Z, the effective charge $Z_{\rm eff}$, and a parameter ν_l.

$$\phi_{njl}(r) = \mathrm{sign}(\kappa)(\kappa-\gamma_j)\left(\frac{Z}{a_0^3\nu_l^3}\right)^{1/2}\frac{2Z_{\rm eff}}{\Gamma(2\gamma_j+1)}\left(\frac{a_0}{2Z\gamma_j r}\right)^{1-\gamma_j} \tag{2.16}$$

$$\xi_{njl}(r) = \mathrm{sign}(\kappa)Z\alpha\left(\frac{Z}{a_0^3\nu_l^3}\right)^{1/2}\frac{2Z_{\rm eff}}{\Gamma(2\gamma_j+1)}\left(\frac{a_0}{2Z\gamma_j r}\right)^{1-\gamma_j}. \tag{2.17}$$

This concludes the brief review of relevant Dirac equation concepts. It is now time to explore the properties of an interaction involving an electron electric dipole moment (eEDM).

2.2 Schiff's theorem

An elementary particle such as the electron, or structured particles such as protons, have this annoying property that when placed in a static electric field they tend to dart quickly away. Therefore, in order to measure their EDMs it is necessary to place them into familiar neutral systems like atoms and molecules. However, this presents a problem formulated first by Purcell and Ramsey [23] and further expounded upon by Garwin and Lederman [24].

Imagine applying an electric field $\vec{\mathcal{E}}_{\rm app}$ to an atom. In equilibrium the electrons move about to and fro in such a manner that the atom remains at rest, thereby implying that the internal electric field $\vec{\mathcal{E}}_{\rm int}$ acting on each electron (and nucleon for that matter) exactly balances $\vec{\mathcal{E}}_{\rm app}$. Therefore there is no electric field whereby the EDM of the electron (or nucleon) can interact and create an energy shift. This is the basic concept of Schiff's Theorem[17]. Ironically, Schiff's own paper [17] was more concerned with how to get around this conundrum. In mathematical terms, this is seen via the following steps. In the atom, there are particles j with intrinsic electric dipole moments $\vec{d}_j$. The

bare EDM of the atom is thereby the expectation of the sum off all the intrinsic dipoles in the state of interest

$$\langle n| \sum_j \vec{d}_j |n\rangle. \tag{2.18}$$

In addition, there is an induced dipole moment due to the interaction with $\vec{\mathcal{E}}_{\rm int}$. By writing $\vec{\mathcal{E}}_{\rm int}$ as the gradient of a potential experienced by the particle,

$$\begin{aligned} H_d &= -\sum_j \vec{\mathbf{d}}_j \cdot \vec{\mathcal{E}}_{\rm int}(\mathbf{r}_j) && (2.19)\\ &= -\sum_j \frac{1}{e_j}\vec{d}_j \cdot \vec{\nabla}_j U(r)_{\rm int} \\ &= \imath \sum_j \frac{1}{e_j} \left[p_j, H_0\right], && (2.20) \end{aligned}$$

where H_0 is the Schrödinger Hamiltonian in the absence of EDM terms. In addition, one assumes the inter particle interactions are solely electrostatic, especially it is assumed the interactions are independent of $\vec{p}$. H_d will cause a mixing of states

$$\begin{aligned} |\tilde{n}\rangle &= |n\rangle + \sum_m \frac{\langle m|H_d|n\rangle}{E_n - E_m}|m\rangle \\ &= \left(1 + \imath \sum_k \frac{1}{e_k}\vec{d}_k \cdot \vec{p}_k\right)|n\rangle, && (2.21) \end{aligned}$$

where here $\vec{d}_k \cdot \vec{p}_k/e_k$ is a sum over states $|m\rangle$ connected by the interaction and the sum on k is a summation over the particles. The expectation value $\langle\tilde{n}|e\vec{r}_k|\tilde{n}\rangle$, which is the non-intrinsic dipole moment of the mixed state, is thus

$$\begin{aligned} \langle\tilde{n}| \sum_k e\vec{r}_k |\tilde{n}\rangle &= \langle n|\imath \left[\sum_l e_l \vec{r}_l, \sum_k \frac{1}{e_k}\vec{d}_k \cdot \vec{p}_k\right]|n\rangle \\ &= -\langle n| \sum_k \vec{d}_k |n\rangle, && (2.22) \end{aligned}$$

which cancels to first order in H_d the effect of the bare dipole moments in Eq. (2.18). It is important to note that the application of the the commutation relations used in Eq. (2.22) requires that the dipole $\vec{d}_k$ be independent of the velocity of the electron in the atom or molecule. In that way, one can invoke the commutation relation between $\vec{r}_l$

and $\vec{p}_k$ to reduce the double sum to one on a single index. This is the heart of Schiff's theorem and intrinsically supposes non-relativistic motion of the electron. Thus, it is left that the total dipole moment of the system is

$$\langle \vec{d} \rangle = \langle \sum_k e_k \vec{r}_k + \sum_j \vec{d}_j \rangle = 0, \tag{2.23}$$

and there is no dipole moment, to first order.

However, all is not lost. A common, although "false and misleading," [25] method of expressing how the electric field acting on the constituents can be non-zero is to invoke the following: electrons in the atom are motional, and therefore create a magnetic field. Thus, there are two internal fields with which to balance the applied electric field thereby allowing a non-zero effective electric field at the electron within the atom. This is the line of reasoning used by Sandars in the original proposal to search for eEDMs in atoms in the 1960s [26, 27, 12, 13]. It has been the standard explanation for the evasion of Schiff's theorem in many papers since [28, 29, 30, 31]. Basically an assertion is made that there exists a velocity dependent piece to the force experienced by the electron.

Yet, one can show that the average electric field is still zero, even in the relativistic sector, i.e. using the Dirac Hamiltonian. The Hamiltonian in Eq. (2.3) combined with the electron EDM Hamiltonian, which is given by [5]

$$H_{\mathrm{EDM}} = -d_e \gamma^0 \vec{\mathbf{\Sigma}} \cdot \vec{\mathcal{E}}, \tag{2.24}$$

where γ^0 is a Dirac matrix and $\vec{\mathbf{\Sigma}}$ is the matrix of Pauli matrices on the diagonal (c.f. Ref. [20]), has an expectation value of zero for the electric field. The standard Dirac Hamiltonian is given by (similar to (2.3) except the electrostatic potential is left as a sum of internal and external terms).

$$H = c\vec{\alpha} \cdot \vec{p} + mc^2\gamma^0 - e(\Phi_i + \Phi_e), \tag{2.25}$$

where $\vec{\alpha}$ is defined in the Sec. 2.1. In addition H has eigenvectors $|\psi\rangle$. The total electric field is $\vec{\mathcal{E}} = -\vec{\nabla}(\Phi_i + \Phi_e)$, where $\Phi_i(\Phi_e)$ is the internal (external) electrostatic potential.

A standard approach (c.f [5, 25]) is to separate (2.24) into two parts

$$H_{\rm EDM} = -d_e\vec{\mathbf{\Sigma}}\cdot\vec{\mathcal{E}} - d_e(\gamma^0-1)\vec{\mathbf{\Sigma}}\cdot\vec{\mathcal{E}}, \tag{2.26}$$

where the first term commutes with Eq. (2.25) and the second term does not. Because the total electric field is the gradient of an electrostatic potential, it is straightforward to show that the first term in (2.26) has an expectation value of

$$\langle\psi| - d_e\vec{\sigma}\cdot\vec{\mathcal{E}}|\psi\rangle = -\frac{\imath d_e}{e}\langle\psi|\left[\vec{\mathbf{\Sigma}}\cdot\vec{p}, H\right]|\psi\rangle = 0, \tag{2.27}$$

because $|\psi\rangle$ is an eigenstate of H. This is merely a restatement of Schiff's theorem because the first term in (2.26) is merely the non-relativistic piece of $H_{\rm EDM}$. The second term in (2.26) is responsible for the evasion of Schiff's theorem, but not because the expectation value of the electric field is non-zero. In fact, it is straightforward to show (using $\Phi = \Phi_i + \Phi_e$)

$$\begin{aligned}\vec{\mathcal{E}} &= -\frac{1}{e}\vec{\nabla}(e\Phi)\\ &= -\frac{\imath}{e}\left[\vec{p}, e\Phi\right]\\ &= \frac{\imath}{e}\left[\vec{p}, (H - c\vec{\alpha}\cdot\vec{p} - mc^2\gamma^0)\right],\end{aligned} \tag{2.28}$$

and since $\vec{p}$ commutes with both $\vec{\alpha}\cdot\vec{p}$ and γ^0, it is evident that

$$\langle\psi|\vec{\mathcal{E}}|\psi\rangle = \frac{\imath}{e}\langle\psi|\left[\vec{p}, H\right]|\psi\rangle = 0 \tag{2.29}$$

because $|\psi\rangle$ is an eigenstate of H. Therefore, the average electric field within the atom is zero.

The true evasion of Schiff's theorem relies on an invocation (or incantation) of relativity: length contraction. As derived in Ref. [25] the dipole moment of the electron has a different value in the lab frame than in the frame of the atom or molecule. After much algebra and relativistic quantum mechanics operator identities that are (summarily) executed in [25], one can arrive at an expression for the EDM of the electron in the

lab frame:

$$\vec{d}_e^{\,\text{lab}} = \vec{d}_e - \frac{\gamma}{1+\gamma}\vec{\beta}\vec{d}_e \cdot \vec{\beta}. \tag{2.30}$$

$\vec{\beta}$ is the velocity vector (and not to be confused with the Dirac β in Eq. (2.3) such that $\vec{p} = m\vec{\beta}\gamma$, and $\gamma = (1-\beta^2)^{-1/2}$ is the usual relativistic factor with $\beta = v/c$. As is evident, Eq. (2.30) has a velocity dependent piece. Therefore, the assumption made in Eq. (2.22), namely $[\vec{r}_l, \vec{d}_j] = 0$, is not valid. The commutation of $\vec{r}_l$ with the non-trivial velocity dependence of the the dipole $\vec{d}_j$ must be worked out. Therefore, that sum will not entirely cancel out the bare dipole moments of the constituent particles in the atom. Therefore, there is a measurable EDM shift in an atom or molecule.

The evasion of Schiff's theorem is now accomplished. It is the Lorentz contraction of the dipole as it moves relativistically near the nucleus that allows for the non-zero expectation value of the interaction $\vec{d}_j \cdot \vec{\mathcal{E}}$ while the expectation value of $\vec{\mathcal{E}}$ is rigorously zero. It is standard to interpret the energy shift due to the interaction with the electric field as arising from an effective electric field $\vec{\mathcal{E}}_{\text{eff}}$ interacting with the dipole moment d_e. For the rest of this chapter, the concern will be with estimating the size of $\vec{\mathcal{E}}_{\text{eff}}$. Therefore, interactions of the form

$$H_{\text{EDM}} = -d_e \vec{\sigma} \cdot \vec{\mathcal{E}}_{\text{eff}}, \tag{2.31}$$

are of interest, where σ is the Pauli matrix for spin and not the version Σ in Eq. (2.2). Even though the relativity is hidden in the length contraction, and the average field in the atom/molecule is still zero, the energy shift will be interpreted as arising from an effective electric field $\vec{\mathcal{E}}_{\text{eff}}$ interacting with electron frame eEDM pointed along the direction of the magnetic spin axis defined by $\vec{\sigma}$.

2.3 Enhancement factor

Sandars [26] noted that the net EDM of an atom can be many times larger than the eEDM because of an enhancement of the applied electric field, the enhancement

associated with relativity. To get a feel for the size of the electric field necessary, very simple arguments can be made. First, the electric field experienced by an electron near the nucleus scales as follows

$$\mathcal{E}_{\text{eff}} \sim \frac{Ze}{r^2} \sim \frac{Z^3 e}{a_0^2}, \tag{2.32}$$

where we use $r \sim a_0/Z$ because of a_0/Z sets the scale for where all the action happens. Again, a_0 is the Bohr length. Therefore, $\mathcal{E}_{\text{eff}}$ scales as Z^3. The larger the value of Z, the larger the effective electric field experienced by the electron.

Now, recall the form of the eEDM Hamiltonian in Eq. (2.26). Even in the presence of multiple electrons in the system, the first term on the LHS of that equation will contribute zero for the same reasons that it did in Sec. 2.2. The electric field $\vec{\mathcal{E}}$ can be written as the gradient of a potential, and will commute with the many electron Hamiltonian, even when including electron-electron interactions. It is the second term on the RHS of (2.26) that is of interest. First, notice that it will only contain terms involving the "small" radial wave function $\xi_{njl}(r)$ because

$$\gamma^0 - \mathbf{1} = 2 \begin{pmatrix} 0 & 0 \\ 0 & -\mathbf{1} \end{pmatrix}, \tag{2.33}$$

and $(\gamma_0 - 1)\vec{\mathbf{\Sigma}} = -2\vec{\sigma}$ The interaction therefore appears as $\sim d_e \vec{\sigma} \cdot \vec{\mathcal{E}}$ and involves only the "small" component of the Dirac wave function. In the non-relativistic limit, this term will vanish completely because $Z\alpha \to 0$ when relativity is unimportant.

Now, let there be a wave function $|\Psi\rangle$ describing an electron in an atom or molecule written as a sum of Dirac wave functions $|njlm\rangle$,

$$|\Psi\rangle = \sum_{njl} \epsilon_{njl} |njlm\rangle, \tag{2.34}$$

where the $|njlm\rangle$ are defined in Eq. (2.4). The parity of each individual solution $|njlm\rangle$ is given by $(-1)^l$. This, combined with the fact that the electric field is an odd parity operator will greatly simplify the calculation. Only states with opposite parity will

be connected, and the Hamiltonian in Eq. (2.33) acts only on the small component. Therefore, terms of the form

$$\begin{aligned}
\langle\Psi|H_{\rm EDM}|\Psi\rangle &= -d_e\langle\Psi|(\gamma_0-1))\vec{\mathbf{\Sigma}}\cdot\vec{\mathcal{E}}|\Psi\rangle \\
&= -2d_e\langle\Psi_{\rm small}|\vec{\sigma}\cdot\vec{\mathcal{E}}|\Psi_{\rm small}\rangle \\
&= 2d_e\langle\Psi_{\rm small}|\vec{\sigma}\cdot\vec{\nabla}U(\vec{r})|\Psi_{\rm small}\rangle \\
&= 2d_e\langle\Psi_{\rm small}|\vec{\sigma}\cdot\hat{r}\frac{Ze^2}{r^2}|\Psi_{\rm small}\rangle \\
&= 2d_e\sum_{njl}\sum_{n'j'l'}\epsilon_{njl}\epsilon_{n',j',l'}\langle{\rm small},n'j'l'm|\vec{\sigma}\cdot\hat{r}\frac{Ze^2}{r^2}|{\rm small},njlm\rangle \quad (2.35)
\end{aligned}$$

are important. In the second line the word "small" is to indicate the small component of the solution, $\xi_{njl}(r)$. From the third to fourth line the potential is assumed to be dependent on the magnitude of the charge of the nucleus and inversely proportional to the separation of the electron from the nucleus. This is valid at distances small enough that the electron experiences the bare nucleus and it is the dominant contribution to the potential energy. At larger separations, the potential is screened and relativistic effects are much smaller due to the smaller velocities involved.

The angular integrand is then going to involve $\Omega^{\star}_{jlm}(\vec{\sigma}\cdot\hat{r})^3\Omega_{j'l'm'}$, where two powers of $\vec{\sigma}\cdot\hat{r}$ come from the "small" angular components and the other from the interaction of the spin with the electric field. Due to properties of the Pauli matrices, $(\vec{\sigma}\cdot\hat{r})^3 = (\vec{\sigma}\cdot\hat{r})$. This is seen using (summation is implied over repeated indexes)

$$\begin{aligned}
(\vec{\sigma}\cdot\hat{r})^2 &= r_i r_j\sigma_i\sigma_j \\
&= r_i r_j(\imath\epsilon_{ijk}\sigma_k+\delta_{ij}) \quad (2.36)\\
&= r_i r_j\delta_{ij}+\imath r_i r_j\epsilon_{ijk}\sigma_k \quad (2.37)\\
&= \mathbf{1}, \quad (2.38)
\end{aligned}$$

where the relations $\epsilon_{ijk}r_i r_j = 0$ and $r_i r_j\delta_{ij}$ is the identity matrix are used. The angular integral is now given by

$$\int\Omega^{\star}_{jlm}(\vec{\sigma}\cdot\hat{r})\Omega_{j'l'm'}d(cos(\theta))d\phi. \quad (2.39)$$

$\vec{\sigma} \cdot \hat{r}$ is a pseudo-scalar which changes the value of l by one. Recall that pseudo-scalars change the parity of a state. Thus, for a given state j, the pseudo-scalar will flip l by one when it flips the parity. Because the pseudo-scalar acts only to change l, j and j' must be the same. So, $l' = l \pm 1$. When $\vec{\sigma} \cdot \hat{r}$ acts on the state $\Omega_{j',l',m'}$, it preserves j and changes the parity thereby changing $l' \rightarrow l' \pm 1$. To evaluate the angular integral, the form of the angular functions for $j = l \pm 1/2$ will be useful (see Ref. [20] for a more detailed account).

$$\Omega_{jlm} = \begin{cases} \varphi^{+}_{jm}; & j = l + 1/2 \\ \varphi^{-}_{jm}; & j = l - 1/2 \end{cases}, \tag{2.40}$$

where

$$\varphi^{+}_{jm} = \begin{pmatrix} \sqrt{\frac{l+1/2+m}{2l+1}} Y_{l,m-1/2} \\ \sqrt{\frac{l+1/2-m}{2l+1}} Y_{l,m+1/2} \end{pmatrix}, \tag{2.41}$$

$$\varphi^{-}_{jm} = \begin{pmatrix} \sqrt{\frac{l+1/2-m}{2l+1}} Y_{l,m-1/2} \\ -\sqrt{\frac{l+1/2+m}{2l+1}} Y_{l,m+1/2} \end{pmatrix}. \tag{2.42}$$

φ^{-}_{jm} only exists when $l > 0$. The $Y_l^{m \pm 1/2}$ are the regular spherical harmonics and m is the projection of j. An important identity to use

$$\varphi^{+}_{jm} = \vec{\sigma} \cdot \hat{r} \varphi^{-}_{jm}. \tag{2.43}$$

Note that unless $l = j \pm 1/2$ and $l' = j \mp 1/2$, the angular integral will be zero. Therefore the angular integral reduces to

$$\begin{aligned} \int \Omega^{\star}_{jlm} (\vec{\sigma} \cdot \hat{r}) \Omega_{j'l'm'} &= \int \varphi^{+}_{jm} (\vec{\sigma} \cdot \hat{r}) \varphi^{-}_{j'm'} \\ &= \frac{l+1}{2l+1} \end{aligned} \tag{2.44}$$

due to the orthogonality and normalization of the spherical harmonics. l takes the value associated with the $j = l - 1/2$ term. For an s connected to a p state, l takes the value $l = 1$ and the angular integral is $2/3$. The angular integration knows that the parity of the two states connected by the H_{EDM} must differ.

Since one starts out in a given $|njlm\rangle$ in an atom one needs to find the $|n'jl'm'\rangle$ states that are connected via the interaction. The radial piece of the integral in Eq. (2.35) reduces to

$$\begin{aligned}\langle njl = j \pm 1/2|\frac{Ze^2}{r^2}|n'jl = j \mp 1/2\rangle &= \langle \xi_{nj(l=j\pm1/2)}|\frac{Ze^2}{r^2}|\xi_{n'j(l'=j\mp1/2)}\rangle, \\ &= \int_0^{r=a_0/Z} \xi^{\star}_{nj(l=j\pm1/2)}(r')\frac{Ze^2}{r'^2}\xi_{n'j(l'=j\mp1/2)}(r')r'^2dr' \\ &= -\frac{4Z^3\alpha^2e^2Z_{\rm eff}^2}{\gamma_j(4\gamma_j^2-1)(\nu'_{l'}\nu_l)^{3/2}}. \end{aligned} \tag{2.45}$$

which is termed the relativistic enhancement factor. The integrand is only taken to distances where the unscreened Coulomb charge of the nucleus is present. Beyond this distance the integrand is vastly smaller and thus, ignorable. For these small values of r the expansions in Eq. (2.17) were used. Therefore, the expectation value of the perturbing Hamiltonian $H_{\rm EDM}$ yields a shift in energy given by

$$\langle\Psi|H_{\rm EDM}|\Psi\rangle = \Delta E = -\frac{4}{3}d_e\sum_{n'l'}\epsilon_{nl}\epsilon_{n'l'}\frac{4Z^3\alpha^2e^2Z_{\rm eff}^2}{\gamma_j(4\gamma_j^2-1)(\nu'_{l'}\nu_l)^{3/2}} \tag{2.46}$$

All that remains is to calculate the ϵ terms.

There is one subtlety to consider. In a molecule, both the $p_{1/2}$ and $p_{3/2}$ electrons have a projection onto the molecular axis defined by λ. Therefore, one must account for this in the angular integrand of Eq. (2.39) where spherical symmetry was assumed. The p orbital can be expanded into

$$|p\rangle = -\frac{2\sigma}{\sqrt{3}}|p_{1/2}\sigma\rangle + \sqrt{\frac{2}{3}}|p_{3/2}\sigma\rangle. \tag{2.47}$$

Then one ignores the contribution from the $p_{3/2}$ state since it does not preserve the value of j. In the end, this introduces a slightly different energy shift for molecules and atoms, which in turn gives a slightly different effective electric field formula. In order to calculate the effective electric field one takes the energy shift and divides by d_e. Thus,

the effective electric field for atoms and molecules are given by

$$\mathcal{E}_{\text{eff,atom}} = -\frac{16}{3}\frac{Z^3\alpha^2 e^2 Z_{\text{eff}}^2}{\gamma_j(4\gamma_j^2-1)(\nu_{ns}\nu_{np})^{3/2}}\epsilon_s\epsilon_p, \tag{2.48}$$

$$\mathcal{E}_{\text{eff,mol}} = -(\sigma\cdot\lambda)\frac{16}{\sqrt{3}}\frac{Z^3\alpha^2 e^2 Z_{\text{eff}}^2}{\gamma_j(4\gamma_j^2-1)(\nu_{ns}\nu_{np})^{3/2}}\epsilon_s\epsilon_p \tag{2.49}$$

In the last line the term $\sigma\cdot\lambda$ takes account of the projection of the spin onto the molecular axis defined by λ. It has magnitude 1/2. Therefore, the two are related in magnitude by $\sqrt{3}/2$ and this factor accounts for the geometry of the molecular system. It is a reduction in the size due to projecting onto the lab frame and the molecule frame.

There is an implicit assumption made about the form of the wave function in the molecular system. When the electron is close to the nucleus, one ignores the molecular properties in favor of the short range atomic ones. Therefore, even in the molecular case the concern lies with the quantum defects of the atom of interest as well as the effective charge.

The next section will address calculating ϵ_s and ϵ_p for the molecule. However, it is instructive to do so for the atom first. In the atom the eEDM interaction does not mix much in the way of p-orbitals into the ground state. Therefore, one could try to enhance the effect by applying an external electric field and perturbatively couple in the excited p state (or more generally the excited state of opposite parity). In this limit

$$\epsilon_s \approx 1, \tag{2.50}$$

$$\epsilon_p \approx \sum_m \frac{\langle s|e\hat{r}\cdot\vec{\mathcal{E}}_{\text{app}}|p\rangle}{E(mp)-E(ns)}. \tag{2.51}$$

An s-ground state has been assumed and the sum is over all p states connected by the applied electric field. Were the ground state p in nature then one has $\epsilon_p \approx 1$ and a sum over connected s states is required. What is directly evident is that the effective field in Eq. (2.48) is proportional to the applied electric field $\vec{\mathcal{E}}_{\text{app}}$, thus defining an enhancement factor. These estimates have been made for many atoms. Two worth mentioning are Cs [26, 27, 32] and Tl [33, 34]. These papers show that the energy shift

in Cs is $\approx 130 d_e \mathcal{E}_{\rm app}$, or that an electric field enhancement of $130 \times \mathcal{E}_{\rm app}$ is achieved. Detailed, fully relativistic calculations yield a value of 114 for the enhancement [32]. In Tl, the estimate yields -500 [5] while detailed calculations yield -585 [34].

Recall from the introduction (Sec. 1) that Tl is the system in which the current best limit on the eEDM was attained $d_e < 4 \times 10^{-27}$ e-cm [7]. Having quite a large enhancement of the applied field is the key to this measurement. Yet, it begs the question of how to improve on this value. Unfortunately, stable atoms do not get much heavier than Tl, and therefore the enhancement that grows with Z so favorably comes to an end. And the ability to apply large electric fields is limited in the laboratory to many kV/cm (perhaps even up to many 10s of kV/cm). One way in which to improve upon this limit is to find systems where s and p orbitals are naturally mixed, or the spacings of opposite parity levels are vastly closer so a smaller applied electric field gains in the enhancement factor. Luckily, nature has provided systems where this occurs.

2.4 Molecular candidates

In a diatomic molecule, the atomic orbitals are naturally mixed. s-states mix with p-states, d with p and f, etc. In so doing, a natural effective electric field is created in the sense of Eq. (2.49) and this field can be many orders of magnitude larger than is achievable in the laboratory. Within a diatomic molecule an s electron is of particular interest for eEDM searches. This electron has zero projection onto the molecular axis (defined by σ) and can be expanded in the following basis

$$|\sigma\rangle = \sum_{l=0}^{l_{\rm max}} \epsilon_l |l\sigma\rangle, \tag{2.52}$$

where the sum indicates all angular momentum with a zero projection along the molecular axis. This is due to the breaking of spherical symmetry in the molecule. Therefore, p_z, d_0, f_0 atomic orbitals all contribute to the σ molecular orbital by the argument of the previous section. This mixing can be interpreted as an effective electric field. $l_{\rm max}$

is the maximum value l can take and will depend on the type of atom being considered. For an alkali-metal atom such as Cs, choosing $l_{\max} = 2$ is sufficient. In order to calculate the contributions ϵ_l one must employ *ab initio* methods. The details of these calculations will be developed in the next chapter (3). The important idea here is that the values of ϵ_s and ϵ_p can be quite close to an even mixture, ideally given by $1/\sqrt{2}$ for each. Moreover, $\mathcal{E}_{\text{eff}}$ is independent of the applied field.

Typically, one uses a basis set designed to accurately reproduce atomic data for a specific atom when performing these calculations. A convenient choice is to use a basis set that consists of Gaussians. One then centers these Guassian sets on each atom with angular momenta from 0–$l_{\max}$, the maximum l in the basis. A basis set $|b\rangle$ (the radial component only) will look like the following

$$|b\rangle = \sum_k s_k |g_k\rangle = \sum_k c_{kl} r^l e^{-\chi_{kl} r^2} \tag{2.53}$$

where l is the angular momentum, and the coefficients c and χ will depend on which value l takes. Thus, an s state is a Guassian, p a first rank polynomial times a Guassian, d a second rank and so on. When there is a one-electron σ molecular orbital, the molecular wave function can be expressed as

$$\begin{aligned} |\Psi_{\text{mol}}\rangle &= \sum_i c_i^h |s\sigma_i^h\rangle + d_i^h |p\sigma_i^h\rangle + \cdots \\ &\quad + \sum_j c_j^\ell |s\sigma_j \ell\rangle + d_j^\ell |p\sigma_j^\ell\rangle + \cdots , \end{aligned} \tag{2.54}$$

where h and ℓ are used to signify the heavy and light atom separately. Distinguishing between h and ℓ serves to separate out the contribution to ϵ_s (ϵ_p) from each atom. Because Gaussians are not necessarily orthogonal to each other, care must be used to normalize molecular orbitals in the definition of the ϵ parameters. The contribution from the heavy atom due to s-type orbitals is

$$\epsilon_s = \frac{\sum_k c_k^h \langle \Psi_{\text{mol}} | s\sigma_k^h \rangle}{\sum_{jk} c_j^{h\star} c_k^h \langle s\sigma_j^h | s\sigma_k^h \rangle}. \tag{2.55}$$

A similar expression for the p-orbital contribution to the heavy atom is

$$\epsilon_p = \frac{\sum_k d_k^h \langle \Psi_{\rm mol} | p\sigma_k^h \rangle}{\sum_{jk} d_j^{h\star} d_k^h \langle p\sigma_j^h | p\sigma_k^h \rangle}. \tag{2.56}$$

The expressions in Eqs. (2.55) and (2.56) do not make a distinction for the principal quantum number n of the atom, and therefore encompass all the excitations that may come into play in forming the molecular bond.

Because these expressions give in principle the entire contribution of the the many ns and $n'p$ excitations, it appears that the definition of the quantum defect parameters ν_s and ν_p are harder to define. However, recall that the expression containing ν_s and ν_p in Eq. (2.49) has the origin of these parameters arising from the short range physics near the nucleus, where the effects of relativity are largest. Therefore, the values of the quantum defects are still tabulated for the individual atom of interest within the molecule.

In Eq. (2.49) the value of $Z_{\rm eff}$ is not quite as it would be for an atom. In a polar molecule there is a transfer of charge from one atom to the other. This transfer does not come in units of the electron charge. A simple model would be to use the measured dipole moment of a molecule of interest and then use a classical approximation to determine the amount of charge on the atom of interest. Then, $Z_{\rm eff}$ would be one more than this number because the electron of interest, when far away from this nucleus, would "see" this charge. Therefore using the system of equations

$$\begin{aligned} d_{\rm mol} &= r_1 q_1 + r_2 q_2 \\ Q_{\rm mol} &= q_1 + q_2, \end{aligned} \tag{2.57}$$

one can solve for the effective charge on either nucleus. $r_{1,(2)}$ is the distance from the center of mass of the molecule to atom 1 (2). In a neutral molecule $Q_{\rm mol} = 0$. It is worth noting that a molecular ion may be of interest since the value of $Z_{\rm eff} = q_{\rm ion} + 1$ can be larger than 2. This further increases the value of the effective electric field. In

order to deal with ions, one must overcome the tendency of ions to dart away in an electric field. Therefore, a rotating electric field is requisite, and the way in which this affects the molecular ions will be addressed in Chap. 4.

There are two other modifications to consider making to Eq. (2.49). In a heavy molecule there are many configurations of the electron that may participate. For example, in a $^3\Delta$ molecule (one where there are two units of orbital angular momentum about the internuclear axis) there are many ways in which the electrons can add up to make Δ. There can be a $|\pi\pi'\rangle$ configuration as well as a $|\sigma\delta\rangle$ configuration. Only the latter will contribute appreciably to the large effective electric field. This is because two π molecular orbitals involve atomic orbitals of a minimum of p angular momentum. While a mixing of p with d orbitals would produce an effective electric field, they would not experience much of the relativistic enhancement near the nucleus since these orbitals have minimal amplitude at the nucleus.

In addition, effects such as spin-orbit can connect states with the same total value of Ω into the state of interest. Ω is the projection of the total spin plus orbital angular momentum onto the molecular axis. A $^2\Sigma_{1/2}$ molecule will mix with a $^2\Pi_{1/2}$ molecule due to spin-orbit effects. Thus, a calculation on a heavy (large Z) diatomic in a $^2\Sigma_{1/2}$ state would have to consider the effects of spin-orbit. The $^2\Pi_{1/2}$ would have negligible contribution to the effective electric field for the same reasons as in the configurations example. Therefore, there would be a reduction in signal for the $^2\Sigma_{1/2}$ state of interest due to the spin-orbit interaction.

In Refs. [28, 35, 36] this method was applied to many molecules. To test the effectiveness of using non-relativistic *ab initio* software (details of which are presented in Chap. 3) along with the relativistic enhancements as calculated above, I produced the values of effective electric fields in Table 2.4. As is evident, the method reproduces the values of the more extensive calculations to within 25%. Considering that some of the more in depth methods produce values to within a certainty of 10%–25% for

the effective electric field, the simple method is a nice alternative. The simple method allows for a quick calculation, taking perhaps a few weeks to complete an in depth study of the molecular properties and arriving at a value of $\mathcal{E}_{\text{eff}}$. More involved methods can take several months to a year to estimate. For experimental groups looking to choose a molecule for an experiment, the simple method is more than sufficient for determining a good candidate. However, it does not replace the need for a fully relativistic calculation once a molecule is chosen and/or a measurement is made.

Now that a simple method has been established, it is worth noting the limitations. Firstly, this approach works well for systems where correlation effects between the electron of interest and the remaining electrons are minimal. Thus, systems with one to two isolated valence electrons are ideal. While the method can be applied to systems with many valence electrons, such as WC [42], the number of configurations begins to take a toll on the time commitment. The accuracy is limited to the diligence of the graduate student in correctly identifying configurations which would contribute to an effective electric field, since many configurations are necessary.

Also, one may try to improve the method by using multi-channel quantum defect theory to find the values of the quantum defect parameters ν_s and ν_p of the individual atoms, i.e. the motion of the electron in the atom of interest [43, 44]. Currently, a single channel approach is all that is used [44, 27]. However, a multi-channel approach adds time to the calculation without necessarily improving the accuracy. The quantum defect contains information about the potential the electron experiences when in the cloud of the other electrons. Yet, it is the information about the region near the nucleus that is most important for these calculations and the essence is already captured in the single channel method.

Lastly, the fully relativistic calculations need to know information about the wave function at the site of the nucleus of interest. Therefore, they need hyperfine parameters measured before the calculation can be put of firm footing. This requires going

Table 2.1: Effective electric field values produced using the above described method compared to values produced using more rigorous methods. All values are in GV/cm.

Molecule	This method	Fully Relativistic
BaF	6.1	7.4 [37]
YbF	32	26 [14]
HgF	95	99 [38]
PbF	-31	-29 [38]
a(1) PbO	23	26.2 [39]
HI^+	0.34	0.34 [40]
HfF^+	30	24 [41]
ThO	104	N/A
ThF^+	90	N/A
RbYb	-0.7	N/A
CsYb	0.54	N/A
$SrYb^+$	-11.3	N/A
$BaYb^+$	1.2	N/A
WC	54	N/A

back to the board to calculate again after the new information is attained. While this simple method can be implemented to reevaluate the hyperfine constants, it takes one down a path of basis set construction which is not at the heart of a speedy calculation. Therefore, using this method is better suited as a preliminary run that aids the experimentalist in choosing a molecule. The experimenter measures the hyperfine parameters and then feeds this information to a theorist who uses it to constrain the fully relativistic calculation from the get go, thereby producing a more accurate prediction the first time through an extensive calculation.

In principle, the non-relativistic *ab initio* software can be constrained using the hyperfine information as well. But, one must again ask whether this is going to improve the overall accuracy compared to the time commitment that would be involved. The simple method is a powerful way to get you into the ball park quickly and start the game — with decent accuracy. However, it can only start the ballgame. A strong closer needs to finish it out in the end. This does not rule out throwing a complete game, it is just rare in this day and age for the starter to close the game[2] .

[2] The baseball analogy may have been carried too far

Chapter 3

A diatom is one atom two many

Technical skill is mastery of complexity while creativity is mastery of simplicity

– Erik Christopher Zeeman

Let's get creative. The study of molecular structure and spectroscopy is quite involved. For many of the molecules presented in Table 2.4 there is no structure or spectroscopic information in the literature. This can make life quite difficult for the experimentalist. However, life is not so strenuous considering the help that can be afforded by a little physical insight mixed with a healthy dose of creativity — simplicity by any other name.

In this chapter I will cover the basics of *ab initio* calculations for gaining insight into the molecular systems of interest. Even with these calculations, there is quite a bit of uncertainty about the analysis of the spectroscopy. Using perturbative treatments, it is possible to extract meaningful parameters which govern the dominant spectroscopy of the atoms. Smaller, more detailed effects can then be understood as deviations from these dominant terms. A general *ab initio* procedure will be developed and used to create surfaces for the molecules of interest in Table 2.4. Then the basic structure and spectroscopy of these molecules will be discussed in in the following sections.

3.1 Chemistry acronym school

Understanding the chemical aspects of heavy diatomic molecules can be a quite daunting task should one try to incorporate every little detail into the calculation and then check that no coding errors are found. Even then, approximations have to be made due to the sheer complexity of the problem. Complexity in science is another way of saying it takes a lot of computer time to solve. The more complex a problem is, the more one needs to make assumptions that simplify the problem. Well, that and the fact that most calculations need to be done within the "lifetime" of a graduate student in the group. Therefore, a natural time limit for the length of the any given calculation is dependent upon weighing the expectations of the student with the professor and trying to leave enough time to write the work up. Somewhere between 4-12 years possibly[1] .

Luckily, there have been many methods introduced due to the innovations of theoretical and computational chemists and physicists over the years. These innovations cut down the computational time required to compute molecular properties. While the methods will not give exact properties, they will contain enough information to qualitatively, or more appropriately, ballpark quantitatively describe the system. In what follows I will walk through the basic steps taken to construct a surface for a diatomic molecule at the various levels needed to understand the eEDM searches presented in Chapter 2. All calculations in this thesis are performed with the MOLPRO suite of *ab initio* codes [45].

As noted in Sec. 2.4 a basis is usually already constructed. In practice, this basis is described by a set of Gaussian functions $|g_i\rangle$ and form an atomic basis set $|b_j\rangle$ as follows

$$|b_j\rangle = \sum_i s_i |g_i\rangle. \tag{3.1}$$

This set is chosen so as to optimize the properties of the individual atom. As an example,

[1] I tried to say 4-8 years but an adviser not to be named said 12

for Rb the basis is optimized so as to reproduce the ionization energy of Rb as well as the polarizability. A good place for obtaining standard basis sets for heavy atoms is given in Ref. [46]. Using a a set of atomic bases on each atom, it is now possible to define a molecular orbital via

$$|\phi_k\rangle = \sum_j c_j |b_j\rangle, \tag{3.2}$$

where each atomic basis is centered on one of the atoms in the molecule. This is an orbital because it has contributions from all atoms in the calculation, and therefore is slightly different from the basis set definition. A configuration is a product of occupations of orbitals given by

$$|\Phi_l\rangle = \mathcal{A} \prod_k d_k |\phi_k\rangle. \tag{3.3}$$

In a Hartree-Fock (HF) calculation the values of d_k can take 0, 1, or 2 for zero, single, or double occupations of the orbital. $\mathcal{A}$ is a shorthand for anti-symmetrization.

For large atoms there is usually another step is reducing the computational time. While it is conceivable to construct an all electron basis for large atoms such as Ba and Yb, it is non-practical. Instead, a core potential can be constructed. This core consisting of N electrons is represented by a pseudo potential. In addition, basis sets can be constructed at the fully relativistic level. Short of creating a basis for one's own use, the quasi-relativistic effective core potentials, which account for a large portion of the relativistic effects (excluding mass corrections and Darwin-type terms), are a great tool to use in these calculations. For the atoms of interest in Table 2.4 there are many great references, chief of which is Ref. [47].

An HF procedure will minimize the energy E of the ground state of the state/symmetry selected and given occupation numbers. Therefore, only one configuration is optimized yielding a HF wave function

$$|\Phi^{\mathrm{HF}}\rangle = \prod_k d_k \ \sum_j c_{jk} |b_j\rangle. \tag{3.4}$$

The procedure will find the d_k and c_{jk} that minimize the total electronic energy E for the configuration. This procedure is exceptionally fast, however it fails to account for the interactions of configurations with each other given that it only optimizes one configuration.

The next step in the procedure is to build a wave function at the multi-configuration self-consistent field (MCSCF) level. A thorough discussion can be found in Refs [48, 49, 50, 51, 52]. The MCSCF takes as a starting point the optimized electronic energy E from the HF step as an initial guess. It then finds appropriate linear combinations of the configurations given in Eq. (3.4) that minimize E over M total configurations. The M configurations can contain many states of a given symmetry as well as different symmetries and spin states. This wave function is

$$|\Phi^{\mathrm{MCSCF}}\rangle = \sum_l f_l |\Phi_l\rangle = \sum_l f_l \left(\prod_k d_{lk} \sum_j c_{kj} |b_j\rangle \right), \tag{3.5}$$

and the procedure finds the f_l, d_{lk}, and c_{kj} which minimize the average E; averaged over all the spin and symmetry states given in the command. Depending on the choice of active, closed, and frozen spaces this can be a quite time consuming part of the procedure due to the non-linear optimization routine. An active space is the space in which one allows the occupations d_{lk} to be optimized to a any number between 0 and 2 for calculating the average energy. Occupations are no longer required to have zero, one, or two electrons on average; some intermediate number can be used to minimize the average E.

Deep within the MCSCF is the wave function that contains a configuration (or many) with the σ-molecular orbital of interest for the eEDM. This orbital mixes s- and p-atomic orbitals to form a molecular orbital $|mol, \sigma\rangle$. It has an explicit expansion into Gaussian basis functions according to Eqs. (3.1) and (3.5).

There still remain two steps in developing the total wave function. After computing the MCSCF wave function we move onto an internally contracted, multi-reference

configuration interaction (MRCI) procedure [53, 54, 52, 55].

$$|\Psi^{\mathrm{MRCI}}\rangle = \sum_m h_m |\Phi_m^{\mathrm{MCSCF}}\rangle, \tag{3.6}$$

where this procedure finds the h_m that minimize the value of E for a given spin multiplicity and space symmetry. The constraint is that the values of f_l, d_{lk}, and c_{kj} in Eq. (3.5) are all fixed to the values determined in the MCSCF procedure. A final step is the spin-orbit MRCI (SO-MRCI) [56] which is only possible when one uses a basis $|b_i\rangle$ that includes the effects of spin-orbit coupling. The SO-MRCI procedure uses single and multi-electron operators to mix the MRCI wave functions with the constraint that the value of Ω, the total projection of all spin and orbital angular momentum onto the molecular axis, is fixed. This procedure does not optimize energies, instead it finds the extent to which the MRCI wave functions are coupled via spin-orbit type interactions.

$$|\Psi^{\mathrm{SO-MRCI}}\rangle = \sum_n l_n |\Psi_n^{\mathrm{MRCI}}\rangle. \tag{3.7}$$

The l_n are the optimized quantities. As alluded to in Sec. 2.4 the h_m and the l_n are parameters which must be factored into the calculation of $\mathcal{E}_{\mathrm{eff}}$. They are straight multiplicative factors because the nominal σ-orbital might get some π-orbital mixed into it, for example. Appendix A shows how to do all this using MOLPRO.

For systems where there is yet to be any experimental measurement of the molecular properties, the above method is employed at many values of the internuclear separation R. This can be time consuming and a smart choice of the active, closed, and core spaces must be employed in order to efficiently and effectively produce a set of potential energy curves. In turn, these curves can then be used to identify the coupling scheme appropriate for writing down a spectroscopic Hamiltonian. These will be discussed in the next two sections.

3.2 Σ molecules

Many of the proposed searches for the eEDM choose $^2\Sigma$ molecules. These molecules are preferred because of their relative simplicity. In this section I will examine the basic properties of Σ-type molecules.

3.2.1 Structure

There are two classes of $^2\Sigma$ molecules presented in Table 2.4: systems with appreciable charge transfer (YbF, BaF, HgF, and PbF) which are ionically bonded and systems with little charge transfer (RbYb, CsYb, $SrYb^+$, and $BaYb^+$) which are van der Waals bonded. Both types of molecules exhibit the same valence electron characteristics. The single unpaired electron is predominantly comprised of an s-electron from one of the atoms.

The reason to choose F-containing molecules is fairly clear. Fluorine is quite adept at taking electrons from atoms. In the case of Yb, Ba, and Hg, the electron taken comes from the outer ns^2 configuration of the heavy atom leaving behind an atomic ns configuration. n refers to the principal quantum number and in all cases is $n = 6$ for the given examples.

In the separated atom limit, the atoms are each neutral while at the minimum of the molecular well, the configuration is more akin to M^+F^-, where M is a stand-in for the heavy atom. Therefore, there is a point in the potential energy surface where F snatches one electron and leads to a location on the surface of an avoided crossing between the the neutral atom configurations and the ionic ones. An example of a surface computed at the HF-MCSCF+MRCI level of computation is given in Fig. 3.1 for the YbF system.

In Fig. 3.1, the black curves represent $^2\Sigma$ states while the red curves are $^2\Pi$ states. There are noticeable avoided crossings in this system. Were one to plot vastly

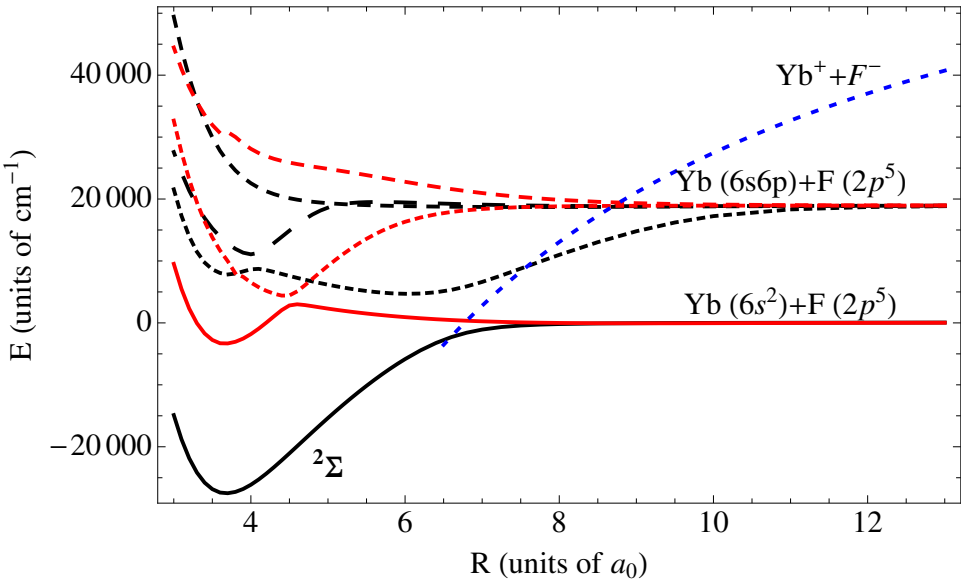

Figure 3.1: YbF potential energy surface calculated at the HF-MCSCF+MRCI level of theory. The black curves represent $^2\Sigma$ states while the red curves represent $^2\Pi$ states. The blue curve is a $1/R$ plot that shows the Yb^++F^- asymptote.

more states of $^2\Sigma$ symmetry a clear emergence of the "ionic" state $Yb^+ + F^-$, which lies around 50,000 cm^{-1} away in energy, would appear. The blue line in Fig. 3.1 is used to guide the eye to the $1/R$ potential that would dissociate to the $Yb^+ + F^-$ asymptote. The avoided crossing in the ground state occurs around $R = 8\ a_0$. It is evident that the $^2\Sigma$ state is well isolated from any other electronic state and therefore is best described by a set of Hund's case (b) coupling numbers. More on Hund's case (b) will be discussed in the next section.

In the calculation of the potential energy surface the ECP68MDF relativistic effective core potential with core polarization terms (CPP) and basis were used for Yb [57]. For the F atom, the cc-pVDZ basis of Dunning was used [58]. The large transfer associated with moving an electron from Yb to F results in a rather large dipole moment of about 4 Debye (D) in the ground state. In the next section I will discuss the benefits of a large dipole moment.

The general feature to take away from this molecular example is that there is one unpaired electron around the Yb^+ ion. This electron, in the free atom, would be of s character alone thus yielding the Σ molecular symmetry in the diatomic orbital. However, the electron sees a rather large negative charge from the F^- ion and tends to repel from it. This in effect polarizes this electron around the Yb atom mixing the s- and p_z-atomic orbitals. It is this mixing that is needed for calculating the effective electric field $\mathcal{E}_{\text{eff}}$ in Eq. (2.49).

The way in which the sign of the effective electric field is defined is based on whether or not its direction conforms to the electric field along the internuclear axis. Electric fields point from positive things to negative things. Therefore, a positive effective electric field is one that lines up with the electric field pointing from Yb^+ to F^- in YbF. Therefore, the unpaired electron around Yb^+ tends to be pushed by the negative charge of F^-. This causes the free electron to sit on the side of Yb^+ away from F^-, yielding larger electron density there. This appears as a mixing of the s- and p_z-atomic

orbitals that has the same effect as an electric field coming from the side of Yb^+ away from F^-. Therefore, the effective electric field is positive. This is borne out by looking at the invention for the dominant configuration in the YbF molecular calculation performed at the equilibrium position of $R_e = 3.6\ a_0$. See Fig. 3.2.

As is evident from Fig. 3.2, there is a large degree of mixing of the s- and p_z-type atomic orbitals around Yb, as evidenced by the asymmetry of the wave function along the internuclear axis $\hat{z}$. This mixing is highlighted by the reddish shading under the molecular orbital curve. The orbital is plotted along the $\hat{z}$-axis and is a projection in the xy-plane. Around the F-atom the mixing is much smaller. The atomic configuration is dominated by the p-atomic orbital characteristics. However, there is evidence of some s-atomic orbital mixing due to the slightly smaller peak on one side of F. This leads one to ask whether the second atom in the diatomic, if it were large enough, can contribute to $\mathcal{E}_{\text{eff}}$.

This leads to a second type of $^2\Sigma$ that has been proposed [36]. Where the benefits of the YbF, BaF, and HgF species have been made apparent, this other species differs. RbYb and CsYb are vastly different from their Fluoride counterparts. These molecular systems do not transfer charge nearly as effectively as the Fluorides. This is due to the relatively similar electronegativities between alkali-metals and Yb. However, Yb is a closed s-shell atom and therefore the only electron in the game is the Rb s-electron. All other electronic states will be separated in energy by an amount comparable to the s-p splitting in Rb. In addition, the well separated electronic states can be taken advantage of when producing the molecular systems. All the atoms considered can be individually laser cooled to extremely cold temperatures. Applying photoassociation techniques one can then produce ultracold samples of these molecular systems. This reduction in temperature would allow for vastly longer coherence times in experimental efforts.

Where F served to take away an electron, Yb serves to perturb the alkali-metal

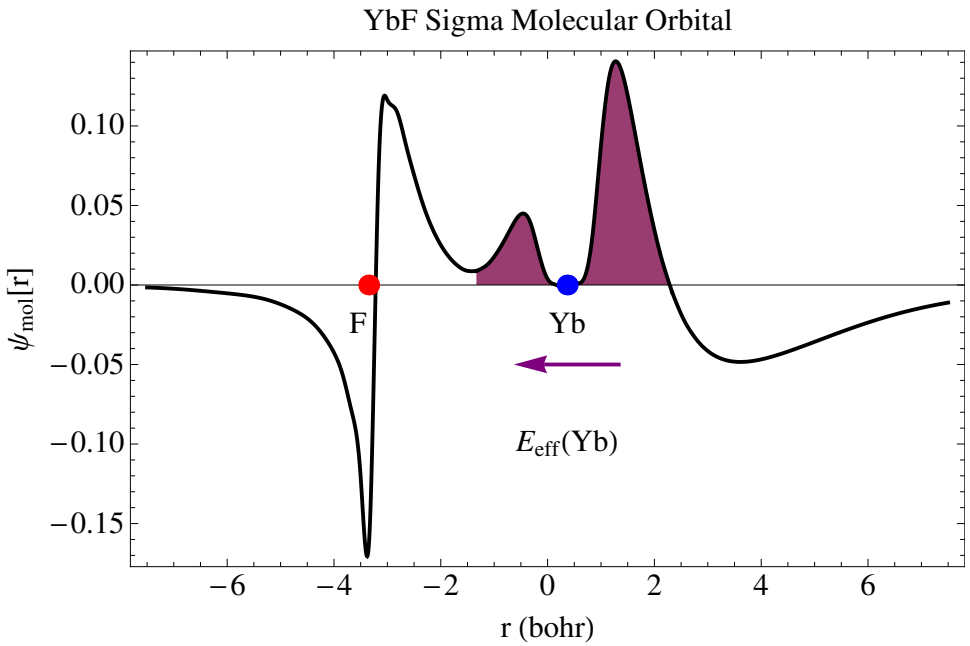

Figure 3.2: YbF σ molecular orbital calculated at the internuclear equilibrium distance. The wave function is plotted along the axis connecting Yb to F. The blue (red) dot represents the Yb (F) atom. Notice the asymmetry in the wave function indicating a larger electron density on the side of Yb away from F.

electron. In the case of Rb and Cs, Yb polarizes the unpaired s-electron. This is simple to see from a van der Waals type argument. Yb and the alkali-metal atom each induce a dipole moment in the other, altering their wave functions. They become slightly distorted, shifting charge in such a way as to attract each other. An alkali-metal electron, being unpaired, reacts to this induced charge separation on Yb and mixes the s and p_z-atomic orbitals along the molecular axis. Yet, the free electron is free to move toward Yb, and hence while around Yb will react to the charge on the alkali-metal.

In Fig. 3.3 I give a calculation of the RbYb potential energy surface in the ground $^2\Sigma$ state. This surface is vastly different than the surface for YbF. First, there is only one electronic state that dissociates to the separated atom limit of $\mathrm{Rb}(5s^1)$ + $\mathrm{Yb}(6s^2)$. The inset in the figure shows a few vibrational levels in the ground electronic state, just in case one could not tell from the figure that the $X^2\Sigma$ state is bound. In this calculation ECP36MDF effective core potential and basis of the Stuttgart group [59, 60] with the CPP terms were used. A RHF-MCSCF+MRCI calculation was performed at several points in the internuclear separation between 25 a_0 and 4.5 a_0. The active space included both the excited p-atomic orbitals for Rb and Yb.

As before, the molecular wave function for the σ-molecular orbital of interest will identify the s-p_z mixing around the individual atoms. This is presented in Fig. 3.4. The electron has an asymmetric distribution about both atoms, but more so around Yb. Because Rb and Yb are of comparable size, relativistic enhancements must be calculated for both. Notice that the direction of the electric field is opposite at the site of each atom. The more comparable in size the two atoms are, the more the fields tend to work against each other, creating a net smaller effective electric field. This is seen in the progression RbYb $\rightarrow$ CsYb in Table 2.4, where the effective electric field in CsYb is smaller than in RbYb because Cs in essence steals some of the glory in Yb's large Z size.

Another interesting item of note is that the RbYb MRCI calculation shows that

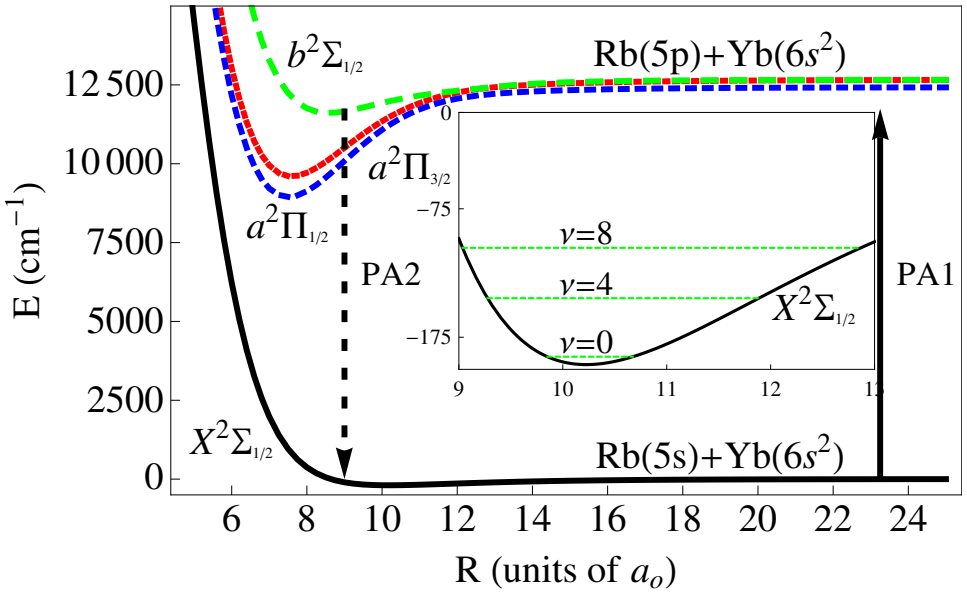

Figure 3.3: RbYb potential energy surface in the ground $^2\Sigma$ state. The calculation was performed at the RHF-MCSCF-MRCI level of theory.

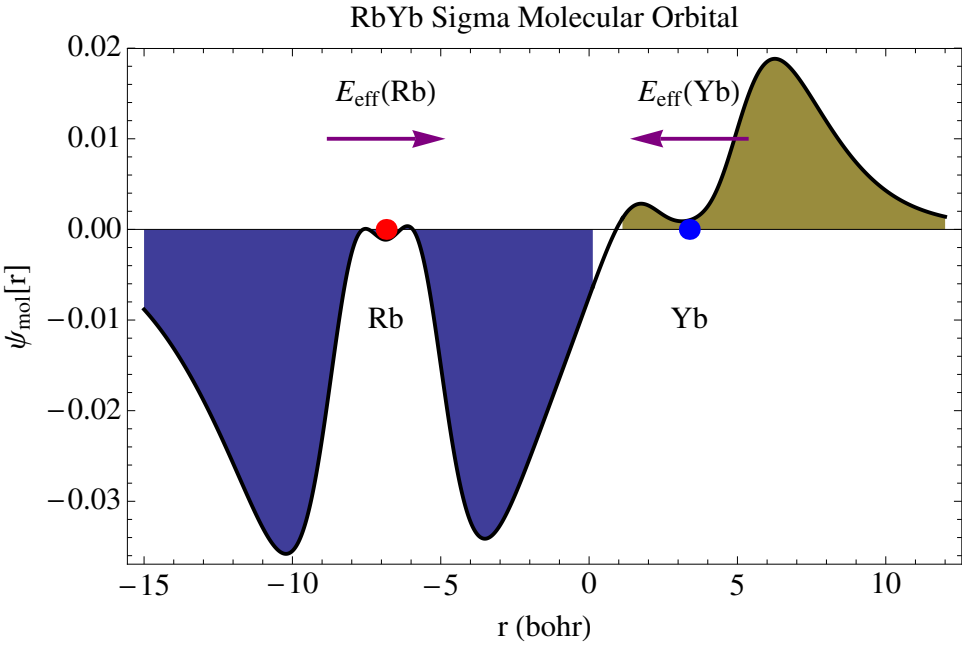

Figure 3.4: RbYb σ molecular orbital calculated at the internuclear equilibrium distance. The wave function is plotted along the axis connecting Yb to Rb. The blue (red) dot represents the Yb (Rb) atom. Notice the asymmetry in the wave function indicating a larger electron density on the side of Yb away from Rb and vice versa on Rb. This leads to a need to find the value of the effective electric field for both atoms.

there are two contributing σ-molecular orbitals, each one dominated by the basis of one of the atoms. The same scenario holds true for all the molecules of these types; RbYb, CsYb, $SrYb^+$, and $BaYb^+$.

3.2.2 Spectroscopy

Spectroscopy for $^2\Sigma$-type molecules is a well known, and widely studied field. There is a separation of energy scales that naturally arises in the systems of interest. Electronic energy separations, the largest in the problem, are of the order 10^5 cm^{-1}. These deal with excitations from one electronic state, the $^2\Sigma$, to another like the $^2\Pi$. For some of the molecules considered, this is a useful bit of information because one way to detect a science signal for the eEDM search is to use transitions from one electronic state to another. The next scale is molecular vibrations, usually of the order 20–50 cm^{-1}, and governs transitions within and between electronic levels. Finally, the next "large" contribution is from end-over-end rotation of the molecule. This scale is 0.01–10 cm^{-1}, depending on the reduced mass and bond length of the system. Further down in energy are all the various interactions between the constituent spins in the molecule that must be understood to gain an appropriate understanding of how to do an eEDM experiment.

Molecule based eEDM searches tend to be on the colder side of physics. The molecules are often studied at temperatures at or below 4 K. For the Fluoride based molecules this is cold enough freeze out all but the lowest vibrational state and to isolate a few rotational levels within the molecule. Therefore, the dominant terms in the spectroscopic Hamiltonian will come from rotational pieces.

Because Σ molecules have no orbital angular momentum about the internuclear axis, they are usually fairly well described by a set of Hund's case (b) quantum numbers. In this representation, the spin $\mathbf{S}$ is decoupled from the molecular axis $\mathbf{N}$. A semi-classical image of this coupling scheme is presented in Fig. 3.5. In this type of coupling, the good quantum numbers are N, S, and the vector sum $J = N + S$ in the absence of

any applied electromagnetic fields. The presence of fields will be addressed shortly.

The basic Hamiltonian for a Hund's case (b) molecule in $^2\Sigma$ can be represented as follows

$$H_{(\mathrm{b})} = B_\nu \mathbf{N}^2 + \gamma_\nu \mathbf{N}\cdot\mathbf{S}, \tag{3.8}$$

where the subscript ν indicates a particular vibrational level of interest. The term B_ν is the rotation constant of the molecule. It sets the energy scale of interest in $^2\Sigma$ eEDM searches because this is the energy which must be overcome to polarize the molecule, without which the large effective electric fields within the molecule would be meaningless. Each rotational level has a different parity given by $(-1)^N$.

γ_ν originates from two sources, of which one is far more important for heavy molecules like YbF. The first order (meaning it arises without the introduction of any other electronic levels) contribution to the spin-rotation parameter γ_ν is given by the interaction of the magnetic moment of the open shell electrons with the rotational magnetic moment of the molecule directed along $\mathbf{N}$. This can be thought of as an interaction akin to the spin-orbit interaction of the electronic spin with the nuclei. The second order term is given by electronic spin-orbit (electronic spin with electronic orbital angular momentum) perturbations which couple in excited states of Π-type symmetry. In heavy molecules, where Z is large for one or both atoms, this is the dominant term. It has the form [16]

$$\gamma_\nu^{(2)} = -2\sum_{\eta'} \frac{\langle \eta,\Lambda,\Sigma|B_\nu L_-|\eta',\Lambda+1,\Sigma\rangle\langle\eta',\Lambda+1,\Sigma|\sum_i a_i \mathbf{l}_i\cdot\mathbf{s}_i|\eta,\Lambda,\Sigma+1\rangle \;+\; \text{s.o.}}{(V_\eta - V_{\eta'})\langle S,\Sigma|S_-|S,\Sigma+1\rangle}, \tag{3.9}$$

where s.o. signifies switching the order of the individual electron spin-orbit operator $\sum_i a_i \mathbf{l}_i\cdot\mathbf{s}_i$ with the rotation operator $B_\nu\ L_-$. η is a stand-in for the other quantum numbers in the molecules. In Eq. 3.9 I have made explicit the dependence on the individual electrons. While the expectation value of the total orbital angular momentum is zero, the individual electrons can have orbital angular momentum and this allows

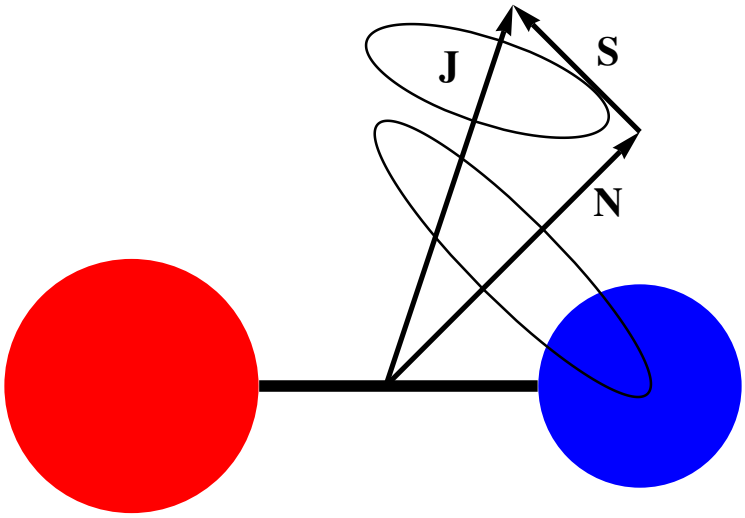

Figure 3.5: The Hund's case (b) coupling scheme vector diagram. The **S** and **N** vectors couple to make the **J**.

communication with excited electronic states via the spin-orbit interaction.

It is not easy to evaluate the matrix elements involving the orbital angular momentum raising and lowering operators $L_\pm$ and $l_{i\pm}$. If one of the atoms is vastly larger than the other, then an approximation can be made called the Van Vleck pure precession hypothesis [61]. The lighter atom is considered a pimple orbiting about the heavier atom and the electron of interest obeys spherical symmetry about the heavy atom. In this approximation, the raising and lowering operators act on atomic orbitals of the heavy atom.

There are significant corrections to the rotation and spin-rotation interactions that are worth addressing. Due to the precise nature of trying to measure an eEDM in a molecule, it is important to understand where tiny corrections can arise. A dominant contribution comes from the centrifugal distortion of the end-over-end rotation of the molecule. Physically, this is related to the stretching of the bond as the molecule rotates about its center of mass. In so doing, there will be corrections to the Hamiltonian presented in Eq. 3.8.

$$H_{(\mathrm{b})} = (B_\nu - D_\nu \mathbf{N}^2)\mathbf{N}^2 + (\gamma_\nu - \gamma_{D_\nu}\mathbf{N}^2)\mathbf{N}\cdot\mathbf{S}. \tag{3.10}$$

In general, any operator acting within the manifold of rotational states will have centrifugal distortions. The general distortion elements are obtained by successive orders of $\mathbf{N}^2$ acting. In the above equation, this is performed once. The value of D_ν is reduced from B_ν by a factor of the m_e/μ_{mol}, where μ_{mol} is the reduced mass of the molecule. This is easily seen from a Dunham-type expansion [62]. While this expansion has the isotopic dependence thoroughly worked out for singlet states [63], the general features of the reduced mass scaling in general hold for doublet states. The expansion of the potential for vibration and rotation terms is

$$E(\nu, J) \approx \sum_{kl} \mu^{-(k+2l)/2} U_{kl} (\nu + 1/2)^k \left(J(J+1) - \Lambda^2\right)^l, \tag{3.11}$$

where $\Lambda = 0$ for Σ molecules. The U_{kl} are isotopically invariant parameters of the interaction potential. Terms with $k = 0$ have no vibrational dependence at this level of theory. The term D_ν is related to the Dunham parameter U_{02} by a minus sign and scales as $(m_e/\mu_{\rm mol})^2$. Thus, for heavier molecules the distortion effects are small. γ_{D_ν} will scale in the same manner as D_ν. Therefore, the higher order distortion terms will be quite small. As an example, in YbF $\gamma_\nu = -13.4$ MHz, $\gamma_{D_\nu} = 4$ kHz, and $\gamma_{H_\nu} = 25$ Hz [64]. Each successive term in the series expansion reduces the interaction energy 2-3 orders of magnitude.

The matrix elements of the rotational Hamiltonian in Eq. 3.10 are given as follows:

$$\begin{aligned}\langle (N\ S)JM_J|H_{\rm (b)}|(N\ S)JM_J\rangle &= (B_\nu - D_\nu\ N(N+1))N(N+1) + (\gamma_\nu - \gamma_{D_\nu}N(N+1)) \times \\ &\quad (-1)^{N+J+S}\left\{\begin{array}{ccc} S & N & J \\ N & S & 1 \end{array}\right\}\Pi\left[S,N\right], \end{aligned} \tag{3.12}$$

where $\Pi\left[S,N\right] = \sqrt{S(S+1)(2S+1)N(N+1)(2N+1)}$. This Hamiltonian is diagonal in S, J, and N. M_J is the projection of J onto the laboratory fixed axis. The deconstruction of the elements into the form above takes advantage of the Wigner-Eckhart theorem. There are many standard references, of which the best are in Refs. [65, 66, 67]. In addition, many extremely useful examples are worked out in the book by Brown and Carrington [16].

The next energy scale to deal with in the spectroscopy is the hyperfine interactions of the F-nucleus with the spin S and rotation N. In the case of the F-bearing molecules in Table 2.4, all of the heavy atoms contain zero nuclear spin isotopes. Thus, the only terms in the hyperfine Hamiltonian to consider are ones where the F nuclear spin interacts with S and N.

$$H_{\rm HFS} = b_F\mathbf{I}\cdot\mathbf{S} - \sqrt{10}g_S\mu_B g_N\mu_N\left(\frac{\mu_0}{4\pi}\right)T^1(\mathbf{S},\mathbf{C}^2)\cdot T^1(\mathbf{I}). \tag{3.13}$$

In the second term, the notation T^1 signifies a first rank tensor. The interaction is the first rank tensor formed from the coupling of $\mathbf{S}$ with the second rank reduced spherical

harmonic $\mathbf{C}^2$ dotted into the first rank tensor of $\mathbf{I}$. To be clear, the term $T^1(\mathbf{S},\mathbf{C}^2)$ is given by

$$T^1_q(\mathbf{S},\mathbf{C}^2) = -\sqrt{3}\sum_{q_1,q_2}(-1)^q T^1_{q_1}(\mathbf{S})T^2_{q_2}(\mathbf{C}) \begin{pmatrix} 1 & 2 & 1 \\ q_1 & q_2 & -q \end{pmatrix}. \tag{3.14}$$

In other words, it is the electron-nuclear spin-spin dipolar interaction. The first term in Eq. (3.13) is the Fermi contact interaction. b_F depends on the amplitude of the wave-function at the F nucleus via

$$b_F = \frac{2}{3} g_S \mu_B g_n \mu_N \mu_0 \left|\Psi_\eta\right|^2, \tag{3.15}$$

where Ψ_ν is the wave function for the ν^{th} vibrational level. The matrix elements of the contact interaction are

$$\begin{aligned}\langle((NS)JI)FM_F|\mathbf{I}\cdot\mathbf{S}|((NS)J'I)FM_F\rangle &= (-1)^{2J'+F+I+N+1+S}\Theta[J,J']\Pi\left[I,S\right]\times \\ &\begin{Bmatrix} I & J' & F \\ J & I & 1 \end{Bmatrix}\begin{Bmatrix} S & J' & N \\ J & S & 1 \end{Bmatrix}\end{aligned} \tag{3.16}$$

$\Theta[J,J'] = \sqrt{(2J+1)(2J'+1)}$. The contact term preserves the values of F, N, and I but couples in differing values of J. Therefore, it modifies the $N=1$ level of the $^2\Sigma$ state by mixing in the two separate J values. The dipole coupling term can bring in states of differing Λ due to the $\mathbf{C}$ functions. However, concentrating on the Σ state alone, yields

$$\begin{aligned}\sqrt{10}g_S\mu_B g_N\mu_N\langle((NS)JI)FM_F|T^1(\mathbf{S},\mathbf{C}^2)\cdot T^1(\mathbf{I})|((NS)J'I)FM_F\rangle = \\ -\sqrt{30}t(-1)^{J'+F+I+N}\Pi\left[I,S\right]\theta[J,J',N,N']\times \\ \begin{Bmatrix} I & J' & F \\ J & I & 1 \end{Bmatrix}\begin{Bmatrix} J & J' & 1 \\ N & N' & 2 \\ S & S & 1 \end{Bmatrix}\begin{pmatrix} N & 2 & N' \\ 0 & 0 & 0 \end{pmatrix},\end{aligned} \tag{3.17}$$

where t is defined as

$$t = g_S\mu_B g_N\mu_N\left(\frac{\mu_0}{4\pi}\right)\left\langle\frac{3\cos^2(\theta)-1}{r^3}\right\rangle_\eta. \tag{3.18}$$

The parameters r and θ refer to distance of the electron from the F nucleus and the angle with respect to the molecular axis. η signifies that the expectation is taken for a particular vibrational level. This interaction can couple in states of different N and J while preserving S and I. Therefore, the ground rotational state $N = 0$ acquires a little of the same parity state $N = 2$ with the differing value of $J' = J + 1$. J can only differ from J' by one as can be seen via one the top row in the $9 - J$ symbol in Eq. 3.17.

In addition to these hyperfine effects, there is one other effect of interest. The nuclear spin can interact with the end-over-end rotation of the molecule $\mathbf{N}$. It takes the form of

$$H_{\mathrm{nRot}} = c_F \mathbf{I} \cdot \mathbf{N} \tag{3.19}$$

c_F is the strength of the interaction for the F nucleus. The elements of this interaction are simple enough to work out. However, a quick glance at the form of c_F will reveal that it is that the interaction is vastly smaller than the contact term. $c_F \sim g_r \mu_B g_N \mu_N$, where g_r is the rotational g factor and is reduced from g_S by the ratio m_e/μ_{mol}; therefore it is 3 orders of magnitude smaller than the interactions in Eqs (3.16) and (3.17).

Lastly, these experiments will be performed in electric and magnetic fields. It is therefore useful to know how these molecules will react to an applied field. The Zeeman interaction is dominated by the magnetic field manipulating the free electron. Another, smaller effect, comes from the magnetic moment of the molecular axis due to rotation. The electron spin-Zeeman interaction is of the form

$$H_{\mathrm{Z}} = g_S \mu_B T^1(\mathbf{B}) \cdot T^1(\mathbf{S}). \tag{3.20}$$

The matrix elements in the coupled representation $|((NS)JI)FM_F\rangle$ (N couples to S to

make J which in turn couples to I to make F)

$$\langle((NS)JI)FM_F|g_S\mu_B T^1(\mathbf{B})\cdot T^1(\mathbf{S})|((NS)J'I)F'M_F\rangle \tag{3.21}$$

$$= g_S\mu_B B_Z(-1)^{F-M_F+F'+2J+I+N+S}\Pi[S]\sqrt{(2J'+1)(2J+1)(2F'+1)(2F+1)} \times \begin{pmatrix} F & 1 & F' \\ -M_F & 0 & M_F \end{pmatrix} \begin{Bmatrix} F & J & I \\ J' & F' & 1 \end{Bmatrix} \begin{Bmatrix} J & S & N \\ S & J' & 1 \end{Bmatrix} .$$

The interaction does not preserve the value of F or J. Since B does not act on the molecular axis, N is unaffected. A simpler way to break this down would be to work in the basis $|NM_N SM_S IM_I\rangle$ since each individual spin interacts with the magnetic field. This would require a different decomposition of the matrix elements in the hyperfine interactions in Eqs.(3.16) and (3.17). However, in eEDM experiments it is usually requisite to have a small magnetic field. This ensures that systematics in the experiment do not contribute much error. Therefore, F is nearly a good quantum number and the completely coupled representation has its merits. A bonus that arises is that one can write down the effective magnetic g-factor in for a given F state.

$$g_F = \sqrt{6}(-1)^{F+2J+N+1}\Theta^2[F,J]\Pi[F] \tag{3.22}$$

$$\times \begin{Bmatrix} F & J & I \\ J & F & 1 \end{Bmatrix} \begin{Bmatrix} J & S & N \\ S & J & 1 \end{Bmatrix} , \tag{3.23}$$

where $\Theta^2[F,J] = (2F+1)(2J+1)$. This is how each level responds to a small applied magnetic field, small when compared to the hyperfine energy splitting.

There are two other magnetic interactions: nuclear moment and molecular rotation can each interact with the applied magnetic field. These interactions will be smaller by the ratio of the nuclear to Bohr magneton, but important in precision measurements. The rotational magnetic moment interacts with an applied field in the following manner

$$H_{\mathrm{Z,rot}} = -g_r\mu_B T^1(\mathbf{N})\cdot T^1(\mathbf{B}), \tag{3.24}$$

with matrix elements

$$\langle((NS)JI)FM_F| - g_r\mu_B T^1(\mathbf{N})\cdot T^1(\mathbf{B})|((NS)J'I)F'M_F\rangle \tag{3.25}$$

$$\begin{aligned} = \quad & -g_r\mu_B B_{\mathrm{Z}}(-1)^{F-M_F+F'+2J+I+N+S}\Pi\left[N\right]\Theta[J',J,F',F] \\ & \times \begin{pmatrix} F & 1 & F' \\ -M_F & 0 & M_F \end{pmatrix} \begin{Bmatrix} F & J & I \\ J' & F' & 1 \end{Bmatrix} \begin{Bmatrix} J & N & S \\ N' & J' & 1 \end{Bmatrix} \quad . \end{aligned}$$

The nuclear spin magnetic moment interacts with the magnetic field via

$$H_{\mathrm{Z,I}} = -g_I\mu_N T^1(\mathbf{I})\cdot T^1(\mathbf{B}), \tag{3.26}$$

yielding elements of the form

$$\langle((NS)JI)FM_F| - g_I\mu_N T^1(\mathbf{I})\cdot T^1(\mathbf{B})|((NS)J'I)F'M_F\rangle \tag{3.27}$$

$$\begin{aligned} = \quad & -g_r\mu_B B_{\mathrm{Z}}(-1)^{2F-M_F+J+I+1}\Pi\left[I\right]\Theta[F,F'] \\ & \times \begin{pmatrix} F & 1 & F' \\ -M_F & 0 & M_F \end{pmatrix} \begin{Bmatrix} F & I & J \\ I & F' & 1 \end{Bmatrix} \quad . \end{aligned}$$

The Stark effect is another matter. An electric field couples to the dipole moment of the molecule which is oriented along the molecular axis. Therefore, an electric field will act on N. However, the electric field will need to be rotated into the frame of the molecule (or vice versa) and this will bring in a new degree of complexity. However, a little patience and thought tells one that an interaction of the form

$$H_{\mathrm{S}} = -\mathbf{d}\cdot\mathcal{E}, \tag{3.28}$$

where $\mathbf{d}$ is the molecular electric dipole moment, will produce matrix elements of the form

$$\langle((NS)JI)FM_F| - \mathbf{d}\cdot\mathcal{E}|((N'S)J'I)F'M_F\rangle \tag{3.29}$$

$$\begin{aligned} = \quad & -d\mathcal{E}(-1)^{F-M_F+F'+J+J'+I+N+S}\Theta[J',J,F',F,N',N] \\ & \times \begin{pmatrix} F & 1 & F' \\ -M_F & 0 & M_F \end{pmatrix} \begin{Bmatrix} F & J & I \\ J' & F' & 1 \end{Bmatrix} \begin{Bmatrix} J & N & S \\ N' & J' & 1 \end{Bmatrix} \begin{pmatrix} N & 1 & N' \\ 0 & 0 & 0 \end{pmatrix} \quad . \end{aligned}$$

It is the last $3-J$ symbol that is of importance; unless $N+1+N'$ is even, this vanishes. Therefore, $N' = N \pm 1$. The Stark effect only couples in states of differing N, or opposite parity since the parity of a state is given by $(-1)^N$. Thus, in order to polarize the molecule, one must over come the splitting between adjacent N levels, or an energy of $2B(N+1)$. An energy of this size requires a polarizing electric field of at least

$$|\mathcal{E}_{\text{polarize}}| \gtrsim |\frac{2B}{d}|(N+1). \tag{3.30}$$

For the $^2\Sigma$ molecules in Table 2.4 this polarizing field ranges from a few to a few 10s of kV/cm. In exchange, one gets an $\mathcal{E}_{\text{eff}}$ of many GV/cm, thereby an enhancement of nearly 10^5, far better than in the atomic case.

When one accounts for all the above, measurements on the transitions between the various sub-levels can be accounted for in an accurate manner. For a $^2\Sigma$ molecule, one wants to measure the transition between a spin-up and a spin-down electron in parallel and anti-parallel electric and magnetic fields. Therefore, in a molecule like YbF, one needs to measure the transition $|F=1, M_F=1\rangle \rightarrow |F=1, M_F=-1\rangle$. This is because the spin of the electron and the spin of the nucleus are coupled, even in the presence of the strong electric field. A diagram is presented in Fig.3.6.

The magnetic fields serve to raise levels with $M_F > 0$ while electric fields push all M_N levels down, thus all M_F levels. In Fig. 3.6, the Stark shift is labeled by the blue lines. The red lines indicate the Zeeman shift, which only affects the $|M_F| = 1$ lines at first order. An eEDM acts on the spin degree of freedom and therefore in parallel fields it enhances (the purple lines) the Zeeman shift while in anti-parallel ($\mathcal{E}$ reversed from $\mathcal{B}$) fields it diminishes (the green lines) the Zeeman effect. One looks to measure the subtle frequency splitting between these two cases, as indicated by the transition W. The difference between parallel fields and anti-parallel fields leads to an expression $W^{\parallel} - W^{anti-\parallel} = 2d_e\mathcal{E}_{\text{eff}}$. However, small uncertainties in the ability to perfectly switch the alignment of the electric to magnetic fields will cause systematics.

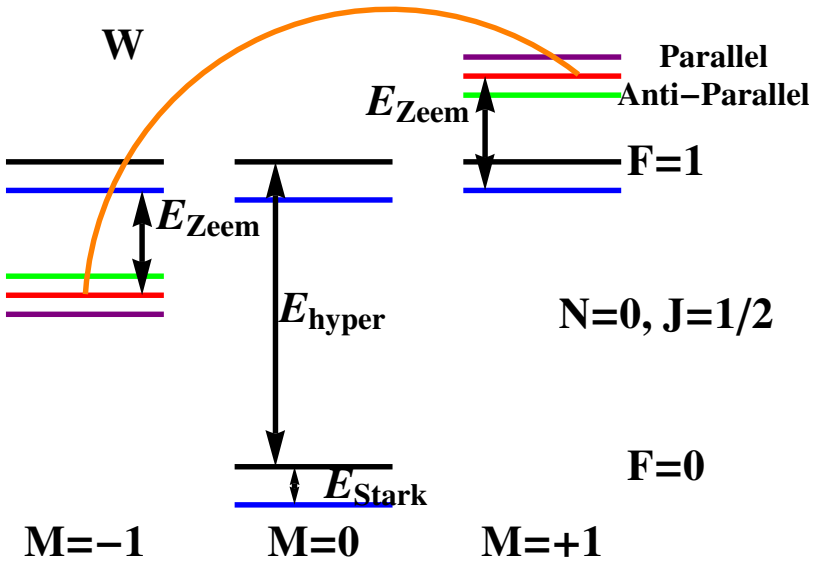

Figure 3.6: The basic hyperfine spectrum for the $N = 0$ rotational state of a $^2\Sigma$ molecule. The Stark shift is denoted by the blue lines while the red lines mark the Zeeman shift. In parallel (anti-parallel) fields the eEDM causes an energy shift labeled by the purple (green) lines. The transition labeled W and marked by an orange curve is of interest in an eEDM experiment. The frequency difference in parallel and anti-parallel fields is due to the eEDM.

Therefore, accurate magnetometers are requisite.

$^2\Sigma$ molecules are a very basic system to consider for an eEDM study. However, the fields required to polarize the molecules are still large. It takes several 10s of kV/cm to align many of these molecules in an external field. While these fields are attainable in a lab, the systematic effects can scale unfavorably. Often, smaller fields are applied and a hit is taken in the effective electric field since the molecule is only partially aligned, one gets some of the effective electric field due to averaging effects. Therefore, a look at systems that are easier to polarize is a natural extension. However, these systems are often composed of more than one valence electron. This causes a collection of electronic surfaces with which the able practitioner of *ab initio* methods much contend.

3.3 Δ-type molecules

Many of the molecules presented in Table 2.4 are not of $^2\Sigma$ symmetry. One of the first molecules to stray from the $^2\Sigma$ doctrine was PbO in the metastable $a(1)$ state [68]. This notation is already a bit different from the standard system. It refers to the first excited state of $\Omega = 1$. Here, Ω is the projection of the sum of orbital and spin angular momentum projections onto the molecular axis. In the case of PbO, only this sum is conserved. PbO in the $a(1)$ excited state is an example of a Hund's case (c) coupling scheme. Fig. 3.7 gives a semi-classical illustration of this scheme.

The reason for the preservation of Ω has to do with the large value of the spin-orbit interaction, which is large enough to overcome the electronic energy separation. In the case of PbO, the $^3\Sigma_1$ and $^3\Pi_1$ states are coupled by the spin-orbit interaction to form two $\Omega = 1$ states. These states are in turn comprised of orbital configurations. The $^3\Sigma_1$ state is primarily of a $\pi_1^\alpha\pi_2^\alpha$ configuration (where α corresponds to a spin-up electron along the internuclear axis), which would nominally be of zero help to an eEDM search. However, there are admixtures of the $\sigma_1^\alpha\sigma_2^\alpha$ configuration when one allows for configuration interaction effects as described in the MCSCF and MRCI calculations in

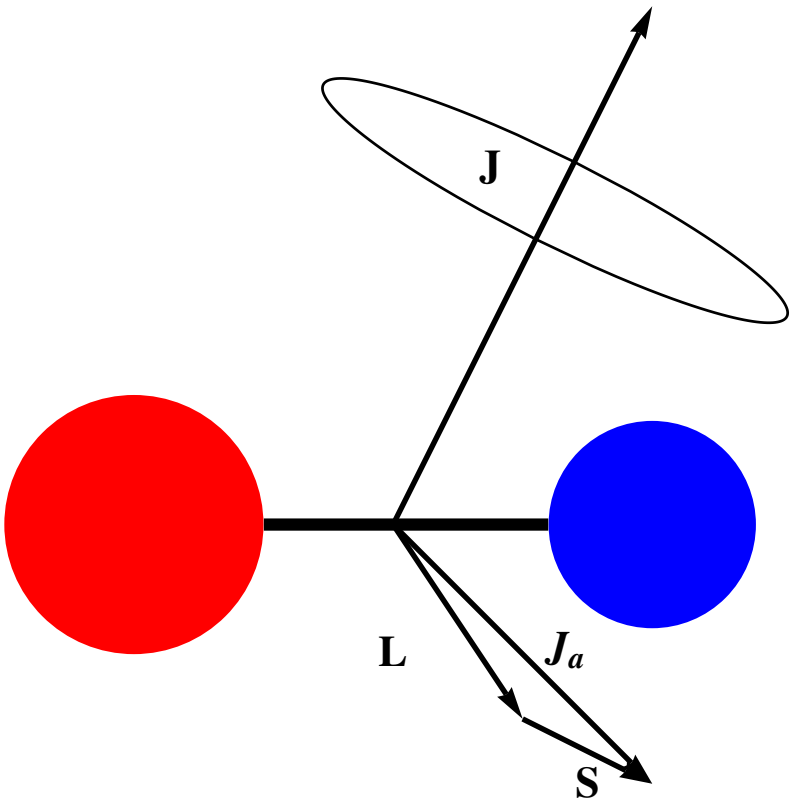

Figure 3.7: The Hund's case (c) coupling scheme vector diagram. The **J** and $\mathbf{J_a}$ vectors each have projection Ω onto the molecular axis. In this case L and S interact so strongly with each other that they overcome the electronic energy separation.

Sec. 3.1. The latter configuration can be very useful in an eEDM search since there are two electrons in distinct σ molecular orbitals. Because the electrons are in distinct orbitals, each can contribute to the calculation of $\mathcal{E}_{\text{eff}}$.

The $^3\Pi_1$ state is composed of a $\pi_1^\alpha\sigma_2^\alpha$-type configuration. This configuration interacts via spin-orbital effects with both of the $^3\Sigma_1$ configurations. The end result is that individual electron spins and orbital angular momenta are inadequate to describe the system. Only the total projection will suffice. The methods outlined in Chapter 2 are applicable so long as one accounts for the contributions from the $^3\Sigma_1$ and $^3\Pi_1$ states individually and appropriately adds them together.

A chief advantage of the metastable PbO system is that it is far easier to polarize than the $^2\Sigma$ system. A phenomenon known as Λ- or Ω-doubling allows the coupling of states of $+|\Omega|$ and $-|\Omega|$, and in the absence of electric fields this coupling forces two states to emerge: the symmetric and anti-symmetric combinations of $|+|\Omega|\rangle$ and $|-|\Omega|\rangle$. Therefore, there is no net orientation of the molecule in the absence of an applied field and therefore no permanent dipole moment. However, this interaction produces an energy difference between states of opposite parity that is considerably less than the rotational splittings of $^2\Sigma$ molecules.

It is the metastable nature of PbO that makes it a tough candidate to work with. It favors rapid decay to the ground state, a state with little to no favorable eEDM characteristics. However, the push to move away from molecules of $^2\Sigma$ flavor had begun. Quickly $^2\Pi$ molecules like HI^+ [28, 40] and PbF [38] were proposed and re-studied for their applicability in eEDM searches. The former were found to be inefficient due to their dominant π-molecular orbital characteristics. However, PbF exhibited strong case (c) type couplings and the mixing of the $^2\Sigma_{1/2}$ with the $^2\Pi_{1/2}$ leads to applicability in an eEDM search. Then a couple of rogue theorists proposed $^3\Delta_1$ molecules for eEDM searches [28]. It was found that the $^3\Delta$ molecules have very favorable Λ-doubling (as will be discussed in Sec. 3.3.2 and arise chiefly from a $\sigma^\alpha\ \delta^\alpha$ configuration. In fact, the

σ-orbital gives the science signal while the δ-orbital makes it easily polarizable. Now it is time to learn more about these fascinating $^3\Delta$ creatures.

3.3.1 Structure

Unlike molecules of the fluoride and alkali-metal variety of the previous sections, $^3\Delta$ molecules are a whole other beast. $^3\Delta$ molecules formed by one atomic d and one atomic s orbital are of interest since they most easily lead to $\sigma^\alpha\delta^\alpha$ configurations. Since d-electrons are of interest one is immediately led to consider transition row elements. Because of large Z favoring, the 3rd row transition metals are ideal. It is here that atoms with the proper characteristics are found. For the purposes of this section the discussion will follow ThF^+ because there is no published work on the molecule[2] as well as HfF^+, because this is being pursued in house at JILA.

Th is a very heavy ($Z = 90$) element in the lanthanide row. Hf is also heavy ($Z = 72$). The thing these two atoms have in common is their atomic ground state, which is comprised of $5d^2\ 6s^2$ for Hf and a $6d^2\ 7s^2$ for Th. By once ionizing and pairing with an F atom, the possibility of an atomic configuration ds on Hf and Th arises, the other electron being whisked away by the ever electronegative F atom. However, there are two other possibilities for the remaining electrons: they can occupy an s^2 or a d^2 configuration. Neither of these is really amenable to an eEDM search without mixing of configurations. Thus, it remains a job for *ab initio* methods to understand the electronic properties.

When there are multiple electrons to consider, then one must use the information given in the prior paragraph to approach the *ab initio* problem efficiently. Namely, the expected atomic configurations are only valid in the region where F is close enough to capture an electron from the heavy atom. Second, the remaining atomic orbitals can be used to predict the dominant molecular orbital configurations. For instance, the

[2] Therefore, this is new material with which to whet your knowledge appetite

s^2 configuration will lead to a σ^2 molecular orbital and hence a $^1\Sigma$ electronic state. However, the sd atomic configuration will lead to $\sigma\delta$, $\sigma\pi$, and $\sigma\sigma'$ configurations, which in turn lead to electronic symmetries $^{1,3}\Sigma$, $^{1,3}\Pi$, and $^{1,3}\Delta$. σ' is the σ-molecular orbital formed by the d electron. The d^2 configuration will lead to a slew of possible states ranging from symmetries similar to those given as well as $^1\Gamma$ and $^{1,3}\Phi$. As is evident, this is many more states than was dealt with in the $^2\Sigma$ molecules. What remains to be see is whether the $^3\Delta$, the one portended to be very useful for eEDM searches, is a viable electronic state for the eEDM search.

In order to calculate the potential energy surfaces of the ThF^+ and HfF^+ molecules I employed the use the MOLPRO suite of codes [45]. The RHF-MCSCF+SO-MRCI method was used at various points in the internuclear separation to determine the ground state [48, 49, 53, 54]. The RHF was performed starting at the atomic densities and finding the wave function for the $^1\Sigma$ arising from the $(s\sigma)^2$ configuration, where the s refers to the Th or Hf s atomic orbital as the dominant contribution to the molecular orbital σ.

After performing the RHF, the MCSCF was gradually built up to include the $^1\Sigma$, $^3\Delta$, $^1\Delta$, $^3\Pi$, $^1\Pi$, $^3\Sigma^+$, and the $^3\Sigma^-$. The last state arises from the $(\delta)^2$ configuration. It was determined that including the $^1\Gamma$, $^1\Phi$, $^3\Phi$ was necessary to converge the lower states. The MRCI calculation was performed separately within each spin and space symmetry group, with the reference spaces of the other spatial symmetries present. This allowed for convergence of Δ, Π, and Γ states which have degeneracies within two spatial groups. This approach is to be contrasted with the previous work on HfF^+ [41]. In that paper only the states arising from the σ^2 and $\sigma\delta$ configurations were studied. The inclusion of the $^3\Sigma^-$ state affects the other $\Omega = 1$ levels arising from the $^{1,3}\Pi_1$ states because the $^3\Sigma^-$ exists in the same energy range as the $^{1,3}\Pi_1$.

In order to account for spin-orbit effects, I employed the fully relativistic effective core potentials (ECP) and triple zeta basis sets of the Stuttgart group for Hf [69] and the

quasi-relativistic (scalar terms only) ECP and segmented basis set for Th [70, 71, 72]. These account for the relativistic effects associated with spin-orbit coupling. It separates out the various Ω sub-levels of a symmetry, e.g. $^3\Delta \rightarrow\ ^3\Delta_1$, $^3\Delta_2$, and $^3\Delta_3$. From this point in the calculation the best determination of the appropriate Hund's case can be made.

To account for the polarizability of the atoms I included in the active space the next-lying atomic p-orbital, i.e. $6p$ for Hf. After each MRCI calculation a spin-orbit (SO) calculation was performed that included all the calculated states and provided mixing amongst the levels with the same value of Ω. The results of the potential energy surface (PES) calculation are presented in Fig. 3.8. As is clearly seen in the figure, the ground state is difficult to declare because it lies within the uncertainty (a few hundred cm^{-1} is a conservative estimate) of the *ab initio* methods. However, given comparison to the known ThO (isoelectronic to ThF^+) electronic levels and a similar calculation's ability[3] to reproduce the lifetime of the metastable $^3\Delta_1$ state, there is confidence in calling the $^1\Sigma_0$ state the ground electronic state.

The admixture of various other $\Omega = 1$ values into the $^3\Delta_1$ state is rather minimal. It is found that most ($\geq 95\%$) is due to the $^3\Delta_1$ and therefore Hund's case (a) quantum numbers are appropriate for describing these $^3\Delta$ systems.

Since it is expected that the ground state may turn out to be the $^1\Sigma_0$ in both HfF^+ and ThF^+, it is instructive to estimate the lifetime of the excited $^3\Delta_1$ state. Nominally, this state would never decay because it needs to change Λ by two units and S by one unit. However, Λ and S are not preserved under the influence of spin-orbit effects. Thus, the admixture of $^1\Pi_1$ into the $^3\Delta_1$ allows for spontaneous emission from $^3\Delta_1 \rightarrow\ ^1\Sigma_0$. I find about a 2% admixture of the $^1\Pi_1$ in both HfF^+ and ThF^+. Using the energy difference between the minima of the respective curves, I obtain a lifetime

[3] I performed the same calculation at the known bond length of ThO in the $^1\Sigma$ state and used the transition moments calculated from the $^3\Delta_1$ state to find the lifetime. I obtained a few ms, and recently the ACME collaboration has measured the lifetime to be ~ 1.8 ms [73]

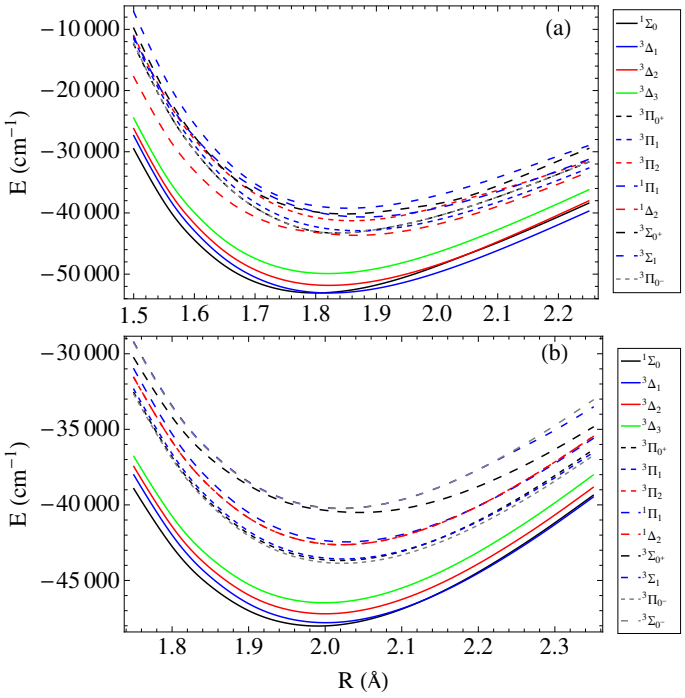

Figure 3.8: Results of the many state calculation on HfF^+ (a) and ThF^+ (b) at the RHF-MCSCF+MRCI+SO level of theory.

on the order of seconds for these two molecules, more than enough time to make a measurement in an ion trap.

3.3.2 Spectroscopy

Given the analysis of the $^3\Delta$ states in Sec. 3.3.1, it is apparent that the electronic state is separated well enough in energy from electronic states with the same value of Ω to be described by a set of Hund's case (a) quantum numbers. These numbers are the total angular momentum *sans* hyperfine J, the total electronic spin S, the projections of orbital and spin angular momentum onto the molecular axis Λ and Σ, the sum of $\Lambda + \Sigma = \Omega$, and in the presence of fields the projection of J onto the axis defined by the field M_J. We will return to the case of hyperfine interactions later in this section. Fig. 3.9 gives a visual of the vector diagram describing Hund's case (a).

While L is drawn in the figure, the value of L is ill-defined due to the lack of spherical symmetry. In some cases, having a defined L is a good approximation, but it must be noted that it is merely that, an approximation. Much of the spectroscopy I will discuss is built from the idea of approximation as a way to guide intuition. Along these lines, various contributions to the spectroscopic Hamiltonian used in analyzing Δ molecules will be discussed.

The first, and most important, is the new energy scale introduced by the non-zero value of L and S. The interaction of L with S induces a splitting between states of different Ω. In the HfF^+ molecule, the splitting between $\Omega = 1$ and $\Omega = 2$ is 1200 cm^{-1}. The splitting between $\Omega = 2$ and $\Omega = 3$ is 1900 cm^{-1}. The reason behind the asymmetry will be dealt with shortly. The main idea to take away is the energy scale. States within the same electronic symmetry are separated by about thousand or so cm^{-1}. Contrast and compare this with the rotational energy splittings of $^2\Sigma$ molecules of 0.1–10 cm^{-1}. This new energy scale will be important in understanding the nature of parity splittings.

The simplest way to construct the interaction is to only consider the diagonal

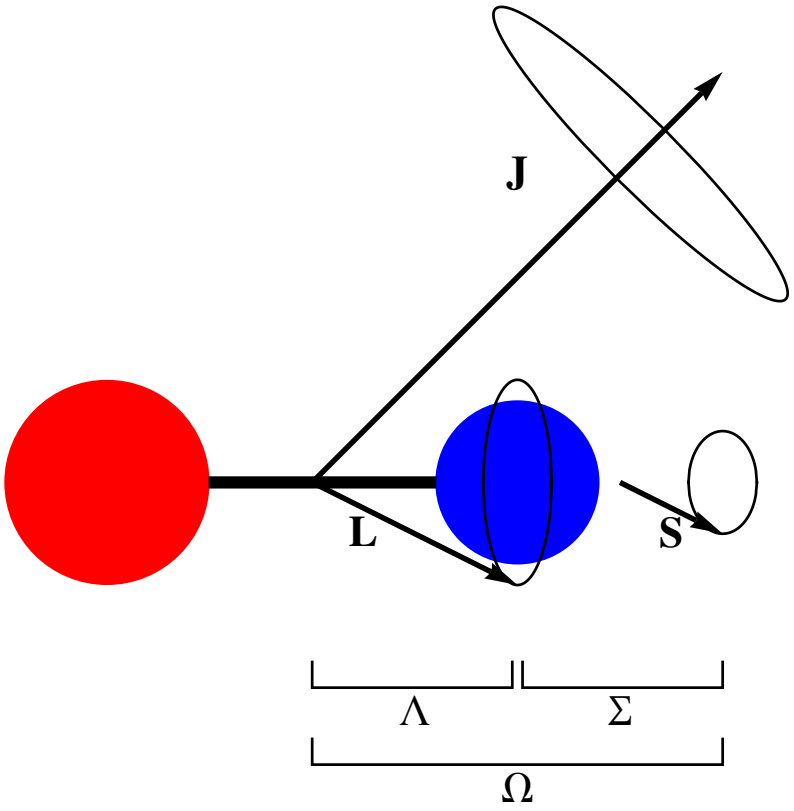

Figure 3.9: The Hund's case (a) coupling scheme vector diagram. The $\mathbf{J}$ and $\mathbf{L}+\mathbf{S}$ vectors each have projection Ω onto the molecular axis. In this case $\mathbf{L}$ and $\mathbf{S}$ interact with the molecular axis as well as with each other.

contribution to the interaction due to the non-sphericity of a diatomic molecule. On the diagonal the contribution from spin-orbit is

$$H_{\rm SO} = A\Lambda\Sigma + \frac{2\lambda}{3}(3\Sigma^2 - \mathbf{S}^2), \tag{3.31}$$

where A is the spin-orbit constant and λ is the electronic spin-dipolar interaction. From the *ab initio* calculation A is about 790 cm^{-1}. Since Hf is much heavier than F, the spin-orbit contribution to the molecular case is dominated by the contribution from the Hf atom. Assuming that the orbital angular momentum l of the d electron from Hf is a good quantum number, then the Van Vleck approximation [61] can be used to calculate the molecular spin-orbit constant.

Using wave functions in terms of Hund's case (a) quantum numbers (labeled by $|\Lambda; S, \Sigma; J, \Omega\rangle$ with $J \geq \Omega$), the energy separation in the molecule can be compared to the atomic system. In terms of Slater determinants, the molecular wave functions are:

$$\begin{aligned} |^3\Delta_3\rangle &= |2; 1, 1; J, 3\rangle & (3.32)\\ &= |d\delta^\alpha s\sigma^\alpha| \\ |^3\Delta_2\rangle &= |2; 1, 0; J, 2\rangle & (3.33)\\ &= \frac{1}{\sqrt{2}}(|d\delta^\alpha s\sigma^\beta| + |d\delta^\beta s\sigma^\alpha|) \\ |^3\Delta_1\rangle &= |2; 1, -1; J, 1\rangle & (3.34)\\ &= |d\delta^\beta s\sigma^\beta|. \end{aligned}$$

The spin-orbit energy shift for the $^3\Delta_3$ is then

$$\begin{aligned} \langle^3\Delta_3|AL_zS_z|^3\Delta_3\rangle &= 2A & (3.35)\\ \langle|d\delta^\alpha s\sigma^\alpha||a(l_1^z s_1^z + l_2^z s_2^z)||d\delta^\alpha s\sigma^\alpha\rangle &= a(2(1/2) + 0(1/2)) \\ &= a. & (3.36) \end{aligned}$$

Now apply the total spin lowering operator (given by $S_- = \sum_i s_i^-$) to Eq. (3.32) to obtain the $^3\Delta_2$ state. Since the projection of Σ is zero, there is no shift. Therefore,

the molecular spin-orbital constant A is half the atomic spin-orbit constant a, seen by comparing Eq. (3.35) with Eq. (3.36). In Hf, this method would predict a molecular spin-orbit constant of $A_{\text{expec}} = 610$ cm^{-1} (obtained via the spectroscopic information in the Moore tables on Hf^+ for the d-electron [74]), which is not too far from the *ab initio* value.

The discrepancy in the energy difference between the three Ω levels has to deal with the fact that the individual electron spin-orbit interaction will couple Slater determinants with $^1\Delta_2$ and $^3\Delta_2$, thereby creating an interaction between the spins; the effect of λ. The singlet state is given by

$$\begin{aligned} |^1\Delta_2\rangle &= |2;1,0;J,2\rangle \\ &= \frac{1}{\sqrt{2}}(|d\delta^\alpha s\sigma^\beta| - |d\delta^\beta s\sigma^\alpha|). \end{aligned} \tag{3.37}$$

The interaction of the atomic spin-orbit constant between the singlet and triplet configurations leads to the estimation of λ. Were the electronic energy separation comparable to the atomic spin-orbit constant, then Hund's case (c) would apply. Since the $^1\Delta_2$ state is over 8000 cm^{-1} away an estimate of the magnitude by which the singlet state pushes down the triplet state via second order perturbation theory can be made. Thus the $^3\Delta_2$ is expected to be pushed down by the $^1\Delta_2$ an amount 260 cm^{-1} whereas the *ab initio* calculation shows it deviates from the expected value by about 360 cm^{-1}. Thus, $|\lambda| \approx 250$ cm^{-1}.

For a $^3\Delta$ molecule, there are quite a few terms in the spectroscopic Hamiltonian. A simple basis is preferred even though the interactions are not necessarily simple. The idea of an effective Hamiltonian, which was used for $^2\Sigma$ molecules earlier, is extremely useful in this case. Firstly, one only wished to include terms which act in the manifold of $^{2S+1}\Delta_\Omega$ states, i.e. interactions that account for the vast array of possible effects but only serve to act within the $^{2S+1}\Delta_\Omega$ parameter space. Therefore, these interactions may change the value of Ω, connect $-|\Lambda|$ to $+|\Lambda|$, and change the value of J, but they will

only do so in such a way as can be described in the basis set $|\Lambda; J\Omega, S\Sigma\rangle$.

The end-over-end rotation of the molecule is described by

$$H_{\mathrm{Rot}} = B(\mathbf{J} - \mathbf{S})^2 + \gamma(\mathbf{J} - \mathbf{S}) \cdot \mathbf{S}, \tag{3.38}$$

In Eq. (3.38) the terms $(\mathbf{J} - \mathbf{S})$ are the equivalent of $\mathbf{N}$ in the $^2\Sigma$ case. In case (a), $\mathbf{N}$ is not a good quantum number. In fact, states with $\mathbf{N}$ differing by unity (but with the same value of $\mathbf{J} - \mathbf{S}$) can be very close in energy. These are related to the phenomenon of Λ-doubling.

Λ-doubling arises from the Coriolis coupling due to the end-over-end rotation of the molecule. States with differing values of L are mixed. Recall the form of the spin-rotation operator in Eq. (3.9). Now consider a Π state and couple in an excited Σ state through the perturbative expansion in (3.9). The interaction returning to the Π state can connect to a state with the same value of $\Lambda = +1$ (which gives the spin-rotation parameter for the Π state), or can connect to the Π state with $\Lambda = -1$. In the latter case a term which couples states of $+|\Lambda|$ to those with $-|\Lambda|$ arises. Therefore, in the absence of an applied electric field, the ground states will be symmetric and antisymmetric combinations of $\pm|\Lambda|$.

In a Δ state, Λ-doubling cannot happen at second order in perturbation theory because a Σ state with $\Lambda = 0$ cannot be coupled in. Therefore, in a perturbative treatment, one will need 4^{th}-order perturbation theory. The mixing caused by this approach will depend on the energy separation of the Δ state from both Π and Σ states.

Recall from Fig. 3.8 that the approximate separation of the electronic states of interest is known. The general process to find the number of parameters is to take an expansion of the sum of H_{Rot} and H_{SO} raised to the $2|\Lambda|$ power. To do so, there will need to be $2|\Lambda| - 1$ energy denominators. In what follows, the first line is a schematic

and the second line is the result after simplifications (see Refs. [16, 75] for more details)

$$\begin{aligned} H_{\Lambda\mathrm{D}} &\propto (H_{\mathrm{Rot}} + H_{\mathrm{Spin}})^{2|\Lambda|}/(\Delta E)^{2|\Lambda|-1} \\ H_{\Lambda\mathrm{D}} &= \frac{1}{2}\tilde{q}_\Delta(J_+^4 + J_-^4) - \frac{1}{2}\tilde{p}_\Delta(J_+^3 S_+ + J_-^3 S_-) + \frac{1}{2}\tilde{o}_\Delta(J_+^2 S_+^2 + J_-^2 S_-^2) - \\ &\quad \frac{1}{2}\tilde{m}_\Delta(J_+ S_+^3 + J_- S_-^3) + \frac{1}{2}\tilde{n}_\Delta(S_+^4 + S_-^4). \end{aligned} \tag{3.39}$$

The last two terms on the bottom line of Eq. (3.39) are irrelevant for $^3\Delta$ molecules because they flip the spin projection Σ beyond the maximal/minimal values and therefore annihilate the state. Each operator is such that $(\Delta\Omega + \Delta\Sigma) - \Delta\Lambda = 0$. For example, the $\tilde{o}_\Delta$ is an operator which takes $\Omega = 1 \rightarrow \Omega = -1$. For the $^3\Delta_1$ states of interest for an eEDM search, this is the operator which causes a direct splitting between the symmetric and antisymmetric combinations of $\pm|\Lambda|$ states. The operators $\tilde{p}_\Delta$ and $\tilde{q}_\Delta$ connect states with $\Delta\Omega = \pm 3$ and ± 4 and therefore affect the $^3\Delta_1$ state via higher orders in perturbation theory.

Expressions for $\tilde{o}_\Delta$, $\tilde{p}_\Delta$, and $\tilde{q}_\Delta$ are given by [75]

$$\tilde{o}_\Delta = 4\sqrt{30}\frac{V_A V_A V_B V_B}{\Delta E_1 \Delta E_2 \Delta E_3} \begin{Bmatrix} S & S & 2 \\ 1 & 1 & S' \end{Bmatrix} \frac{(2S-2)!}{(2S+3)!} \tag{3.40}$$

$$\tilde{p}_\Delta = 4\sqrt{35}\frac{V_A V_B V_B V_B}{\Delta E_1 \Delta E_2 \Delta E_3} \tag{3.41}$$

$$\tilde{q}_\Delta = 8\frac{V_B V_B V_B V_B}{\Delta E_1 \Delta E_2 \Delta E_3}, \tag{3.42}$$

where $V_{A(B)}$ is the matrix element of the spin-orbit (rotational) Hamiltonian between differing states. $\langle ^3\Delta_1 | AL_- | ^3\Pi_1 \rangle$ is an example of V_A, whereas $\langle ^3\Delta_1 | BL_- | ^3\Pi_0 \rangle$ is an example of V_B. The ΔE_i are the energy differences between the state of interest and the intermediate states. For a $^3\Delta$ state built from s and d atomic orbitals, the number of Π and Σ states is limited to a few. The sum is fairly straightforward to calculate. In HfF^+, the $\Omega = 1$ state is of concern, and it is governed by the $\tilde{o}_\Delta$ parameter. E_{doub} is

thus (recall that $J = 1$ in the ground state)

$$\begin{aligned} E_{doub}^{\Omega=1} &= 2\tilde{o}_{\Delta} J(J+1) \\ &\approx \frac{\frac{8}{6\times 5!}\sqrt{30}A^2B^2}{(E_{^3\Delta} - E_{^3\Pi})^2(E_{^3\Delta} - E_{^1\Sigma})} J(J+1)\epsilon_d^2 \\ &= 2\times 10^{-7}\ \mathrm{cm}^{-1}. \end{aligned} \tag{3.43}$$

Using methods similar to the polarizing field in Eq. (3.30), one can write

$$\mathcal{E}_{\mathrm{polarize}} \gtrsim \frac{E_{doub}^{\Omega=1}}{d_{\mathrm{mol}}}, \tag{3.44}$$

which leads to an $\mathcal{E}_{\mathrm{polarize}} \approx 50$ mV/cm. The value of $d_{\mathrm{mol}} = 4$ Debye obtained via the MOLPRO calculations is used. In HfF^+ the splitting between states of opposite parity in the ground $J = 1$ level is $\omega_{\mathrm{ef}} = 4\tilde{o}_{\Delta} = 10$ kHz. It should be noted that this is including the $^1\Sigma$ state which is actually dominated by the atomic s^2 configuration. Thus, the estimate includes a reduction which arises from the mixing of d_0 contributions into the s^2 state, which is accounted for by the presence of ϵ_d in Eq. (3.43). There are two powers of ϵ_d because it appears twice in the summation; once for each appearance of $^1\Sigma$.

3.3.3 Hyperfine interactions in $^3\Delta_1$ molecules

Because Fluorides are present again, there will be hyperfine structure. Being a bit more complicated because of the orbital motion, there are three terms, two of which are similar to $^2\Sigma$ molecules given in Eq. (3.13). Because there is orbital angular momentum, a new term $\propto \mathbf{I}\cdot\mathbf{L}$ is present.

$$H_{\mathrm{HFS}} = \aleph\vec{\mathbf{I}}\cdot\vec{\mathbf{L}} + b\vec{\mathbf{I}}\cdot\vec{\mathbf{S}} + cI_zS_z. \tag{3.45}$$

The term with $\aleph$ is the orbital angular momentum interacting with the nuclear spin. I've included a simplified form of the contact and spin-dipolar interactions from Eq. (3.13). Due to the expected strong Hund's case (a) nature of these molecules, spectroscopic measurements will not identify individual parameters in the above equation, instead

only finding the net energy shift

$$\langle \dots | H_{\rm HFS} | \dots \rangle = (\aleph\Lambda + (b+c)\Sigma)\Omega = h_\Omega. \tag{3.46}$$

$|\dots\rangle$ signifies a state with the relevant quantum numbers of interest. Note that changing $\Omega \to -\Omega$ implies $\Sigma \to -\Sigma$ and $\Lambda \to -\Lambda$ therefore leaving this expression invariant, as it should be in order to be time-reversal invariant. In the limit of pure case (a), there are no Ω changing operators. However, given enough measured transitions, it is possible to assign values to $\aleph$, b, and c in the hyperfine Hamiltonian. For clarity, the relation of b to b_F is given by $b_F = b + (1/3)c$. b_F absorbs part of the spin-dipolar coupling into it's definition. It is a little easier to deal with in the $^3\Delta$ molecules. In addition, the spin-dipolar term has been greatly simplified with many of the constants being lumped into c.

Because there exists a term proportional to $\vec{\mathbf{I}} \cdot \vec{\mathbf{L}}$ in Eq. (3.45), one may ask whether it can contribute to terms similar to the Λ-doubling Hamiltonian; the answer is yes. In order to see the origin of the exact terms an expansion is needed. Note that the hyperfine interaction is smaller than the spin and rotation interactions since it is reduced by a factor proportional to μ_N/μ_B, the ratio of the nuclear to Bohr magneton. Thus, a perturbative approach can be taken akin to the method used to find the Λ-doubling terms. Once again, $4^{\rm th}$-order perturbation theory is required to connect $\Lambda = \pm 2$ to $\Lambda = \mp 2$. Thus

$$H_{\rm P.E.} \propto ((H_{\rm Rot} + H_{\rm Spin}) + H_{\rm HFS})^{2|\Lambda|}, \tag{3.47}$$

where P.E. refers to perturbative expansion and terms that involve the first power of $H_{\rm HFS}$ are kept. Because terms proportional to $H^2_{\rm HFS}$ are going to be even smaller, they are ignored. The first term in the expansion of Eq. (3.47) is just the usual Λ-doubling Hamiltonian as in Eq. (3.39), so it has already been worked out. The next term is

$$H_{\rm HFS\Lambda D} \propto 2|\Lambda| H_{\rm HFS} (H_{\rm Rot} + H_{\rm Spin})^{2|\Lambda|-1} / (\Delta E)^{2|\Lambda|-1} / (\Delta E)^{2|\Lambda|-1}. \tag{3.48}$$

In spectroscopic terms this yields an expression of the form

$$H_{\mathrm{HFS}\Lambda\mathrm{D}} = \frac{1}{2}c_\Delta(J_+^3 I_+ + J_-^3 I_-) - \frac{1}{2}d_\Delta(J_+^2 I_+ S_+ + J_-^2 I_- S_-) + \frac{1}{2}e_\Delta(J_+ I_+ S_+^2 + J_- I_- S_-^2) - \frac{1}{2}f_\Delta(I_+ S_+^3 + I_- S_-^3). \tag{3.49}$$

Here the notation I_+ and I_- is used to indicate the raising and lowering operators of I that act on the internuclear axis. Therefore, I_+ and I_- raise and lower the value of Ω because I couples to J.

Of the four terms in (3.49), only the d_Δ term has been previously published, in a study of the NiH molecule where there is a curiously large Λ-doubling for a Δ electronic state [76, 77]. From what is known, the remaining three terms are new. The simple explanation for the algebra that leads to the expression in (3.49) is that since $I_\pm$ acts on the internuclear axis projection, one merely is swapping instances of the interaction $BL_\pm$ with $\aleph L_\pm$, or replacing one instance of the rotational Hamiltonian with the hyperfine orbital Hamiltonian. Therefore, the term e_Δ can be written as a perturbative sum in a manner similar to $\tilde{o}_\Delta$ in Eq. (3.40). Note that there are many ways in which to permute this interaction, three times more than ways in which one can permute the regular Λ-doubling interaction.

Using this, the expectation for the size of the hyperfine Λ-doubling parameters can be expressed in terms of their regular Λ-doubling counterparts. The four terms c_Δ, d_Δ, e_Δ, and f_Δ can be related to the terms $\tilde{q}_\Delta$, $\tilde{p}_\Delta$, $\tilde{o}_\Delta$, and $\tilde{m}_\Delta$. Thus

$$c_\Delta \approx -2\frac{\aleph}{B}\tilde{q}_\Delta, \tag{3.50}$$

$$d_\Delta \approx -\frac{3}{2}\frac{\aleph}{B}\tilde{p}_\Delta, \tag{3.51}$$

$$e_\Delta \approx -\frac{\aleph}{B}\tilde{o}_\Delta, \tag{3.52}$$

$$f_\Delta \approx -\frac{1}{2}\frac{\aleph}{B}\tilde{m}_\Delta. \tag{3.53}$$

The minus sign is due to the replacement of $-2BL_\pm$ with $\aleph L_\pm$. There is no term proportional to $\tilde{n}_\Delta$ because this parameter contains only terms which raise and lower

on Σ. Now, since $\aleph$ is not an easily determinable parameter in a pure Hund's case (a) molecule, either many measurements are needed, or this scaling relation is to be treated as very approximate. If one can measure the term h_Ω (c.f. Eq (3.46)) for both $^3\Delta_1$ and $^3\Delta_3$, the average will yield a value of $\aleph$. In addition, measuring h_2 in the $^3\Delta_2$ state will give the value of $\aleph$ as well since $\Sigma = 0$ in that state. Therefore $\aleph = h_2/2 = (h_1 + h_3)/4$. The ability of the terms in Eqs. (3.50)–(3.53) to predict the size of the interaction can be seen in NiH. There, $(h_{3/2} + h_{5/2})/4 = 22.8$ MHz and $\tilde{p}_\Delta = 188.6$ MHz. This would yield a prediction for $d_\Delta = -0.03$ MHz. The measured value is $d_\Delta = 0.8(1)$ MHz. As is evident, this estimate is off by more than an order of magnitude and has the wrong sign. The discrepancy is hard to locate since the experimental work is not entirely positive about the assignment of d_Δ. However, NiH is a rather complicated molecule in the sense that there are many d electrons to account for. This complicates the perturbative calculations. In HfF^+, there is only one d electron and this simplifies the number of electronic states to consider. Thus, the scaling rule developed in Eqs. (3.50)–(3.53) is expected to be a better predictor.

3.3.4 $^3\Delta_1$ molecules in electric and magnetic fields

$^3\Delta_1$ molecules are interesting. Because N is no longer a good quantum number, the electric and magnetic fields will both act on J, the sum of N and S. I will separate the electric and magnetic interactions in what follows.

3.3.4.1 Electric fields

I now turn to the calculation of the application of electric and magnetic fields. First, I will address the Stark effect. As in the case of $^2\Sigma$ molecules, the Stark effect acts along the internuclear axis. However, N is not a good quantum number. Thus, the electric field acts on J. The form of the interaction is the same as in Eq. (3.28). The

matrix elements are

$$\begin{aligned}\langle \eta J\Omega IFM_F| -\mathbf{d}\cdot\mathcal{E}|\eta J'\Omega' IF'M_F\rangle &= -d\mathcal{E}(-1)^{F-M_F+F'+2J+1+I-\Omega}\Theta[J,J',F,F']\times \\ &\begin{pmatrix} F & 1 & F' \\ -M_F & 0 & M_F \end{pmatrix}\begin{pmatrix} J & 1 & J' \\ -\Omega & 0 & \Omega \end{pmatrix} \\ &\times\begin{Bmatrix} J' & F' & I \\ F & J & 1 \end{Bmatrix},\end{aligned} \tag{3.54}$$

where $\Theta[J,J',F,F']$ is the same as in Eq. (3.16). This interaction preserves the value of Ω and M_F. In fact, this would seem to imply a linear Stark shift since $\begin{pmatrix} J & 1 & J' \\ -\Omega & 0 & \Omega \end{pmatrix} \propto \Omega$ when $J = J'$. However, in the presence of the interactions in Eq. (3.39), the ground state is given by linear combinations of $+|\Omega|$ and $-|\Omega|$. Thus, the Stark effect is zero to first order in $\mathcal{E}$ because the two terms cancel. However, should one be in a field large enough to overcome the splitting caused by the parameter in Eq. (3.40), the term responsible for splitting levels of symmetric and anti-symmetric combinations of $\pm|\Omega|$, then the linear Stark regime enters. The field must be larger than that given by Eq. (3.44). The intent is two work with fully polarized molecules, thus the best choice of basis is the Ω basis.

The way in which to define whether the regime of a signed Ω, i.e. linear Stark shifts, is by whether or not the inequality

$$|d\mathcal{E}|\frac{J(J+1)+F(F+1)-I(I+1)}{2F(F+1)J(J+1)} \gg |\tilde{o}_\Delta|J(J+1), \tag{3.55}$$

holds. Given the numbers for d and $\tilde{o}_\Delta$ in HfF^+, the requisite field needs to be $|\mathcal{E}| \gg$ 50 mV/cm, same as the result in Eq. (3.44); the polarizing field. Thus, fields on the order of several V/cm will suffice for polarizing the molecule and choosing the signed Ω basis. Luckily, these fields can be efficiently constructed in the lab in contrast to the fields required to polarize $^2\Sigma$ molecules. In addition, the Stark shift illustrates that states with the same $M_F\Omega$ go the same way in energy. Thus, unlike Fig. 3.6, there will

be an upper and lower component. This is due to the Λ-doubling and provides a way to check systematics by measuring shifts in the upper component and compare them to shifts in the lower component. This will be discussed a little later after we understand the Zeeman interactions.

3.3.4.2 Zeeman interaction

Next is the Zeeman interaction. Unlike the Stark effect, the Zeeman terms are horrendous. The magnetic field will act on anything that has a magnetic moment, hence the electron spin, the electron orbital angular momentum, the rotational angular momentum, the nuclear spin, and then even higher order corrections. You guessed it, I will go through each in a simple manner and estimate the size of the effect. The basic Zeeman Hamiltonian is given by 4 terms:

$$\begin{aligned} H_{\rm Zeem} &= (g_L + g_r)\mu_B \mathcal{B}\cdot\mathbf{L} + (g_S + g_r)\mu_B \mathcal{B}\cdot\mathbf{S} \\ &\quad -g_r\mu_B\mathcal{B}\cdot\mathbf{J} - g_N\mu_N\mathcal{B}\cdot\mathbf{I}. \end{aligned} \tag{3.56}$$

The spin and orbital pieces combine to give

$$\begin{aligned} \langle\kappa|H_{\rm Zeem}(\mathbf{S},\mathbf{L})|\kappa'\rangle &= ((g_L+g_r)\Lambda + (g_S+g_r)\Sigma)\mu_B\mathcal{B}\times \\ &\quad (-1)^{F-M_F+F'+2J+I+1-\Omega}\Theta[F,F',J,J']\times \\ &\quad \begin{pmatrix} F & 1 & F' \\ -M_F & 0 & M_F \end{pmatrix}\begin{pmatrix} J & 1 & J' \\ -\Omega & 0 & \Omega \end{pmatrix}\begin{Bmatrix} J' & F' & I \\ F & J & 1 \end{Bmatrix} \\ &\quad +(g_S+g_r)\mu_B\mathcal{B}\sum_{q=\pm1}\begin{pmatrix} J & 1 & J' \\ -\Omega & q & \Omega \end{pmatrix}\begin{pmatrix} S & 1 & S \\ -\Sigma & q & \Sigma' \end{pmatrix} \\ &\quad \times(-1)^{F-M_F+F'+2J+I+1-\Omega+S-\Sigma}\Theta[F,F',J,J']\Pi[S] \\ &\quad \times\begin{pmatrix} F & 1 & F' \\ -M_F & 0 & M_F \end{pmatrix}\begin{Bmatrix} J' & F' & I \\ F & J & 1 \end{Bmatrix}. \end{aligned} \tag{3.57}$$

The use of κ is to signify the quantum numbers of interest. They are the same as the quantum numbers in the Stark effect in Eq. (3.54). I have separated out the contribu-

tions that preserve the value of Ω and those that change it. Notice that those which change the value of Ω also change the value of Σ. This is to keep zero change in Λ. This term is usually labeled the anisotropic spin-Zeeman effect. It is responsible for decoupling the electron spin from the molecular axis as the strength of the magnetic field is increased. It is often easiest to denote the interaction via g_l multiplied by the Ω-changing operators.

The nuclear and rotational Zeeman terms are

$$\begin{aligned}\langle\kappa| - g_N\mu_N\mathcal{B}\cdot\mathbf{I}|\kappa'\rangle &= -g_N\mu_N\mathcal{B}(-1)^{F-M_F+J+I+1+F}\Theta[F,F']\Pi[I] \\ &\times \begin{pmatrix} F & 1 & F' \\ -M_F & 0 & M_F \end{pmatrix} \begin{Bmatrix} F' & I & 1 \\ I & F & J \end{Bmatrix} \end{aligned} \tag{3.58}$$

$$\begin{aligned}\langle\kappa| - g_r\mu_B\mathcal{B}\cdot\mathbf{J}|\kappa'\rangle &= -g_r\mu_B\mathcal{B}(-1)^{F-M_F+J+I+1+F'}\Theta[F,F']\Pi[J] \\ &\times \begin{pmatrix} F & 1 & F' \\ -M_F & 0 & M_F \end{pmatrix} \begin{Bmatrix} F' & J' & 1 \\ J & F & I \end{Bmatrix} \end{aligned} \tag{3.59}$$

These Zeeman interactions are the dominant ones. Their size is easy to estimate. For the spin and orbital pieces collect terms to find that $g_L\Lambda + g_S\Sigma \approx 0$. This is because $g_L\Lambda = 1$ and $g_S\Sigma = -2$ in the $^3\Delta_1$. Small perturbations originating from QED effects as well as interactions with excited electronic states will cause g_L to differ from 1 and g_S to differ from 2. While QED is hard to discern, the electronic effects scale from the inclusion of excited states with the same value of Ω into the state of interest, i.e. $^3\Delta_1$. The inclusion of spin-orbit coupling will bring in $^{1,3}\Pi_1$ states into the $\Omega = 1$ wave function. The Zeeman matrix element $\langle{}^3\Pi_1|H_{\rm Zeem}|{}^3\Delta_1\rangle \neq 0$. Therefore, the cross terms arising from taking the $\langle\Omega = 1|H_{\rm Zeem}|\Omega = 1\rangle$ matrix element (which is a combination of $^{1,3}\Pi_1$ and $^3\Delta_1$ states) will not be zero. The size of this effect will scale as $A/\Delta E$, where A is the spin-orbit constant and ΔE is the electronic energy separation. From the *ab initio* calculations, this is a 0.1–1% effect depending on the state coupled in. Thus, the sum $g_L\Lambda + g_S\Sigma \approx 0.1$ at the largest.

This is one of the appealing features of a $^3\Delta_1$ state, it is relatively immune to

small variations in an applied magnetic field. The dominant contributions nearly cancel each other out. The remaining terms are g_N and g_r, both of which are of the order and $m_e/\mu_{\rm mol}$. Therefore, these interactions are of the order 10^{-3} and thus also quite small. The anisotropic g-factor g_l, which accounts for the mixing in of other Ω states and helps to decouple the electron spin from the molecular axis, is also of order 10^{-3}. Because it works to decouple spin, it can be related to the other spin-decoupling interactions, like spin-rotation. In fact, to make an estimate, swap one instance of $BL_\pm$ in the expression for γ in Eq. (3.9) with the magnetic field. In so doing, it is seen that $g_l \approx \gamma/B$, where B is the rotation constant. In OH, where extremely detailed spectroscopy has been performed, $g_l = \gamma/B = 6 \times 10^{-3}$, while the measured value is $g_l = 4 \times 10^{-3}$ [16]. This is excellent agreement for such a simple argument.

The remaining Zeeman terms are all related to the orbital Zeeman interaction and involve higher orders. As in the case of the Λ-doubling and hyperfine induced Λ-doubling, the orbital Zeeman interaction will cause Λ-doubling to occur. Interactions which connect $+|\Lambda| \rightarrow -|\Lambda|$ will be Λ-doubling related. However, there will also be terms that connect $\Lambda \rightarrow \Lambda$ and thus will not be parity dependent. Brown and coworkers [77, 16] have written down the effective Zeeman Hamiltonian. It is arrived at by taking the sum of the $H_{\rm Spin} + H_{\rm Rot}$ and $\mathcal{B} \cdot \mathbf{L}$ to the $2|\Lambda|$ power and dividing by the energy differences, as was done in Eq. (3.47). The result is

$$\begin{aligned} H_{\rm Zeem}^{\rm other} &= \\ &- \frac{\mu_B}{2} g_{rD} (\mathcal{B}_+ J_- J_+ J_- + \mathcal{B}_- J_+ J_- J_+) + \frac{\mu_B}{2} g'_{rD} (\mathcal{B}_+ J_+ J_+ J_+ + \mathcal{B}_- J_- J_- J_-) \\ &+ \frac{\mu_B}{2} g_{lD} (\mathcal{B}_+ S_- J_+ J_- + \mathcal{B}_- S_+ J_- J_+) - \frac{\mu_B}{2} g'_{lD} (\mathcal{B}_+ S_+ J_+ J_+ + \mathcal{B}_- S_- J_- J_-) \\ &- \frac{\mu_B}{2} g_{rS} (\mathcal{B}_+ S_- S_+ J_- + \mathcal{B}_- S_+ S_- J_+) + \frac{\mu_B}{2} g'_{rS} (\mathcal{B}_+ S_+ S_+ J_+ + \mathcal{B}_- S_- S_- J_-) \\ &- \frac{\mu_B}{2} g_{lS} (\mathcal{B}_+ S_- S_+ S_- + \mathcal{B}_- S_+ S_- S_+) - \frac{\mu_B}{2} g'_{lS} (\mathcal{B}_+ S_+ S_+ S_+ + \mathcal{B}_- S_- S_- S_-) \end{aligned} \tag{3.60}$$

In the above I have collected the terms that are similar. Primes denote Λ-doubling terms. The first line describes the coupling of the rotation of the molecule with the

magnetic field. This is very much akin to centrifugal distortion effects and is thus labeled with a rD for distortion due to rotation. The second line is akin to a distortion of the anisotropic correction (think g_l). Thus, they are labeled with an lD. The $\mathcal{B}_\pm$ signify the raising and lowering of angular momentum along the internuclear axis, thus are Ω changing. Each interaction changes Ω. Terms with an same number of $B_\pm$ and $J_\mp$ operators will return Ω to the same initial value; g_{rD} and g_{lD}.

The final two lines are higher-order spin interactions and are thus labeled with rS for spin-spin-type corrections to the rotation and lS for spin-spin-type corrections to the anisotropic terms. The last line is anisotropic because the final Ω state must be different from the initial one.

Provided that the electronic states that are coupled in are limited to configurations arising from the *sd*-atomic configuration, then the magnitude of the higher-order g-factors are expected to be the same in the primed and unprimed interactions. This is because they are limited to talking with excited Π and Σ states only. However, if one has Φ and Γ states, then the primed and unprimed g-factors will differ from each other in magnitude.

Assuming that the primed and unprimed terms will be of similar size because they talk with the same electronically excited states, the size of the g-factors can be estimated in a manner similar to the c_Δ etc. terms:

$$g'_{rD} \approx -2\frac{\tilde{q}_\Delta}{B} \tag{3.61}$$

$$g'_{lD} \approx -\frac{3}{2}\frac{\tilde{p}_\Delta}{B} \tag{3.62}$$

$$g'_{rS} \approx -\frac{\tilde{o}_\Delta}{B} \tag{3.63}$$

$$g'_{lS} \approx -\frac{1}{2}\frac{\tilde{m}_\Delta}{B} \tag{3.64}$$

For the $^3\Delta_1$ state, it is the g'_{rS} term that is of interest. It connects states of $\Omega = pm1 \rightarrow \Omega = \mp 1$ and therefore acts differently on the states of opposite parity in the absence of the electric field. $\tilde{o}_\Delta = 10$ kHz was estimated, which yields this term to be of the order

$g'_{rS} = 10^{-6}$.

This is important since it changes the way in which states with even (odd) parity respond to the application of a magnetic field, thus causing a systematic shift that mimics an eEDM signal in an eEDM measurement. However, in the absence of the electric field this term is of order 2×10^{-6}. In the presence of the electric field strong enough to polarize the molecule, where Ω is a signed quantity, this interaction is off-diagonal and therefore only contributes in second order and thus is negligible. The scale will be $(g'_{rS}\mu_B\mathcal{B})^2/2d_{\rm mol}\mathcal{E}$, or the strength of the Λ-doubling Zeeman shift to the Stark splitting between states of opposite Ω (but same M_F).

However, there is an important effect to consider. The electric field couples in excited rotational states of the molecule. Thus, there could be an electric field dependent difference in the way the molecules respond to an applied magnetic field. See Fig. 3.10 for a physical picture. As is evident in the figure, the lines with $J' = J+1$ and $M\Omega < 0$ (> 0) are gained upon (gaining on) the lines of J with $M\Omega < 0$ (> 0). This causes the states with $M\Omega < 0$ to have a stronger coupling to the magnetic field as a function of applied electric field than their $M\Omega > 0$ counterparts. This can be seen from a perturbative approach

$$|\tilde{J}, M\Omega > 0\rangle = |J, M\Omega > 0\rangle + \eta_{>}|J+1, M\Omega > 0\rangle, \tag{3.65}$$

$$|\tilde{J}, M\Omega < 0\rangle = |J, M\Omega < 0\rangle + \eta_{<}|J+1, M\Omega < 0\rangle, \tag{3.66}$$

where

$$\eta_{\gtrless} = \frac{\langle JM\Omega \gtrless 0|H_{\rm Stark}|J+1, M\Omega \gtrless 0\rangle}{2B(J+1) \mp \gamma_F M\Omega d\mathcal{E}}. \tag{3.67}$$

The factor γ_F is given by

$$\gamma_F = \frac{J(J+1) + F(F+1) - I(I+1)}{2F(F+1)J(J+1)}, \tag{3.68}$$

the diagonal contribution to the Stark interaction. It is like an electric g-factor. Now apply the Zeeman Hamiltonian to the the states $|\tilde{J}\rangle$ ($\langle\tilde{J}|H_{\rm Zeem}|\tilde{J}\rangle$). Taking the appro-

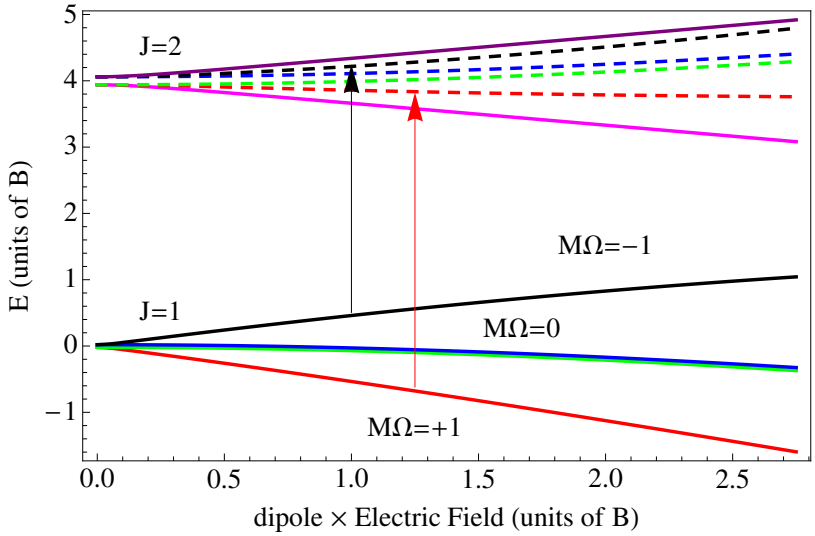

Figure 3.10: The Stark effect in $^3\Delta$ molecules that shows how the application of an electric field can change the way in which the molecule responds to an applied magnetic field in different Ω states. The axes are in units of the rotational constant B. When the energy of the field is comparable to B, we enter a new regime of the Stark shift as it deviates from linear. The Λ-doubling constant has the exaggerated value $B/100$ so as to be somewhat visible. This distorts the range over which the linear Stark effect is applicable. The dashed lines in the upper part of the panel correlate to the solid lines of the same color in the lower portion of the panel. The black and red arrows indicate the coupling of $M\Omega$ states.

priate matrix elements by applying Eqs. (3.57) and (3.54) to the terms and expanding the denominators in Eqs. (3.65) and (3.66) to the first order in $d\mathcal{E}/B$ yields

$$\begin{aligned}\delta g_F(\mathcal{E}) &= \sum_{J',F'} \frac{d\mathcal{E}}{B(J+1)} \frac{g_F}{\gamma_F \Omega} \Pi[F,F',J,J'] \\ &\times \begin{pmatrix} F & 1 & F' \\ -M_F & 0 & M_F \end{pmatrix}^2 \begin{pmatrix} J & 1 & J' \\ -\Omega & 0 & \Omega \end{pmatrix}^2 \begin{Bmatrix} F' & J' & I \\ -J & F & 1 \end{Bmatrix}^2 .\end{aligned} \tag{3.69}$$

In the level of interest ($J = 1, M\Omega = \pm 1$) for eEDM spectroscopy the difference between positive and negative $M\Omega$ is

$$\frac{\delta g_{F=3/2}}{g_{F=3/2}} = \frac{9}{40} \frac{d\mathcal{E}}{B}. \tag{3.70}$$

This is about a part in 10^5.

The two transitions of interest are labeled in Fig. 3.11. The upper transition W^u will have a slightly different shift in frequency than the lower one W^ℓ due to the eEDM. A systematic that must be controlled is the difference in magnetic response due to the electric field dependent g-factor difference. What is nice here is that there is no need to reverse the sign of the magnetic field relative to the electric field because the $^3\Delta_1$ molecules have a built in co-magnetometer; the Λ-doublet. However, whereas in the $^2\Sigma$ case the sensitivity was limited to the ability to exactly reverse the applied magnetic field, here the sensitivity is to the difference in magnetic response. The difference $W^u - W^\ell \propto d_e \mathcal{E}_{\text{eff}} + \delta g_F \mu_B B$.

The blue lines indicate the Stark shift while the red lines indicate the Zeeman shift. The $\tilde{o}_\Delta$ has been greatly exaggerated. The eEDM shift is denoted by the green lines. One way in which to cancel out the effect of the varying g-factors is to chop the magnetic field. This is discussed in the forthcoming paper from the JILA eEDM collaboration [78]. In so doing, the difference in the transitions W^u and W^ℓ is

$$W^u(\mathcal{B}) + W^u(-\mathcal{B}) + W^\ell(\mathcal{B}) + W^\ell(-\mathcal{B}) = 8 d_e \mathcal{E}_{\text{eff}} + \frac{\delta g_F}{g_F} \mu_B \mathcal{B}, \tag{3.71}$$

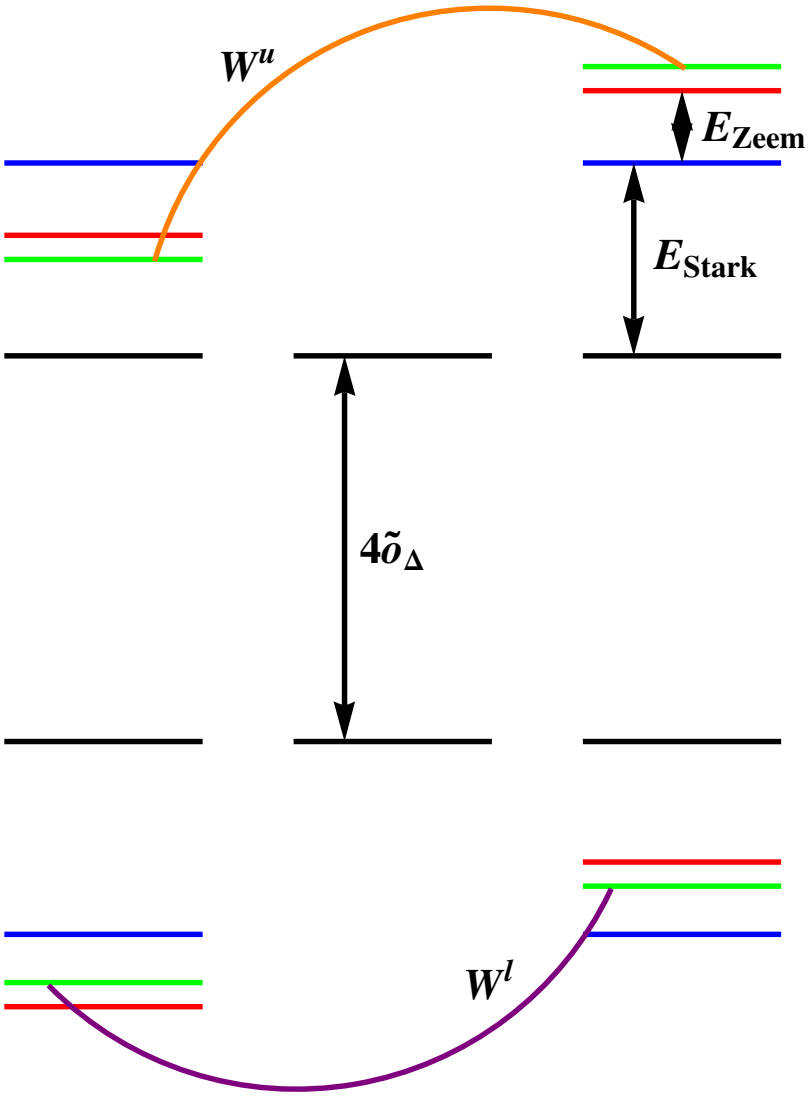

Figure 3.11: The basic Stark (blue lines)and Zeeman (red lines) spectrum of a $^3\Delta_1$ molecule. The transition labeled W^u is of interest in an eEDM experiment. The "co-magnetometer" transition labeled W^ℓ is also of interest as the difference between W^u and W^ℓ will cancel out the magnetic field shifts provided the g-factors are the same in the upper and lower components of the Λ-doublet. The Λ-doublet splitting has been greatly exaggerated as well as the eEDM shift labeled by the green lines. Black lines indicate the zero field shifts.

which is 4 times stronger than the $^2\Sigma$ case with the added benefit of having a weaker dependence on the systematic control of $\mathcal{B}$ due to the smaller g-factors.

Chapter 4

Beyond the Geometric Phase

The mathematical difficulties of a theory of rotation arise chiefly from a want of geometrical illustrations and sensible images, by which we might fix the results of the analysis in our minds.

– James Clerk Maxwell

And so begins over 25 years of research into the geometric phase introduced by Berry in 1984 [18]. In the proposed experiment by the JILA eEDM team, the molecular ions will be in a rotating electric field [78]. This electric field will couple to the electric dipole moment of the molecule and in so doing introduce an additional phase into the dynamic evolution of the internal states of the molecule. It is this additional phase, which will appear as an energy shift in the measurement, which must be understood. The ions will rotate in the plane defined by $\theta_r = \pi/2$ (the angle the electric field makes with the axis of rotation), which gives the maximum coupling between states of M differing by unity (as will be seen in the following discussion).

In addition, the ions will be confined in the z-direction by an electric field that will change the value of the $\theta_r = \pi/2$ small amounts and the plane of rotation is shifted up and down. While this effect will be ignored in the development of the dressed state picture, it will be included in the final section (4.6) as a discussion of how it may affect a measurement in the $^3\Delta_1$ system. I will develop a formalism whose punchline is that, while it complicates a measurement of the eEDM, does not prohibit such a search. This

formalism takes many steps, and some simple examples will be worked out so as to build intuition.

4.1 The basics

Any quantum mechanical system in a stationary state accumulates a dynamical phase over time proportional to the energy of that state. To determine energy differences, based on phase differences accumulated between two such states, is the basis of Ramsey spectroscopy; the workhorse of high-precision measurement. For this reason, small effects that can add spurious phase shifts must be understood and kept under control. What effects, you may ask? Effects like the ones which crop up when a particle is driven by a periodically rotating field, which creates non-stationary states.

If the total Hamiltonian $H(t)$ has an explicit time dependence, then this dependence will generate an additional phase evolution. For example, precision spectroscopy of trapped ions must contend with the fact that the ions are in motion, and experience varying ambient fields during the course of their orbit. Otherwise, these ions would leave the trap, thereby making an electron electric dipole moment (eEDM) search irrelevant.

In the case of a Hamiltonian with a slow, periodic time dependence $H(t+\tau) = H(t)$, Berry [18] has given a famous description of the additional phase. Berry's original treatment requires that the period τ be far larger than any other relevant time scale of the system, and thus finds an "adiabatic" phase shift. This shift is largely independent of the detailed way in which the Hamiltonian varies with time, and leads to an elegant geometric description of the phase [18, 79, 80, 81, 82, 83, 84]. Maxwell would be so proud for finding such a description.

Extensions to this formalism have considered the next-order corrections if the rate of change of the Hamiltonian is not strictly adiabatic [85, 86, 87, 88, 89, 90, 91]. A more general Floquet theory has also been advanced, which allows one to consider the effect of overtones of the fundamental period τ [92, 93, 91]. In addition, the ideas

have been extended to particles with dynamic properties [94], gauge structure [95], the quantum Hall effect [96], to relativistic effects using the Dirac equation [97], and to supersymmetric black holes in 5 dimensions [98]. Yes, I said supersymmetric black holes in 5 dimensions thereby bringing us full circle to supersymmetry from the introduction. This will be the last mention of supersymmetric black holes in 5 dimensions.

Thus far, applications of the Berry phase have mostly considered the effect of the time-dependence on quantum mechanical particles without internal structure, although atoms with two or several levels have been considered [99, 93, 100]. However, the job of precision spectroscopy is precisely to reveal this internal structure. Corrections to Berry's phase arising from degrees of freedom internal to an atom or molecule is our concern in understanding the intricacies of a trapped molecular ion in an eEDM experiment. To establish a concrete formalism for this, we will consider a particular case, namely, a diamagnetic or electrically polar species in the presence of a magnetic or electric field, whose direction precesses on a cone with an angular frequency ω_r (see Fig. 4.1). The system evolves in time according to the field variation, combined with whatever intrinsic Hamiltonian governs the particle's internal structure. The internal structure dictates regimes of linear and quadratic Zeeman (Stark) shifts with respect to the applied magnetic (electric) field.

A main point in deriving the non-dynamic phase in this situation is to recognize the periodicity of the driving field. By analogy to the periodic driving of a near-resonant laser field applied to a two-level atom, we consider "field-dressed" states of the Hamiltonian in the spirit of quantum optics [101, 100]. This viewpoint effectively counts the energy of the atom itself, plus that of the photons of frequency ω_r arising from the driving field. The additional energy shift due to the rotating field is then equivalent to the ac Stark effect in optics. By constructing the complete Hamiltonian in this way, we are able to accommodate the particle's internal structure. We are also able to consider arbitrary rates of rotation, not just those that are adiabatic with respect to the parti-

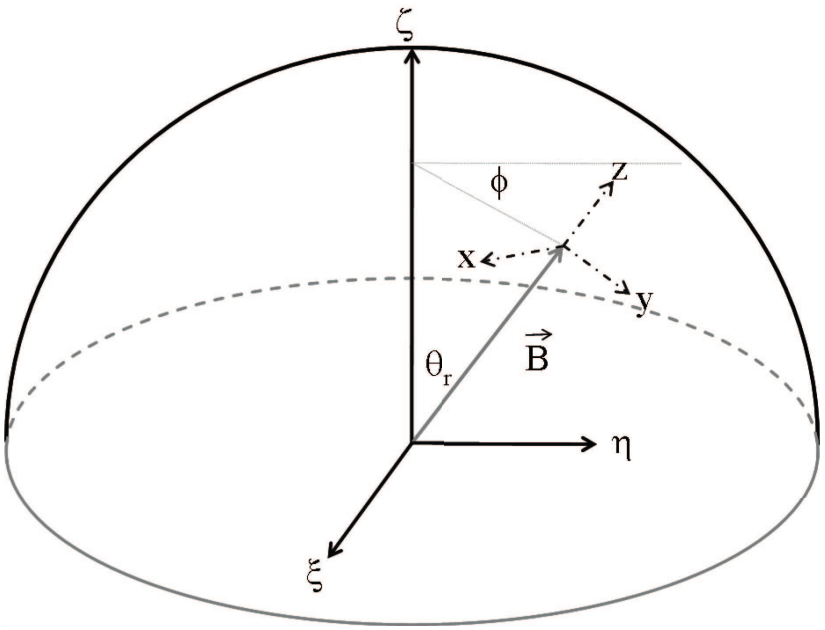

Figure 4.1: The axis of rotation with laboratory-fixed coordinates $\{\xi, \eta, \zeta\}$ as well as the field coordinates defined by $\{x, y, z\}$. The field direction rotates about the ζ-axis with angular frequency ω_r.

cle's Hamiltonian. Nevertheless, in what follows we will focus primarily on results for low rotation rates, to better draw analogies with the usual adiabatic phase [18]

I will walk through the basic derivation of the dressed state formalism in Sec. 4.2 and find the general transformation from a Hamiltonian with an explicit time-rotating field, into an effective dressed Hamiltonian whose eigen-energies yield the shifted energies. I'll illustrate this transformation first with a simple two-level atom, then generalize it to an arbitrary atom or molecule. In Sec. 4.3 I'll briefly re-visit a structureless particle with arbitrary total spin, showing that the results reduce to Berry's in the limit of slow rotation. Sec. 4.4 illustrates the application of the method to a particle composed of two interacting spin-1/2 objects, to show most clearly the effect of their fine structure on the Berry phase. Sec. 4.5 considers a simple case of a dipolar molecule in a rotating electric field, to assess the influence of molecular end-over-end rotation on the phase. After having understood these basics, I'll address the form of $^3\Delta_1$ molecules in a rotating electric field and a complexity that arises due to the Λ-doubling and rotation of the electric field (Sec. 4.6).

4.2 General spin-j system: A dressed state derivation

A general derivation for the spin-j system will entail the use of a dressed state *ansatz*. A dipole $\vec{\mu}$ interacting with a time-varying field $\vec{\mathcal{F}}(t)$ can be described by the following Hamiltonian

$$H(t) = H_0 - \vec{\mu} \cdot \vec{\mathcal{F}}(t), \tag{4.1}$$

where $\vec{\mathcal{F}}(t)$ can be electric or magnetic that acts on an appropriate moment $\vec{\mu}$ of the atom or molecule. $\vec{\mathcal{F}}$ rotates on a cone at frequency ω_r and tilt angle θ_r as depicted in Fig. 4.1. Here H_0 is a Hamiltonian in the absence of the applied rotating field. It can be used to describe the hyperfine elements of an atom or it can be a detailed molecular Hamiltonian that includes such items as rotation, spin-spin, nuclear spin, or λ-doubling.

The Hamiltonian can equally be represented in a basis referred to the axis of rotation or to the instantaneous field axis. Later I will take the instantaneous field axis. I'll begin by quantizing along the axis of rotation. Place this structured object in a rotating field $\vec{\mathcal{F}}$; let there be an electric or magnetic dipole that interacts with the field in the usual way, i.e. it is a scalar interaction of two vectors.

To work with this Hamiltonian, it is convenient to pick two basis sets:

$$|(\kappa)jm_\zeta\rangle$$
$$|(\kappa)jm_j\rangle \tag{4.2}$$

Because j is the total of all relevant angular momenta, its projection onto an axis is unambiguously defined as m_ζ in the lab fame and m_j in the rotating frame, as above. Here κ is a shorthand notation for all the other quantum numbers required to specify the state.

To deal with the explicit time dependence of the field rotation, I will expand into the lab basis first, and will a trial wave function motivated by dressed states with a little ingenuity in the choice of phase;

$$|\psi(t)\rangle = \sum_{\kappa',j',m'_\zeta} C_{\kappa',j',m'_\zeta} e^{-im'_\zeta\omega_r t}|(\kappa')j'm'_\zeta\rangle. \tag{4.3}$$

We have explicitly included a time dependent phase factor with phase $m_\zeta\omega_r$. Taking the time derivative for the time-dependent Schrödinger equation (TDSE) and projecting onto a particular state, gives

$$\langle(\kappa)jm_\zeta|i\frac{d|\psi\rangle}{dt} = \left(i\dot{C}_{\kappa,j,m_\zeta} + m_\zeta\omega_r C_{\kappa,j,m_\zeta}\right)e^{-im_\zeta\omega_r t}. \tag{4.4}$$

As for the internal Hamiltonian H_0, it may or may not be diagonal in this basis, but it does not depend on any external field. Therefore it can be represented in a basis where it is diagonal in m_ζ, whereby

$$\langle(\kappa)jm_\zeta|H_0|\psi\rangle = \sum_{\kappa',j',m'_\zeta} e^{i(m_\zeta-m'_\zeta)\omega_r t}\langle(\kappa)jm_\zeta|H_0|(\kappa')j'm'_\zeta\rangle C_{\kappa',j',m'_\zeta}\delta_{m_\zeta,m'_\zeta} \tag{4.5}$$

To treat the field interaction, I'll use the language of tensor algebra, and express the spherical components of $\vec{\mathcal{F}}$ in the lab frame as an explicit rotation from $\vec{\mathcal{F}}$ in the rotating frame (whose z axis is, of course, defined by the instantaneous direction of $\vec{\mathcal{F}}$ itself):

$$\begin{aligned} \mathcal{F}_\iota &= \sum_\iota \mathcal{F}_q \mathcal{D}^{1\star}_{\iota q}(\omega_r t, \theta_r, 0) \\ &= \mathcal{F}\mathcal{D}^{1\star}_{\iota q}(\omega_r t, \theta_r, 0). \end{aligned} \tag{4.6}$$

$\mathcal{F}$ is the magnitude of the field, and q is its spherical projection in the rotating frame. But $\vec{\mathcal{F}}$ defines this frame so only the values of $q = 0$ will contribute. $\mathcal{D}$ is a Wigner rotation matrix. In a similar manner, the dipole moment $\vec{\mu}$ is determined by its spherical components such that

$$\begin{aligned} -\vec{\mu}\cdot\vec{\mathcal{F}} &= -\sum_\iota (-1)^\iota \mu_\iota \mathcal{F}_{-\iota} \\ &= -\mathcal{F}\sum_\iota (-1)^\iota \mu_\iota \mathcal{D}^{1*}_{-\iota 0}(\omega_r t, \theta_r, 0) \\ &= -\mathcal{F}\sum_\iota \mu_\iota e^{-i\iota\omega_r t} d^1_{-\iota 0}(\theta_r). \end{aligned} \tag{4.7}$$

This uses the explicit expression for $\mathcal{D}$ in terms of a little-d function [102].

Just as I treated the internal degrees of freedom in H_0 I must now treat the field interaction.

$$\begin{aligned} \langle(\kappa) j m_\zeta| - \vec{\mu}\cdot\vec{\mathcal{F}}|\psi\rangle &= -\mathcal{F}\sum_{\kappa' j' m'_\zeta \iota} (-1)^\iota \langle(\kappa) j m_\zeta|\mu_\iota|(\kappa') j' m'_\zeta\rangle \times \\ &\quad C_{\kappa', j', m'_\zeta} d^1_{-\iota 0}(\theta_r) e^{i\omega_r t(-\iota - m'_\zeta)}. \end{aligned} \tag{4.8}$$

Piecing together the different parts, and multiplying through by $e^{i m_\zeta \omega_r t}$, a new TDSE is arrived at for the coefficients C:

$$\begin{aligned} i\dot{C}_{\kappa,j,m_\zeta} + \omega_r m_\zeta C_{\kappa,j,m_\zeta} &= \sum_{\kappa', j'} \langle(\kappa) j m_\zeta|H_0|(\kappa') j' m_\zeta\rangle C_{\kappa', j', m_\zeta} - \\ &\quad \mathcal{F}\sum_{\kappa' j' m'_\zeta \iota} (-1)^\iota \langle(\kappa) j m_\zeta|\mu_\iota|(\kappa') j' m'_\zeta\rangle C_{\kappa', j', m'_\zeta} \times \\ &\quad d^1_{-\iota 0}(\theta_r) e^{i\omega_r t(-\iota - m'_\zeta + m_\zeta)}. \end{aligned} \tag{4.9}$$

Now, nowhere is specified what the field $\vec{\mathcal{F}}$ is, nor which structural degrees of freedom are involved in making the dipole $\vec{\mu}$, and it does not matter. All that matters is that $\vec{\mu}$ is a vector, in which case the Wigner-Eckhart theorem applies [102]. In the total angular momentum basis, it must be

$$\langle(\nu)jm_\zeta|\mu_\iota|(\nu')j'm'_\zeta\rangle \propto \begin{pmatrix} j & 1 & j' \\ -m_\zeta & \iota & m'_\zeta \end{pmatrix}, \tag{4.10}$$

where the proportionality constant involves the reduced matrix element. Then the conservation of angular momentum implies that $m'_\zeta - m_\zeta = -\iota$. However, this immediately removes the time-dependence in the exponential term in (4.9). In fact, this statement says that any angular momentum imparted by the rotating field must be accounted for in the projection m_ζ.

In some cases it will prove more useful to keep track of the individual spin components $m_{\zeta i}$ separately. For instance, suppose there were two angular momenta, $m_{\zeta 1}$ and $m_{\zeta 2}$: we would have two projection terms that would each evolve as $e^{i\, m_{\zeta 1}\omega_r t}$ and $e^{i\, m_{\zeta 2}\omega_r t}$. Terms in the Hamiltonian which describe the interaction of the two spins are of the form $\vec{s}_1 \cdot \vec{s}_2$ for which the interaction scales as

$$\langle s_1\ m_{\zeta 1}\ s_2\ m_{\zeta 2}|\vec{s}_1 \cdot \vec{s}_2|s'_1\ m'_{\zeta 1}\ s'_2\ m'_{\zeta 2}\rangle \propto$$
$$\begin{pmatrix} s_1 & 1 & s'_1 \\ -m_{\zeta 1} & p & m'_{\zeta 1} \end{pmatrix} \begin{pmatrix} s_2 & 1 & s'_2 \\ -m_{\zeta 2} & -p & m'_{\zeta 2} \end{pmatrix} e^{i\,(m_{\zeta 1}-m'_{\zeta 1})\omega_r\, t} e^{i\,(m_{\zeta 2}-m'_{\zeta 2})\omega_r\, t}. \tag{4.11}$$

The proportionality involves a reduced matrix element. By the conservation of angular momentum it is noted that $m_{\zeta 1} - m'_{\zeta 1} = -(m_{\zeta 2} - m'_{\zeta 2})$ and the phase factor is still canceled out. In fact, for any such interaction between two spins, the conservation of angular momentum forces the time dependence to cancel out.

With the time-dependence removed, Eq. (4.9) reduces to the Schrödinger equation for a non-rotating field tilted at an angle θ_r from the rotation axis. This introduces an additional term on the left of (4.9), which is moved to the RHS and interpreted as an

effective Hamiltonian. Thus if H_0 is presented in the basis $|(\kappa)j\ m_j\rangle$ diagonal with respect to the field, then the matrix to be diagonalized is

$$\begin{aligned} H_{\text{dressed}} &= H_0 - \vec{\mu}\cdot\vec{\mathcal{F}} - \omega_r m_\zeta \\ &= H_0 - \vec{\mu}\cdot\vec{\mathcal{F}} - \omega_r j_\zeta, \end{aligned} \tag{4.12}$$

where m_ζ is the eigenvalue of the j_ζ operator. Now rotate this Hamiltonian from the m_ζ basis to the m_j basis. Since H_0 does not depend on the either m_ζ or m_j, it is unaffected by this rotation. In the frame of the instantaneous field, where m_j is the good quantum number, the dressed Hamiltonian is written as

$$\begin{aligned} H_{\text{dressed}} &= H_0 - \vec{\mu}\cdot\vec{\mathcal{F}} - \hat{\omega}_r\cdot\vec{j}, \\ &= H_0 - \vec{\mu}\cdot\vec{\mathcal{F}} - \omega_r(\cos(\theta_r)j_z - \sin(\theta_r)j_x). \end{aligned} \tag{4.13}$$

Here is the *key* result. All the time-dependence is removed. This Hamiltonian has been previously formulated in NMR studies [103]. In the following sections I will apply it to a few elementary cases of interest.

4.3 Pure spin-s system

As the simplest application of the general method beyond the spin-j particle, I consider in this section a structureless particle of arbitrary spin s, as was considered in the original formulation of Berry [18]. This spin interacts with a magnetic field that rotates at an angle θ_r with respect to the axis of rotation. Using the result from Eq. (4.13), this system is described by the Hamiltonian

$$H_{\text{dressed}} = \omega_L s_z - \omega_r(\cos(\theta_r)s_z - \sin(\theta_r)s_x), \tag{4.14}$$

where $\omega_L = g_s\mu_B\mathcal{B}$ is the m-independent Larmor precession frequency and g_s is the g-factor for the spin-s. For this section, I have reverted to the usual notation s and m for the spin and it's projection onto the instantaneous field axis.

For this structureless particle, the Hamiltonian (4.14) is represented by a $(2s+1)$ $\times$ $(2s+1)$ tridiagonal matrix, in the basis of states $|s\,m\rangle$. This matrix is explicitly given by

$$H = \begin{pmatrix} m\,a & b(s,m) & 0 & 0 & \dots \\ b(s,m) & (m-1)\,a & b(s,m-1) & 0 & \vdots \\ 0 & b(s,m-1) & \ddots & \ddots & b(s,-m+1) \\ \vdots & 0 & b(s,-m+1) & -(m-1)\,a & b(s,-m) \\ \dots & 0 & 0 & b(s,-m) & -m\,a. \end{pmatrix}, \quad (4.15)$$

where $a = \omega_L - \omega_r \cos(\theta_r)$ and $b(s,m) = (1/2)\sqrt{s(s+1) - m(m-1)}\ \omega_r \sin(\theta_r)$. Appendix B sketches a derivation of the eigenvalues of this matrix, which are

$$\lambda_m = m\sqrt{\omega_L^2 + \omega_r^2 - 2\omega_r\omega_L \cos(\theta_r)}, \quad (4.16)$$

where m takes on the values $-s, \dots, +s$ in integer steps.

The usual Berry phase is obtained in the adiabatic limit where $\omega_r \ll \omega_L$, in which case

$$\lambda_m \approx m\omega_L - m\omega_r \cos(\theta_r). \quad (4.17)$$

The magnetic field completes one rotation in a time $\tau = 2\pi/\omega_r$. In this time the spin accumulates a dynamical phase $\varphi_m = m\omega_L\tau$. Beyond this, it acquires an additional phase $\gamma_m = \phi_m - \varphi_m$, where $\phi_m = \lambda_m\tau$, given to lowest order by

$$\gamma_m^{(0)} = -m2\pi \cos(\theta_r) \Rightarrow 2\pi m(1 - \cos(\theta_r)). \quad (4.18)$$

In the final step, the fact that adding $2\pi m$ (where m is either integer or half-integer) amounts to adding a phase of ± 1 to the system is used. Since Ramsey-type measurements are the main concern, i.e. knowledge of phase differences between two sub-levels, this added phase is unobservable. However, in interferometric measurements, half integer spins will introduce a sign change in the state which is observable. However, this a

additional phase contributes an apparent extra energy of $2\pi\Delta M$ to a Ramsey-type measurement, which is always an integer multiple of 2π and hence, unobservable. The phase $\gamma_m^{(0)}$ accumulated is exactly that given by the result of Berry; m times the solid angle subtended by the rotation. This solution can be extended to regimes of non-adiabaticity. The first order correction in ω_r/ω_L is

$$\gamma_m^{(1)} = 2\pi\ m\frac{\omega_r}{2\omega_L}\sin^2(\theta_r), \tag{4.19}$$

which has already been identified elsewhere [85, 91]. Based on our explicit formula, we can extract corrections to any desired order, at least for fields undergoing the simple motion in Fig. 4.1. This additional phase can be expanded to any desired order in the adiabatic parameter ω_r/ω_L. For example, the second and third-order $\gamma^{(k)}$ corrections are

$$\gamma_m^{(2)} = 2\pi m\frac{\omega_r^2}{2\omega_L^2}\cos(\theta_r)\sin^2(\theta_r) \tag{4.20}$$

$$\gamma_m^{(3)} = 2\pi m\frac{\omega_r^3}{16\omega_L^3}(3+5\cos(2\theta_r))\sin^2(\theta_r) \tag{4.21}$$

Using the general dressed formalism, the limit of fast field rotation can also be described. The phase γ_m (after one field period) can be approximated in this limit ($\omega_r \gg \omega_L$):

$$\gamma_m \approx 2\pi m - 2\pi m\frac{\omega_L}{\omega_r}\cos(\theta_r), \tag{4.22}$$

and the first term is unobservable. In this case the dominant energy, as manifested in the phase, is the photon energy due to the time-periodic field. On top of this, the magnetic field interaction itself makes a small correction. This is clearly not the appropriate limit in which to perform precision spectroscopy, since small uncertainties in the field rotation rate would dominate the observable Larmor frequency.

A spectroscopic measurement would involve finding the energy difference between two states with different values of m, with difference Δm. In a Ramsey-type

experiment, this measurement seeks to measure the phase difference $\omega_L \Delta m \tau = \Delta\varphi$. In a rotating field, however, the experiment will produce a measurement of $\Delta\phi = \Delta m \sqrt{\omega_L^2 + \omega_r^2 - 2\omega_L \omega_r \cos(\theta_r)}\tau$, and thus will introduce an error. This error is given by the difference $\Delta\gamma = \gamma_m - \gamma_{m'} = \Delta\phi - \Delta\varphi$, and is plotted in Fig. 4.2 as a function of rotation rate. The different curves represent different values of the tilt angle θ_r.

4.4 Structured spin-J system

More generally, atoms and molecules are composite objects made of individual spins, which are moreover coupled together to create fine or hyperfine structure. For example, alkali atoms couple the electronic and nuclear spins into a total hyperfine state. The resulting angular momentum structure will have a bearing on the non-adiabatic corrections to the geometric phase accumulated. Ref. [104] has studied the effects of an atomic spin-J system with $\vec{L} \cdot \vec{S}$ coupling while Ref. [105] analyzed the Breit-Rabi Hamiltonian assessing the influence of hyperfine structure on the Berry phase. Both coupling schemes can be easily addressed with the method illustrated below.

As a simple illustration of the formalism, consider a composite particle composed of two spin-1/2 objects. This example goes beyond the structureless particle often envisioned by the usual Berry theory. The dressed Hamiltonian is given by

$$H_{\text{dressed}} = \omega_1 j_{1z} + \omega_2 j_{2z} + \Delta \vec{j}_1 \cdot \vec{j}_2 - \omega_r(\cos(\theta_r) J_z - \sin(\theta_r) J_x), \tag{4.23}$$

where $\omega_i = g_i \mu_B \mathcal{B}$ is the Larmor precession frequency of spin j_i; $\vec{J}$ is the vector sum of $\vec{j}_1$ and $\vec{j}_2$; and Δ is parameter that governs the splitting between levels $J = 0$ and $J = 1$.

The Hamiltonian (4.23) can be represented by a 4×4 matrix, in the basis

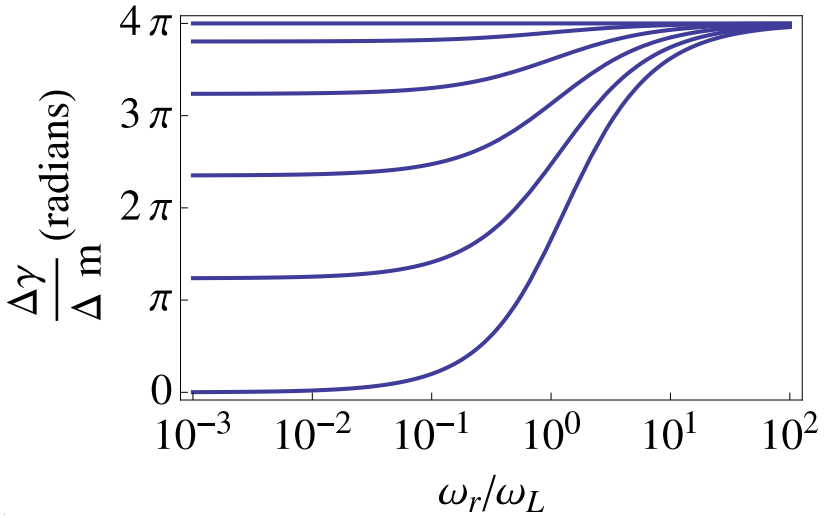

Figure 4.2: The extra phase accumulated due to the rotation of the field. In the limit of very fast rotation, $\omega_r \gg \omega_L$, the system accumulates a phase of 4π, which is unobservable. In this limit, the states are best represented by projections onto the axis of rotation. The various lines represent values of θ_r between $\pi/2$ (bottom line) and 0 (top line) in steps of $\pi/10$. As can be seen, when θ_r is zero, there is no measurable phase shift, since there is no enclosed solid angle.

$$\{|(j_1\, j_2)J\, M_J\rangle\} = \left\{|(\tfrac{1}{2}\ \tfrac{1}{2})0\ 0\rangle,\ |(\tfrac{1}{2}\ \tfrac{1}{2})1\ 1\rangle,\ |(\tfrac{1}{2}\ \tfrac{1}{2})1\ 0\rangle,\ |(\tfrac{1}{2}\ \tfrac{1}{2})1\ -1\rangle\right\}$$

$$H_{\text{dressed}} = \begin{pmatrix} -\frac{3\Delta}{4} & 0 & \frac{1}{2}(\omega_1 - \omega_2) & 0 \\ 0 & \frac{\Delta}{4} + \omega_{\text{Z}} - \omega_r\cos(\theta_r) & \frac{\omega_r}{\sqrt{2}}\sin(\theta_r) & 0 \\ \frac{1}{2}(\omega_1 - \omega_2) & \frac{\omega_r}{\sqrt{2}}\sin(\theta_r) & \frac{\Delta}{4} & \frac{\omega_r}{\sqrt{2}}\sin(\theta_r) \\ 0 & 0 & \frac{\omega_r}{\sqrt{2}}\sin(\theta_r) & \frac{\Delta}{4} - \omega_{\text{Z}} + \omega_r\cos(\theta_r) \end{pmatrix}, \tag{4.24}$$

where $\omega_{\text{Z}} = \frac{1}{2}(\omega_1 + \omega_2)$, is the average of the individual Larmor frequencies. The first item to note is that if the two spins have identical Larmor frequencies, $\omega_1 = \omega_2$, then this Hamiltonian is equivalent to that of a spin-0 particle and a spin-1 particle that are independent of each other, there is no coupling between the two states. Each would then evolve according to the previous section on pure spins. This would be the case for the singlet and triplet excited states of the helium atom, $(1s2s)^{1,3}S$ state, for example. However, should these spins be different from one another (such that $\omega_1 \neq \omega_2$) then coupling corrections arise.

The ordinary adiabaticity criterion specifies that the rotational frequency ω_r be small as compared to the Larmor precession frequency ω_L, which in this example is given by ω_{Z}. However, now it becomes also necessary to specify whether the Larmor frequency itself is large or small compared to the splitting Δ between adjacent J-levels. This is because the Berry phase arises from a correction to the eigenvalues of the dressed Hamiltonian relative to the non-rotating Hamiltonian. It is therefore worthwhile to cast the non-rotating Hamiltonian in the basis in which it is as diagonal as possible. In the following sections we treat the two limits separately. Since our emphasis here is on the Berry-phase limit, I consider only the limit where $\omega_r \ll \omega_{\text{Z}}$, where the rotation rate of the field is small compared to the Larmor frequency. The resulting phase shifts are of course implicit in the theory, however.

4.4.1 Weak magnetic field, $\omega_r \ll \omega_Z \ll \Delta$

In the low-field limit, but assuming that each Larmor frequency ω_i is still far larger than the rotational frequency ω_r, one can write down expressions for the energy quite simply. Note that in the absence of rotation, the leading-order energy shift is the sum of the Larmor frequencies themselves, i.e., $(1/2)(\omega_1 + \omega_2)M_J = \omega_Z M_J$. Leaving this correction on the diagonal to break the degeneracy of the $J = 1$ level, one now treats as perturbations the difference $(1/2)(\omega_1 - \omega_2)$ and the rotation rate ω_r.

Doing so, the leading-order correction due to rotation of the field is given by the diagonal terms in (4.24) that contain the rotation rate ω_r. This correction is the usual Berry phase found above,

$$\gamma^{(0)}(|J\ M_J\rangle) = -2\pi M_J \cos\theta_r, \tag{4.25}$$

and it depends on the atomic state only through the total projection of angular momentum M_J. Thus the ordinary Berry phase in the limit of zero rotation rate is still intact, and is independent of the internal structure.

However, the higher order corrections do depend on this structure. To leading order in the rotation frequency ω_r, a correction to the Berry phase in the $|(\frac{1}{2}\ \frac{1}{2})1\ 1\rangle$ state is given by:

$$\gamma^{(1)}(|11\rangle) = 2\pi \frac{\omega_r}{2\omega_Z} \sin^2(\theta_r) \left(1 + \frac{(\omega_1 - \omega_2)^2}{4\omega_Z(\Delta + \omega_Z)}\right). \tag{4.26}$$

The first term is the usual first order correction for a structureless particle (cf. (4.19)), with the replacement of ω_L by ω_Z. This should be expected since the energy splitting between the two states is given by ω_Z, and thus is what must be overcome by the rotating field that couples together the differing projections. The second term in the parentheses depends on how strongly the rotating field couples states with differing total J, as manifested by $\omega_1 - \omega_2$. This new correction arises from 4^{th}-order mixing in perturbation theory, it is nevertheless linear in the adiabaticity parameter ω_r/ω_Z. A

similar expression is found for the $|1-1\rangle$ state,

$$\gamma^{(1)}(|1-1\rangle) = -2\pi\frac{\omega_r}{2\omega_{\rm Z}}\sin^2(\theta_r)\left(1-\frac{(\omega_1-\omega_2)^2}{4\omega_{\rm Z}(\Delta-\omega_{\rm Z})}\right). \tag{4.27}$$

As is expected from the pure spin case, this state picks up an overall negative sign. However, due to slight changes introduced by the structure, we find a slightly different correction to the second term in parentheses. In fact, one can write down an expression that encapsulates the first order (in $\omega_r/\omega_{\rm Z}$) correction as

$$\gamma^{(1)}(|J\ M_J\rangle) = 2\pi M_J\frac{\omega_r}{2\omega_{\rm Z}}\sin^2(\theta_r)\left(1+M_J\frac{(\omega_1-\omega_2)^2}{4\omega_{\rm Z}(\Delta+M_J\omega_{\rm Z})}\right). \tag{4.28}$$

While the first term is exactly of the form in (4.19), the second term describes how the distant $|J=0, M_J=0\rangle$ state affects the accumulated first order phase $\gamma^{(1)}_{M_J}$; namely that the quadratic Zeeman shift in the two $M_J=0$ levels distorts the system such that the $|J=1, M_J=1(-1)\rangle$ state is affected more (less) by the $|J=1, M_J=0\rangle$ state.

The two states with $M_J=0$ do not acquire a geometric phase at lowest order in ω_r, which is appropriate. In this case the leading order perturbation to the dressed Hamiltonian is $E_{\rm Z}^{(\pm)} = \pm[(1/2)(\omega_1-\omega_2)]^2/\Delta$, which denotes the quadratic Zeeman shift already present in the non-rotating system, and which does not contribute to the Berry phase γ. The quadratic shift after a period $\tau = 2\pi/\omega_r$ is the dynamical phase the $M_J=0$ would nominally acquire. To the first order in ω_r in which there is a correction to the $|J=0, M_J=0\rangle$ state arises in $4^{\rm th}$-order perturbation theory. It is given by

$$\gamma^{(1)}(|0\,0\rangle) = 2\pi\frac{\omega_r}{2\Delta}\sin^2(\theta_r)\frac{2E_{\rm Z}^{(-)}}{\Delta\left(1-\left(\frac{\omega_{\rm Z}}{\Delta}\right)^2\right)}, \tag{4.29}$$

where as always the superscript "1" denotes a correction linear in ω_r. Here we find a term that appears similar to the $M_J=1$ states, with the exception that it occurs in an $M_J=0$ state. A new energy scale has been introduced into the problem by adding Δ and this allows the $|0\,0\rangle$ state to acquire a first order Berry phase. However, the strength of this phase is reduced by a term proportional to the ratio of the quadratic Zeeman

shift in the lower level to the spin-spin energy splitting. Given our assumptions, this term — while linear in ω_r — is a product of multiple small parameters, and is generally smaller than $\gamma^{(0)}$ for $M_J = \pm 1$ states.

For the case of the $|J = 1, M_J = 0\rangle$ state, there is also a 4^{th}-order correction, but it takes a very different form. After much algebra,

$$\gamma^{(1)}(|1\,0\rangle) = -2\pi \frac{\omega_r}{2\omega_{\text{Z}}} \sin^2(\theta_r) \frac{2E_{\text{Z}}^{(+)}}{\omega_{\text{Z}}}. \tag{4.30}$$

This is very different from the $|0\,0\rangle$ state correction in (4.29). The important energy scale is the linear Zeeman shift ω_{Z}. Eqs. (4.29) and (4.30) carry an important insight; the energy scale responsible for higher-order Berry phases is different for the two $M_J = 0$ states. The dominant scale in the $|0\,0\rangle$ is the spin-spin splitting Δ. In the $|1\,0\rangle$, the dominant energy scale is the linear Zeeman shift. To first order in ω_r, there is a correction to the $M_J = 0$ states that, while similar to the shift in the $|M_J| = 1$ states, is reduced in magnitude. This reduction is due to the structure, the structure that provides a quadratic Zeeman shift in the $M_J = 0$ states. For the lower (upper) level, the correction depends on the relative strength of the quadratic Zeeman shift to the spin-spin splitting (linear Zeeman shift). In the regime considered, both of these contributions are very small. The same ideas apply to the $F = 0$ and $F = 1$ hyperfine states of Hydrogen, where the magnetic field is coupling states of the same parity. Briefly, $\gamma^{(1)}$ is influenced by "nearby" $M_J = \pm 1$ states for the $|1\,0\rangle$ level, and comparatively less influenced by the "far away" $M_J = \pm 1$ levels in the $|0\,0\rangle$ state.

It is instructive to examine these results for different cases of individual Larmor frequencies. In the case where both particles experience the same Larmor frequency in a field, $\omega_1 = \omega_2$, then these first-order corrections reduce to the usual first-order corrections for a structureless spin-1 particle, as in Eqn. (4.19), and the additional $M_J = 0$ pieces are zero as well. In another limit where one Larmor frequency dominates the other, say $\omega_1 \gg \omega_2$, then $\gamma^{(1)}$ for the $|M_J| = 1$ states reduce to the first order

correction of the dominant spin alone, reflecting the fact that the weaker spin is coupled to the stronger one and gets dragged along for the ride. This happens, for example, in the $F = 1$ hyperfine ground state of the hydrogen atom, where the nuclear g-factor is far smaller than the electron g-factor.

4.4.2 Strong magnetic field, $\omega_1, \omega_2 \gg \Delta \gg \omega_r$

In the other limit, where the magnetic field is large compared to the splitting between adjacent J-levels, it is more useful to construct the dressed Hamiltonian in an alternative basis. Namely, the non-rotating Hamiltonian is more nearly diagonal in the independent-spin basis $|j_1\, m_1\, j_2\, m_2\rangle$, where the four Zeeman energies $E_{m1,m2}$ are given simply by $m_1\omega_1 + m_2\omega_2$:

$$\begin{aligned} E_{\frac{1}{2},\frac{1}{2}} &= \frac{1}{2}(\omega_1 + \omega_2) \\ E_{\frac{1}{2},-\frac{1}{2}} &= \frac{1}{2}(\omega_1 - \omega_2) \\ E_{-\frac{1}{2},-\frac{1}{2}} &= -\frac{1}{2}(\omega_1 + \omega_2) \\ E_{-\frac{1}{2},\frac{1}{2}} &= -\frac{1}{2}(\omega_1 - \omega_2), \end{aligned} \tag{4.31}$$

as appropriate to this Paschen-Back limit of the Zeeman effect. This is an example of the aside in Sec. 4.2 where the *ansatz* $(\alpha,\ \beta)\ e^{-i\, m_1\omega_r t}e^{-i\, m_2\omega_r t}$ was made. The remaining Hamiltonian, which includes the rotation of the field and the spin-spin interaction, is recast as follows

$$H_{\text{dressed}} = \begin{pmatrix} E_{\frac{1}{2},\frac{1}{2}} + \frac{\Delta}{4} - \omega_r\cos(\theta_r) & \frac{\omega_r}{2}\sin(\theta_r) & 0 & -\frac{\omega_r}{2}\sin(\theta_r) \\ \frac{\omega_r}{2}\sin(\theta_r) & E_{\frac{1}{2},-\frac{1}{2}} - \frac{\Delta}{4} & \frac{\omega_r}{2}\sin(\theta_r) & -\frac{\Delta}{2} \\ 0 & \frac{\omega_r}{2}\sin(\theta_r) & E_{-\frac{1}{2},-\frac{1}{2}} + \frac{\Delta}{4} + \omega_r\cos(\theta_r) & -\frac{\omega_r}{2}\sin(\theta_r) \\ -\frac{\omega_r}{2}\sin(\theta_r) & -\frac{\Delta}{2} & -\frac{\omega_r}{2}\sin(\theta_r) & E_{-\frac{1}{2},\frac{1}{2}} - \frac{\Delta}{4} \end{pmatrix} \tag{4.32}$$

Once again, one immediately reads the Berry-phase contribution from the diagonal components, as

$$\begin{aligned}\gamma^{(0)}(|j_1\ m_1\ j_2\ m_2\rangle) &= -2\pi(m_1+m_2)\cos(\theta_r) \\ &= -2\pi M_J\cos(\theta_r). \end{aligned} \tag{4.33}$$

The phase accumulates due to the individual spins separately, as expected when the spins interact weakly with each other compared to their interaction with the field.

This independent accumulation of phase leads to a different interpretation of the $M_J = 0$ states: in the limit of small magnetic field compared to the spin-spin energy splitting, we had attributed this to an $M_J = 0$ projection while here, we can attribute this to $m_1 = \pm\frac{1}{2}$ accumulating $\pm(\omega_r/2)\cos(\theta_r)$ extra energy and the $m_2 = \mp\frac{1}{2}$ accumulating $\mp(\omega_r/2)\cos(\theta_r)$. To cement this idea even further, there are two independent first-order contributions to the first-order non-adiabatic correction $\gamma^{(1)}$, computed first neglecting Δ:

$$\gamma^{(1)}(|j_1\ m_1\ j_2\ m_2\rangle) = 2\pi\ m_1\frac{\omega_r}{2\omega_1}\sin^2(\theta_r) + 2\pi\ m_2\frac{\omega_r}{2\omega_2}\sin^2(\theta_r) \tag{4.34}$$

$$= \gamma_1^{(1)}(|j_1\ m_1\rangle) + \gamma_2^{(1)}(|j_2\ m_2\rangle). \tag{4.35}$$

This is exactly the contribution one would expect from two *independent* spins following a rotating field. When the spins are anti-aligned, or $m_1 = -m_2$, no correction exists at this order. It is worth noting that this perturbative expansion breaks down if $\omega_r \sim \omega_i$. Thus, should the rotation rate be fast with respect to one of the Larmor frequencies, but not the other, then the measured phase difference cannot be treated perturbatively in this regime.

The explicit effect of internal structure, manifested in the splitting Δ, appears as

a next-order correction:

$$\gamma_1^{(1)} \rightarrow 2\pi\, m_1 \frac{\omega_r}{2\omega_1} \sin^2(\theta_r) \left(1 + \left(\frac{\Delta}{2\omega_2}\right)^2\right) \tag{4.36}$$

$$\gamma_2^{(1)} \rightarrow 2\pi\, m_2 \frac{\omega_r}{2\omega_2} \sin^2(\theta_r) \left(1 + \left(\frac{\Delta}{2\omega_1}\right)^2\right). \tag{4.37}$$

Of course, there are many routes by which 4^{th}-order perturbation theory can affect this state. Only the one route which produces a phase shift proportional to ω_r after one period of oscillation is given. There is a structure correction for each non-adiabatic spin that depends on the relative strength of the spin-spin splitting to the other Larmor frequency. Thus, it is evident that the spin-spin splitting need be small compared to each of the Larmor frequencies in order to make this expansion. Again, this is a more restrictive condition on adiabaticity than is usually employed for two independent spins.

4.5 Polar molecules in a rotating electric field

Molecules bring yet another degree of freedom to the picture, namely end-over-end rotation with eigenstates $|N\ M_N\rangle$. In addition, if the molecule is polar, it has an electric dipole moment that can be acted upon by a rotating electric field. In this section I'll consider only diatomic molecules, and only one of a fairly simple structure, to illustrate how the formalism applies to them. The lowest-order Berry phase was worked out recently in this system [100], but the higher-order corrections are implicit there as well.

For the sake of illustration why not choose the simplest of diatomic molecules, a $^1\Sigma$ molecule with no hyperfine structure. In a rotating electric field this system is described by a Hamiltonian of the form

$$H_{\text{dressed}} = B\vec{N}^2 - \vec{\mu}_m \cdot \vec{\mathcal{E}} - \omega_r(\cos(\theta_r)N_z - \sin(\theta_r)N_x), \tag{4.38}$$

where $\vec{N}$ is the end-over-end rotational angular momentum of the molecule, μ_m is the electric dipole moment of the molecule and $\mathcal{E}$ is the electric field strength. Working in

the frame of the electric field along with the electric dipole moment pointing along the molecular axis, there are no couplings of M_N or Λ, where Λ is the projection of total angular momentum onto the internuclear axis. For Σ-molecules, this means there are no couplings to excited electronic states by the applied electric field at the low fields considered.

For simplicity, only the coupling only between the $N = 0$ and $N = 1$ rotational levels of the molecule is considered, which assumes weak coupling of rotational states due to the electric field, i.e., $\mu_m \mathcal{E} \ll B$. The formalism can of course be extended to arbitrarily large N values as needed. It is nice to note that this formalism has an atomic analog: the $^1S_0$ and $^1P_1$ states of noble gas and alkaline-earth atoms have opposite-parity and are coupled by the Stark interaction. This approach gives the corrections for states of opposite parity coupled by the Stark interaction. The dressed Hamiltonian reads, in the basis $\{|NM_N\rangle\} = \{|00\rangle, |1-1\rangle, |10\rangle, |1+1\rangle\}$

$$H_{\text{dressed}} = \begin{pmatrix} 0 & 0 & -\frac{1}{\sqrt{3}}\mu_m\mathcal{E} & 0 \\ 0 & 2B - \omega_r\cos(\theta_r) & \frac{1}{\sqrt{2}}\omega_r\sin(\theta_r) & 0 \\ -\frac{1}{\sqrt{3}}\mu_m\mathcal{E} & \frac{1}{\sqrt{2}}\omega_r\sin(\theta_r) & 2B & \frac{1}{\sqrt{2}}\omega_r\sin(\theta_r) \\ 0 & 0 & \frac{1}{\sqrt{2}}\omega_r\sin(\theta_r) & 2B + \omega_r\cos(\theta_r) \end{pmatrix} \tag{4.39}$$

Note the the electric Hamiltonian is off-diagonal in the basis of parity eigen-states. In the absence of the perturbation ω_r, this Hamiltonian appears to have a complete degeneracy among the three states with $N = 1$. In the magnetic field case above, this degeneracy was broken by the linear Zeeman effect acting on the diagonal matrix elements. To achieve the same feat here, one must account for the off-diagonal mixing due to electric field. Note the similarity of this procedure to that of Vutha and DeMille [100].

First diagonalize the $M_N = 0$ subspace, using the mixing angle δ defined by

$$\tan(\delta) = -\frac{\mu_m\mathcal{E}}{\sqrt{3}\,B} = -x, \tag{4.40}$$

with the usual eigenvectors $(\cos(\delta/2), \sin(\delta/2))$ and $(-\sin(\delta/2), \cos(\delta/2))$. The explicit

values in terms of the parameter x are

$$\cos\left(\frac{\delta}{2}\right) = \sqrt{\frac{\sqrt{1+x^2}+1}{2\sqrt{1+x^2}}} \tag{4.41}$$

$$\sin\left(\frac{\delta}{2}\right) = \sqrt{\frac{\sqrt{1+x^2}-1}{2\sqrt{1+x^2}}}. \tag{4.42}$$

In terms of this mixing angle the transformed Hamiltonian, with electric-field-dependent terms on the diagonal only, reads

$$H_{\text{dressed}} = \begin{pmatrix} B(1-\sqrt{1+x^2}) & -\frac{\omega_r}{\sqrt{2}}\sin(\frac{\delta}{2})\sin(\theta_r) & 0 & -\frac{\omega_r}{\sqrt{2}}\sin(\frac{\delta}{2})\sin(\theta_r) \\ -\frac{\omega_r}{\sqrt{2}}\sin(\frac{\delta}{2})\sin(\theta_r) & 2B-\omega_r\cos(\theta_r) & \frac{\omega_r}{\sqrt{2}}\cos(\frac{\delta}{2})\sin(\theta_r) & 0 \\ 0 & \frac{\omega_r}{\sqrt{2}}\cos(\frac{\delta}{2})\sin(\theta_r) & B(1+\sqrt{1+x^2}) & \frac{\omega_r}{\sqrt{2}}\cos(\frac{\delta}{2})\sin(\theta_r) \\ -\frac{\omega_r}{\sqrt{2}}\sin(\frac{\delta}{2})\sin(\theta_r) & 0 & \frac{\omega_r}{\sqrt{2}}\cos(\frac{\delta}{2}\sin(\theta_r) & 2B+\omega_r\cos(\theta_r) \end{pmatrix} \tag{4.43}$$

In the limit that $x \ll 1$ the diagonal terms for the two $M_N = 0$ states are merely the quadratic Stark shift $E_{\text{S}}^{(\pm)} = \pm(\mu_m\mathcal{E})^2/6B$. Now read off the ordinary Berry phase from the diagonal perturbations linear in ω_r, yielding the usual

$$\gamma^{(0)}(|\tilde{N}\, M_N\rangle) = -2\pi M_N \cos(\theta_r), \tag{4.44}$$

where by $\tilde{N}$ is meant the appropriate eigenstate of the field-mixed $M_N = 0$ states [100]. This diagonalization removed the degeneracy of the $M_N = 0$ level with the $M_N = \pm 1$ levels of the $N = 1$ subspace. However, the degeneracy among the $M_N = \pm 1$ states still exists.

Having quasi-broken the degeneracy in the $N = 1$ levels, evaluation of the first-order non-adiabatic correction term using standard second-order perturbation theory seems a logical next step. It is evident that both states $|N, M_N = \pm 1\rangle$ experience the same additional phase at this order (due to their degeneracy in the non-perturbing Hamiltonian), given by

$$\gamma^{(1)}(|1,\, \pm 1) = -\pi\left(\frac{6\,B}{(\mu_m\mathcal{E})^2}\right)\omega_r \sin^2(\theta_r), \tag{4.45}$$

where an expansion in the small parameter x has been applied. Requiring this to be a small correction identifies the adiabaticity criterion for this situation. If this case were analogous to the magnetic field case, one would only be concerned about the magnitude of ω_r with respect to $\mu_m \mathcal{E}$, which is the stand-in for the Larmor frequency. However, Eqn. (4.45) suggests a slightly different criterion, namely $\omega_r B \ll (\mu_m \mathcal{E})^2$ must hold in order to recover the simple leading-order Berry phase. To understand the origin of this criterion look at the term in the large parentheses in (4.45). It is the inverse of the Stark energy in the absence of field rotation for the upper level. Now rewrite (4.45) as

$$\gamma^{(1)}(|N\, M_N = \pm 1\rangle) = -2\pi \frac{\omega_r}{2\, E_{\mathrm{S}}} \sin^2(\theta_r), \tag{4.46}$$

and recover a form reminiscent of the pure spin case (cf. (4.19)), where the Larmor frequency, ω_L, is replaced by E_{S}, the quadratic Stark shift. In order to be an adiabatic correction, it is immediately evident why $\omega_r B \ll (\mu_m \mathcal{E})^2$ must hold; the rotation rate must be small compared to the energy splitting in that level. In this case, the splitting is quadratic in electric field and therefore a secondary energy scale — the rotational level splitting or internal structure — must come into play.

By similar reasoning, $\gamma^{(1)}$ corrections for the $M_N = 0$ states can be obtained as well. That of the lower level is given by

$$\gamma^{(1)}(|\tilde{N} \sim 0\,, 0\rangle) = -2\pi \frac{\omega_r}{2B} \sin^2(\theta_r) \frac{E_{\mathrm{S}}}{2\, B}, \tag{4.47}$$

where the requirement that $\omega_r\, E_{\mathrm{S}} \ll B^2$ must hold. In this case, our assumptions clearly support this adiabatic criterion since the regime $\omega_r \ll \mu_m \mathcal{E} \ll B$ is assumed. This correction is linear in ω_r, but suppressed by the ratio of the Stark energy to the rotational constant of the molecule. Physically, this is because this state is far removed from the "degeneracy" in the $N = 1$ levels. It is the electric analogue of the weak magnetic field limit of the spin-spin interaction. The correction for the upper level is given by

$$\gamma^{(1)}(|\tilde{N} \sim 1\,, 0\rangle) = 4\pi \frac{\omega_r}{2\, E_{\mathrm{S}}} \sin^2(\theta_r). \tag{4.48}$$

This correction is in the opposite direction to and twice that of the $|N\, M_N = \pm 1\rangle$ states because the $|\tilde{N} \sim 1\,, 0\rangle$ state is influenced by the two states, $M_N = \pm 1$, that are below it in energy. This is in contrast to the coupled spins in a magnetic field case, where each $M_N = \pm 1$ contributed equally in magnitude but opposite in sign. This is due to the lack of any linear Stark shift in the $M_N = \pm 1$ levels.

It is evident that polar molecules in a rotating electric field are quite similar to magnetic dipoles in rotating magnetic fields. There is an energy splitting in comparison with which the rotation of the field must be small to ensure adiabaticity. If there is a shift in energy that is linear with the applied field, then the rotation rate must be small compared to this energy. However, if the energy scales quadratically with the applied field, the rate of rotation must be small in comparison to the energy shift in the field. Thus, the internal structure is quite important in regimes of quadratic field shifts and introduces different adiabaticity requirements on ω_r in terms of the applied field and internal structure.

4.6 $^3\Delta_1$ molecules

$^3\Delta_1$ molecules are a whole other bag of worms. In Sec. 3.3.2 it was made apparent that they can be quite complicated. Adding a rotating electric field to the mix will make it even more so. However, in this section only nuclear spin free systems will be considered, so as to only present the necessary new physics. Recall Fig. 3.11. The upper component shifts in energy with the application of an electric field. The Hamiltonian which describes the object in the rotating field is given by

$$H_{\rm dress} = -\vec{\mu}\cdot\vec{\mathcal{E}} - \tilde{o}_\Delta J^2 \delta_{\Omega,-\Omega'} + BJ^2 - \omega_r(\cos(\theta_r)J_z - \sin(\theta_r)J_x). \tag{4.49}$$

The first term is the Stark interaction, the second the Λ-doubling which connects states of $\Omega \to -\Omega$, the third end-over-end rotation, and the last the rotating contribution. For inclusion of any J, the total number of channels in the system scales as $\sum_J 2(2J+1)$,

where the extra 2 encapsulates the two Ω's in the problem.

The concern is primarily with the Stark degenerate states $M\Omega = \pm 1$, and therefore it would be beneficial if there were a way to understand the new physics that arises from the rotating field. I shall choose the regime where the electric field is vastly larger than $\tilde{o}_\Delta$ and ω_r yet ridiculously small compared to the rotational splitting given by $2B(J+1)$. Therefore, the Stark energy is the dominant energy in the system. Treating the other two interactions, Λ-doubling and rotation, as small one can try to build an effective Hamiltonian in the basis of $M\Omega = \pm 1$. The reason for this is to try to understand the the degenerate states in terms of a 2×2 matrix.

The interesting item to note is that the rotating field ω_r couples M to $M \pm 1$ while Λ-doubling couples $\Omega = \pm 1$ to $\Omega = \mp 1$. Thus, in a perturbative approach, it is evident that states with $M = 1, \Omega = -1$ are coupled at some level to states with $M = -1, \Omega = 1$. Yet, in Fig. 3.11, these were the states where the upper transition W^u is to be measured to determine the eEDM. This is potentially hazardous because should there ever be a case where the two states are degenerate then the rotation would introduce a complete mixing of states, yielding new eigenfunctions proportional to $|M, \Omega\rangle \pm |-M, -\Omega\rangle$. If the electron being measured in the experiment spends half its time up against the applied axis and half its time down, the effect cancels out. And apparently, when $\theta_r = \pi/2$ the situation is just so that the two levels are degenerate, as is evident from staring at Eq. (4.49) long enough.

Now, in the ion trap of the JILA eEDM experiment, $\theta_r = \pi/2$, or at least will vary around this choice of angle. Therefore, there will need to be some way to understand the eigenfunctions in the plane. Because the $|M\Omega = \pm 1\rangle$ states are coupled by the combined interactions of the rotating field and Λ-doubling, the states at the value of

$\theta_r = \pi/2$ are given by (in the $|M\Omega\rangle$ basis)

$$||M\Omega|,+\rangle = \frac{1}{\sqrt{2}}\left(|1,-1\rangle + |-1,1\rangle\right) \tag{4.50}$$

$$||M\Omega|,-\rangle = \frac{1}{\sqrt{2}}\left(|1,-1\rangle - |-1,1\rangle\right). \tag{4.51}$$

Neither of these states is conducive to measuring the eEDM. Therefore, the size of the energy splitting between these states needs to be understood as well as a way to move back into a regime of good M and Ω.

The matrix elements of interest in a fixed J-level are given by

$$\begin{aligned}
\langle JM\Omega|\tilde{o}_\Delta J^2|JM-\Omega\rangle &= 2\tilde{o}_\Delta J(J+1) \\
\langle JM\Omega| - \vec{\mu}\cdot\vec{\mathcal{E}}|JM\Omega\rangle &= -\mu\mathcal{E}\frac{M\Omega}{J(J+1)} \\
\langle JM\Omega| - \omega_r\cos(\theta_r)J_z|JM\Omega\rangle &= -\omega_r\cos(\theta_r)M \\
\langle JM\Omega| - \omega_r\sin(\theta_r)J_x|JM\Omega\rangle &= \langle JM\Omega| - \omega_r\sin(\theta_r)(J_+ + J_-)/\sqrt{2}|JM\Omega\rangle \\
&= \Big(\sqrt{(J+M)(J-M+1)}/2 + \\
&\quad \sqrt{(J-M)(J+M+1)}/2\Big)\,\omega_r\sin(\theta_r)
\end{aligned} \tag{4.52}$$

The raising and lowering here operators act on the laboratory defined axis of the instantaneous field, as opposed to earlier in Sec. 3.3.2.

In order to understand the energies associated with the terms in Eqs.(4.50) and (4.51), one can take a sum of the perturbative terms and raise them to the $2|M|+1$ power, then divide by ΔE^{2M}. This is because the order at which the two states are coupled requires $2|M|$ applications of the rotating field and one application of the Λ-doubling term.

$$\begin{aligned}
H_{\text{peturb}} &\propto \frac{(H_{\Lambda\text{D}} + H_{\text{rot field}})^{2|M|+1}}{\Delta E^{2M}} \\
&\propto H_{\Lambda\text{D}}H_{\text{rot field}}^{2|M|} + \text{permutations.}
\end{aligned} \tag{4.53}$$

The permutations have to deal with whether the Λ-doubling occurs first, second, or third. In fact, there are $2|M|+1$ permutations in general. In the case of $^3\Delta_1$ with no

hyperfine, this reduces to $H_{\Lambda D}H^2_{\text{rot field}}$, $H_{\text{rot field}}H_{\Lambda D}H_{\text{rot field}}$, and $H^2_{\text{rot field}}H_{\Lambda D}$. One must account for each term because the energy denominators are different in each case. To illustrate, the first term takes (using $|M\Omega\rangle$ basis functions) $|11\rangle \rightarrow |01\rangle \rightarrow |-11\rangle \rightarrow |-1-1\rangle$. The second term is $|11\rangle \rightarrow |01\rangle \rightarrow |0-1\rangle \rightarrow |-1-1\rangle$. These multiple paths can constructively or destructively interfere with each other, and therefore must be accounted for separately.

The energy denominators are given by either $M-(M\pm 1)$ or $\pm 2\Omega$ times the the Stark parameter $\mu\mathcal{E}/(J(J+1))$. Using some algebra one arrives at an expression for the matrix element connecting $|M\Omega\rangle$ to $|-M-\Omega\rangle$ (at $\theta_r = \pi/2$)

$$\langle M\Omega|H_{\text{peturb}}|-M-\Omega\rangle = y[J,M]\tilde{o}_\Delta\left(\frac{\omega_r}{\mu\mathcal{E}}\right)^{2|M|}. \tag{4.54}$$

The function $y[J,M]$ depends on the many ways in which the operators can act and in what order. It is not enlightening to write down the form since it is merely a complicated expression, however in the case of $^3\Delta_1$ ground state molecules, $y[J,M] = 16$. What is enlightening is that the interaction has a scaling law. The larger the value of M in which one starts, the smaller is the term which couples $|M,\Omega\rangle$ to $|-M,-\Omega\rangle$. In the absence of Λ-doubling or field rotation there is no coupling between these states. It is an artifact of the combined effects.

It is worth noting that the way in which the interaction was developed is entirely akin to the way in which one creates the effective Hamiltonian for Λ-doubling, of the regular, hyperfine induced, or Zeeman induced varieties. In the plane of rotation defined by $\theta_r = \pi/2$, this method lends itself to being dubbed $M\Omega$-doubling (pronounced "momega"-doubling), because states with the same value of $M\Omega$ are degenerate and split by an "effective" parity interaction. This parity is related to the sense of rotation in cahoots with the orientation of the molecular axis. An outward pointing Ω (dipole moment of the molecule pointing along instantaneous field direction) with an outward M rotating in a positive sense is degenerate with an inward Ω, inward M rotating in a

positive sense. If one were to look at the case of magnetic spins and bring Ω into the definition of the g-factor, then the two states have equal and opposite g-factors such that a positive g-factor for state M for all intents and purposes is the same as a negative g-factor for state $-M$.

In the basis of $|M\Omega\rangle$, the effective 2×2 Hamiltonian describing the interaction between the degenerate Stark states near the value $\theta_r = \pi/2$ is

$$H_{2\times 2} = \begin{pmatrix} \frac{d\mathcal{E}}{2} + \omega_r \alpha & 16\left(\frac{\omega_r}{d\mathcal{E}}\right)^2 \tilde{o}_\Delta \\ 16\left(\frac{\omega_r}{d\mathcal{E}}\right)^2 \tilde{o}_\Delta & \frac{d\mathcal{E}}{2} - \omega_r \alpha \end{pmatrix}, \tag{4.55}$$

where the small angle approximation has been applied and $\alpha = \theta_r - \pi/2$. Now, should one want to "push" the crossing to a different value of α so as to be able to do the experiment at $\theta_r = \pi/2$, one would have to shift the $M = 1$ and $M = -1$ level in addition to the shift that is applied by α. The Zeeman interaction does this because it does not care about the sign of $M\Omega$, just the sign of M. Therefore, applying a magnetic field collinear with the electric field will shift the crossing to a different value of α. The Hamiltonian in Eq. (4.55) is modified such that

$$H_{2\times 2} = \begin{pmatrix} \frac{d\mathcal{E}}{2} + \frac{g_J \mu_B \mathcal{B}}{2} + \omega_r \alpha & 16\left(\frac{\omega_r}{d\mathcal{E}}\right)^2 \tilde{o}_\Delta \\ 16\left(\frac{\omega_r}{d\mathcal{E}}\right)^2 \tilde{o}_\Delta & \frac{d\mathcal{E}}{2} - \frac{g_J \mu_B \mathcal{B}}{2} - \omega_r \alpha \end{pmatrix}, \tag{4.56}$$

where $g_J = (g_L \Lambda - g_S \Sigma)\Omega$. Now, the new value α where the coupling is maximal and $|M\Omega\rangle$ states are degenerate is

$$\alpha = -\frac{g_J \mu_B \mathcal{B}}{2\omega_r}. \tag{4.57}$$

Recall that the value of $g_J \approx 0.1$. Now, in the proposed experiment the ratio of the Zeeman energy to ω_r is expected to be around 0.012 [78]. Thus, the angle is shifted an amount $\alpha = 0.06$, which is small enough that the small angle approximation still holds. What remains to be seen is whether a shift this small brings one back to the regime of good M and Ω at the value of $\alpha = 0$.

This crossing, as a function of α is presented in Fig. 4.3. The upper panel (Eq. (4.55) solutions) shows the avoided crossing. The units on the x-axis are in terms

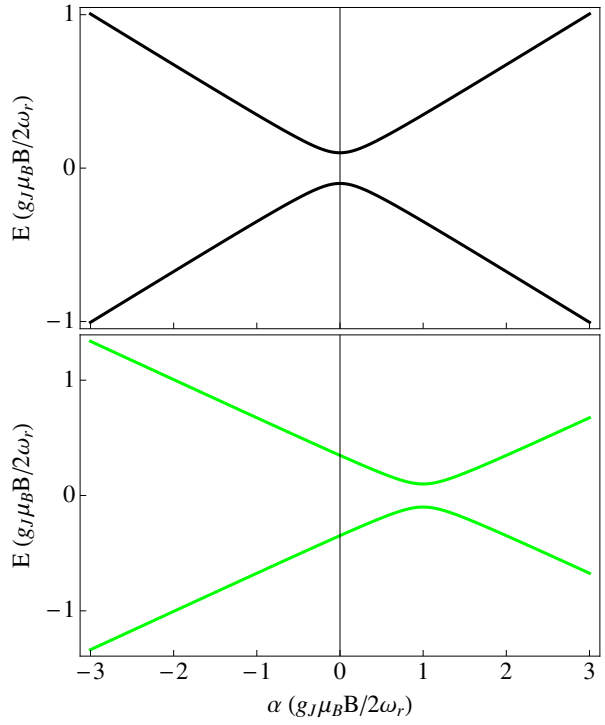

Figure 4.3: The upper panel shows the avoided crossing for a purely Stark interaction. At $\alpha = 0$ (corresponds to $\theta_r = \pi/2$), the two states are maximally mixed, which is bad for an eEDM measurement. However, the application of a magnetic field will move the crossing to a new value of α that is governed by the ratio of the Zeeman energy to the field rotation energy (bottom panel).

of $g_J\mu_B\mathcal{B}/2\omega_r$, and on the y-axis the energy has been offset so as to center the crossing around zero. The units on the y-axis are in terms $g_J\mu_B\mathcal{B}/2\omega_r$ as well. The application of a magnetic field, which like the rotation of the electric field acts only on M, will move the degeneracy to a different value of $\alpha = g_J\mu_B\mathcal{B}/2\omega_r$. Now, to determine whether the eigen-states at $\alpha = 0$ are states of good M and Ω one compares the energy difference between the states $|1-1\rangle$ and $|-11\rangle$ (in the $|M\Omega\rangle$) basis to the strength of the coupling

$$|g_J\mu_B\mathcal{B}| \gg 16\left(\frac{\omega_r}{d\mathcal{E}}\right)^2 \tilde{o}_\Delta, \tag{4.58}$$

which is met in the proposed experiment [78]. The LHS of Eq. (4.58) has the value of $g_J\mu_B\mathcal{B} \approx 2.5$ kHz while the RHS has the value 0.25 kHz, or a factor of 10 smaller. Thus, the values of M and Ω are fairly good in this regime.

By applying the magnetic field to shift the location of the crossing to values of $\theta_r \neq \pi/2$, one recovers states of good M and good Ω in the plane defined by $\theta_r = \pi/2$. Now, should the ions oscillate up and down across this plane, as ions in an ion trap invariably do, they will not experience this crossing provided the amplitude of the oscillation is less than $|\alpha_{\rm osc}| \ll 0.06$. The axial electric field is expected to cause oscillations in $|\alpha_{\rm osc}| \approx 0.0005$, from the parameters in the proposed experiment [78]. Therefore, the ability to perform an eEDM measurement on molecular ions in an ion trap is completely feasible.

One item to note is that in the proposed experiment, there is hyperfine structure, which makes the total angular momentum basis $F = 3/2$ in the ground state. In this state, $M_F = 3/2$ is the total M and this further reduces the size of the coupling strength. The Stark and Zeeman energies will be comparable up to a geometric factor describing the coupling of the spins J to F. Therefore, the extra complexity of hyperfine structure actually helps to alleviate the symptomatic effects of rotating in the plane $\theta_r = \pi/2$ by further reducing the coupling strength between states of $|M\Omega\rangle$ and $|-M-\Omega\rangle$.

Chapter 5

. . . In the End

The best way to be boring is to leave nothing out.

– Francois Voltaire

And now you are either wondering what it is I have left out, or you are really bored. I do hope it is the former.

5.1 A mild review

In this thesis I have presented three ideas all linked by their goal to understand diatomic molecular candidates for an eEDM search. Perturbation theory played a pivotal role in understanding the estimation of $\mathcal{E}_{\text{eff}}$. Standard *ab initio* techniques were used to create potential energy surfaces for the new candidates and these surfaces were in turn used to place a size on the interactions that lead to spectroscopic observables. The theory of Λ-doubling was extended to the hyperfine realm by applying perturbative rules and scaling laws. While the spectroscopy of $^3\Delta$ molecules may be complicated, each term can be understood by applying simple arguments. The goal of understanding even the most minute detail of the spectroscopy is to isolate the spectroscopic shift due to an eEDM. Finally, a dressed state approach to Berry's phase was developed to address the effects of structure on the additional phases. The role that structure plays is to systematically shift the levels of interest in an eEDM experiment, but in such a way for which it is easily accounted.

5.2 The future

There are other avenues to explore EDM effects. An interesting one with molecules is to search for the neutron or proton EDM (nEDM, where n stands for nucleon). $^1\Sigma$ molecules such as TlF have been proposed as candidates for measuring the nEDM and measurements have been made [106]. Here I offer a slightly different approach. Great work has been performed on ^{199}Hg as an atomic candidate for a nEDM search [107]. Since Hg can be laser cooled as well as Sr, one may consider HgSr a viable candidate for a nEDM search in its $^1\Sigma$ ground state because the molecule has the possibility to be produced at ultracold temperatures. The Sr atom acts as a "handle" by which the molecule can be polarized. There is much work to be done regarding this field, but it is but one example of the use of molecules in precision studies. The same *ab initio* methods employed to calculate the wave functions in for the $^3\Delta$ molecules can be used to construct the wave functions for the $^1\Sigma$ candidates.

A further examination of Berry's phase in a dressed state picture can also be explored. Currently, only time-variations in the angle ϕ, the azimuthal angle, have been explored. One can imagine simple time-dependent θ models which would also lead to additional phases. Trying to understand simple oscillations in θ would be an ideal next step since these oscillations occur in ion trap environments. This oscillation would effectively take the system through the avoided crossing in Fig. 4.3 and one can ask how the time scale of this oscillation will affect an eEDM search.

Bibliography

[1] I.I. Bigi and A.I. Sanda. CP Violation. Cambridge university press, 2000.

[2] T.E. Browder and R. Faccini. Establishment of cp violation in b decays. Ann. Rev. Nucl. Part. Sci., 53:353, 2003.

[3] J. Schwinger. On guage invariance and vacuum polarization. Phys. Rev., 82:664, 1951.

[4] N.F. Ramsey. Electric-dipole moments of particles. Ann. Rev. Nucl. Part. Sci., 32:211, 1982.

[5] I.B. Khriplovich and S.K. Lamoreaux. CP Violation without Strangeness. Springer-Verlag, Berlin, 1997.

[6] W. Bernreuther and M. Suzuki. Electric dipole moment of the electron. Rev. Mod. Phys., 63:313, 1991.

[7] B.C. Regan, E.D. Commins, C.J. Schmidt, and D. DeMille. New limit on the electron electric dipole moment. Phys. Rev. Lett., 88:071805, 2002.

[8] M.E. Peskin and D.V. Schroeder. An Introduction to Quantum Field Theory. Westview Press, USA, 1995.

[9] Sarah Bickman. Progress Towards a Measurement of the Electric Dipole Moment of the Electron using PbO*. PhD thesis, Yale University, 2007.

[10] D. DeMille, S. Bickman, P. Hamilton, Y. Jiang, V. Prasad, and R. Paolina. Search for the electron electric dipole moment. In Particles and nuclei international conference, number 669 in 842. AIP, 2005.

[11] F.J. Gilman, K. Kleinknecht, and B. Renk. The cabibbo-kobayashi-maskawa quark mixing matrix. Review of Particle Physics, Physics Letters B, 592:1, 2004.

[12] P.G.H. Sandars. The electric dipole moment of an atom i: Some general considerations. J. Phys. B, 1:499, 1968.

[13] P.G.H. Sandars. The electric dipole moment of an atom ii: The contribution from an electric-dipole moment of the electron with particular reference to the hydrogen atom. J. Phys. B, 1:511, 1968.

[14] J.J. Hudson, B.E. Sauer, M.R. Tarbutt, and E.A. Hinds. Measurement of the electron electric dipole moment using ybf molecules. Phys. Rev. Lett., 89:023003, 2002.

[15] R. Stutz and E. Cornell. Bull. Am. Soc. Phys., 49:76, 2004.

[16] J. Brown and A. Carrington. Rotational Spectroscopy of Diatomic Molecules. Cambridge University Press, Cambridge, 2003.

[17] L.I. Schiff. Measurability of nuclear electric dipole moments. Phys. Rev., 132:2194, 1963.

[18] M. V. Berry, F.R.S. Quantal phase factors accompanying adiabatic changes. Proc. R. Soc. Lond. A, 382:45–57, 1984.

[19] L.L Foldy and S.A. Wouthuysen. On the dirac theory of spin 1/2 particles and its non-relativistic limit. Phys. Rev., 78:29, 1950.

[20] J.D. Bjorken and S.D. Drell. Relativistic Quantum Mechanics. McGraw-Hill, New York, 1964.

[21] V.B. Berestetskii, E.M. Lifshitz, and L.P. Pitaevskii. Quantum Electrodynamics. Pegamon Press, Oxford, 1982.

[22] U. Fano, C.E. Theodosiou, and J.L. Dehmer. Electron-optical properties of atomic fields. Rev. Mod. Phys., 48:49, 1976.

[23] E.M. Purcell and N.F. Ramsey. On the possibility of electric dipole moments for elementary particles and nuclei. Phys. Rev., 78:807, 1950.

[24] R.L. Garwin and L.M. Lederman. Nuovo Cim., 11:776, 1959.

[25] E.D. Commins, J.D. Jackson, and D.P. DeMille. The electric dipole moment of the electron: An intuitive explanation for the evasion of schiff's theorem. Am. J. Phys., 75:532, 2007.

[26] P.G.H. Sandars. The electric dipole moment of an atom. Phys. Lett., 14:194, 1965.

[27] P.G.H. Sandars. Enhancement factor for the electric dipole moment of the valence electron in an alkali atom. Phys. Lett., 22:290, 1966.

[28] E.R. Meyer, M.P. Deskevich, and J.L. Bohn. Candidate molecular ions for an electron electric dipole moment experiment. Phys. Rev. A, 73:062108, 2006.

[29] E.A. Hinds. Probing the electron edm with cold molecules. Phys. Sc., T, T70:34, 1997.

[30] E.D. Commins. Electric dipole moments of leptons. Adv. in At., Mol., and Opt. Physics, 40:1, 1999.

[31] E.N. Fortson, P.G.H. Sandars, and S. Barr. The search for a permanent electric dipole moment. Physics Today, June:33, 2003.

[32] A.C. Hartley, E. Lindroth, and A.-M. Mårtensson-Pendrill. Parity non-conservation and electric dipole moments in caesium and thallium. J. Phys. B, 23:3417, 1990.

[33] V.V. Flambaum. Sov. J. Nucl. Phys., 24:383, 1976.

[34] Z.W. Liu and H.P. Kelly. Analysis of atomic electric dipole moment in thallium by all order calculations in many-body perturbation theory. Phys. Rev. A, 45:R4210, 1992.

[35] E.R. Meyer and J.L. Bohn. Prospects for an electron electric dipole moment search in tho and thf^+. Phys. Rev. A, 78:010502(R), 2008.

[36] E.R. Meyer and J.L. Bohn. Electron electric dipole moment searches based on alkali-metal or alkaline-earth-metal bearing molecules. Phys. Rev. A, 80:042508, 2009.

[37] M.G. Kozlov, A.V. Titov, N.S. Mosyagin, and P.V. Souchko. Enhancements of the electric dipole moment of the electron in the baf molecule. Phys. Rev. A, 56:R3326, 1997.

[38] Y.Y. Dmitriev *et al.* Calculation of the spin-rotational hamiltonian including $p-$ and $t-$ odd weak interaction terms for hgf and pbf molecules. Phys. Lett. A, 167:280, 1992.

[39] A.N. Petrov, A.V. Titov, T.A. Isaev, N.S. Mosyagin, and D. DeMille. Configuration interaction calculation of the hyperfine and p,t-odd constants on the ^{207}pbo excited states for electron electric dipole moment experiments. Phys. Rev. A, 72:022505, 2005.

[40] T.A. Isaev, N.S. Mosyagin, A.N. Petrov, and A.V. Titov. In search of the electron electric dipole moment: Relativistic correlation calculations of the p,t-violating effect in the ground state of hi^+. Phys. Rev. Lett., 95:163004, 2005.

[41] A.N. Petrov, N.S. Mosyagin, T.A. Isaev, and A.V. Titov. Theoretical study of hff^+ in search of the electron electric dipole moment. Phys. Rev. A, 76:030501(R), 2007.

[42] J. Lee, E.R. Meyer, R. Paudel, J.L. Bohn, and A.E. Leanhardt. An electron electric dipole moment search in the $x^3\delta_1$ ground state of tungsten carbide molecules. J. Mod. Opt., 56:2005, 2009.

[43] M.J. Seaton. Quantum defect theory. Rep. Prog. Phys., 46:167, 1983.

[44] U. Fano and A.R.P. Rau. Atomic collisions and spectra. Academic Press, Inc., New York, 1986.

[45] H.-J. Werner, P. J. Knowles, R. Lindh, F. R. Manby, M. Schütz, et al. Molpro, version 2008.3, a package of ab initio programs, 2008. see http://www.molpro.net.

[46] D. Feller. J. Comp. Chem., 17:1571, 1996. see https://bse.pnl.gov/bse/portal.

[47] various authors. Institut for theoretical chemistry, 2010. see http://www.theochem.uni-stuttgart.de/pseudopotentials/index.en.html.

[48] H.-J. Werner and P.J. Knowles. A second order multiconfiguration scf procedure with optimum convergence. J. Chem. Phys., 82:5053, 1985.

[49] P. J. Knowles and H.-J. Werner. An efficient second-order mccsf method for long configuration expansions. Chem. Phys. Lett., 115:259, 1985.

[50] H.-J. Werner and W. Meyer. A quadratically convergent multiconfiguration–self consistent field method with simultaneous optimization of orbitals and ci coefficients. J. Chem. Phys., 73:2342, 1980.

[51] H.-J. Werner and W. Meyer. A quadratically convergent mcscf method for the simultaneous optimization of several states. J. Chem. Phys., 74:5794, 1981.

[52] H.-J. Werner. Adv. Chem. Phys., LXIX:1, 1987.

[53] H.-J. Werner and P.J. Knowles. An efficient internally contracted multiconfiguration–reference configuration interaction method. J. Chem. Phys., 89:5803, 1988.

[54] P.J. Knowles and H.-J. Werner. An efficient method for the evaluation of coupling coefficients in configuration interaction calculations. Chem. Phys. Lett., 145:514, 1988.

[55] H.-J. Werner and E.A. Reincsh. The self-consistent electron pairs method for multiconfiguration reference state functions. J. Chem. Phys., 76:3144, 1982.

[56] A. Berning, M. Schweizer, H.-J. Werner, P. J. Knowles, and P. Palmieri. Mol. Phys., 98:1823, 2000.

[57] Y. Wang and M. Dolg. Pseudopotential study of the ground and excited states of yb_2. Theor. Chem. Acc., 100:124, 1998.

[58] Jr. T.H. Dunning. Gaussian basis sets for use in correlated molecular calculations. i. the atoms boron through neon and hydrogen. J. Chem. Phys., 90:1007, 1989.

[59] L.v. Szentpaly, P. Fuentealba, H. Preuss, and H. Stoll. Psuedopotential calculations on rb_2^+.

[60] P. Fuentealba, H. Stoll, L.v. Szentpaly, P. Schwerdtfeger, and H. Preuss. On the reliability of semi-empirical pseudopotentials: simulation of hartree-fock and dirac-fock results. J. Phys. B, 16:L323, 1983.

[61] V.V. Van Vleck. On σ-type doubling and electron spin in the spectra of diatomic molecules. Phys. Rev., 33:467, 1929.

[62] J.L. Dunham. The energy levels of a rotating vibrator. Phys. Rev., 41:721, 1932.

[63] J.K.G. Watson. The isotope dependence of diatomic dunham coefficients. J. Mol. Spect., 80:411, 1980.

[64] J. Wang B.E. Sauer and E.A. Hinds. Laser-rf double resonance spectroscopy of ^{174}ybf in the $x^2\sigma^+$ state: Spin-rotation, hyperfine interactions, and the elctric dipole moment, journal =.

[65] A.R. Edmonds. Angular Momentum in Quantum Mechanics. Princeton University Press, Princeton, 1960.

[66] M.E. Rose. Elementary Theory of Angular Momentum. John Wiley and Sons, Inc., New York, 1957.

[67] D.M. Brink and G.R. Satchler. Angular Momentum. Oxford University Press, Oxford, 1962.

[68] D. DeMille, F. Bay, S. Bickman, D. Kawall, Jr. D. Krause, S.E. Maxwell, and L.R. Hunter. Investigation of pbo as a system for measuring the electric dipole moment of the electron. Phys. Rev. A, 61:052507, 2000.

[69] D. Figgen, K.A. Peterson, M. Dolg, and H. Stoll. J. Chem. Phys., 130:164108, 2009.

[70] W. Kuechle, M. Dolg, H. Stoll, and H. Preuss. Energy adjusted pseudopotentials for the actinides. parameter sets and test calculations for thorium and thorium monoxide. J. Chem. Phys., 100:7535, 1994.

[71] X. Cao, M. Dolg, and H. Stoll. Valence basis sets for relativistic energy-consistent small-core actinide pseudopotentials. J. Chem. Phys., 118:487, 2003.

[72] X. Cao and M. Dolg. Segmented contraction scheme for small-core actinide pseudopotential basis sets. J. Molec. Struct. (Theochem), 673:203, 2004.

[73] A.C. Vutha *et al.* Search for the electric dipole moment of the electron with thorium monozide. ArXiV:0908.2412v1, 2009.

[74] C. E. Moore. Atomic Energy Levels, Circ. 467. Vol. III. Natl. Bur. Stand. (U.S.), 1958.

[75] J.M. Brown, A.S-C. Cheung, and A.J. Merer. λ-type doubling parameters for molecules in δ electronic states. J. Mol. Spec., 124:464, 1987.

[76] T.C. Steimle, D.F. Nachman, J.E. Shirley, D.A. Fletcher, and J.M Brown. The microwave spectrum of nih. Mol. Phys., 9:923, 1990.

[77] T. Nelis, S.P. Beaton, K.M. Evenson, and J.M Brown. A determination of the molecular parameters for nih in its $^2\delta$ ground state by laser magnetic resonance. J. Mol. Spectr., 142:462, 1991.

[78] R. Stutz *et al.* On measuring the electron electric dipole moment in trapped molecular ions. In preparation, 2010.

[79] B. Simon. Holonomy, the quantum adiabatic theorem, and berry's phase. Phys. Rev. Lett., 51(24):2167–2170, 1983.

[80] J. Anandan and L. Stodolsky. Some geometrical considerations of berry's phase. Phys. Rev. D, 35(8):2597–2600, 1987.

[81] Y. Aharonov and J. Anandan. Phase change during a cyclic quantum evolution. Phys. Rev. Lett., 58(16):1593–1596, 1987.

[82] D. N. Page. Geometrical description of berry's phase. Phys. Rev. A, 36(7):3479–3481, 1987.

[83] J. C. Garrison and E. M. Wright. Complex geometrical phases for dissipative systems. Phys. Lett. A, 128(3,4):177–181, 1988.

[84] J. M. Robbins and M. V. Berry. A geometric phase for $m = 0$ spins. J. Phys. A: Math. Gen., 27:L345–L348, 1994.

[85] M. V. Berry, F.R.S. Quantum phase corrections from adiabatic iteration. Proc. R. Soc. Lond. A, 414:31–46, 1987.

[86] M. V. Berry, F.R.S. Histories of adiatbatic quantum transitions. Proc. R. Soc. Lond. A, 469:61–72, 1990.

[87] M. V. Berry, F.R.S. Geomtric amplitude factors in adiabatic quantum transitions. Proc. R. Soc. Lond. A, 430:405–411, 1990.

[88] Shi-Min Cui. Nonadiabatic berry phase in rotating systems. Phys. Rev. A, 45(7):5255–5237, 1992.

[89] J. H. Hannay. The berry phase for spin in the majorana representation. J. Phys. A: Math. Gen., 31:L53–L59, 1998.

[90] D. J. Moore. Berry phases and hamiltonian time dependence. J. Phys. A: Math. Gen., 23:5523–5534, 1990.

[91] D. J. Moore. The calculation of nonadiabatic berry phases. Physics Reports, 210(1):1–43, 1991.

[92] D. J. Moore. Floquet theory and the nonadiabatic berry phase. J. Phys. A: Math. Gen., 23:L665–L668, 1990.

[93] D. J. Moore and G. E. Stedman. Adiabatic and nonadiabatic berry phase for two-level atoms. Phys. Rev. A, 45(1):513–519, 1991.

[94] S. A. R. Horsley and M. Babiker. Topological phases for composite particles with dynamic properties. Phys. Rev. Lett., 99:090401, 2007.

[95] F. Wilczek and A. Zee. Appearance of gauge strucure in simple dynamical systems. Phys. Rev. Lett., 52(24):2111–2114, 1984.

[96] J. E. Avron, R. Seiler, and L. G. Yaffe. Adiabatic theorems and applications to the quantum hall effect. Commun. Math. Phys., 110:33–49, 1987.

[97] Z.-C. Wang and B.-Z. Li. Geometric phase in relativistic quantum theory. Phys. Rev. A, 60(6):4313–4317, 1999.

[98] J. de Boer, K. Papadodimas, and E. Verlinde. Black hole berry phase. Phys. Rev. Lett., 103:131301, 2009.

[99] P. Hoodbhoy. Berry's phase for atomic levels. Phys. Rev. A, 38(7):3766–3768, 1988.

[100] A. Vutha and D. DeMille. Geometric phases without geometry. ArXiV:0907.5116, pages 1–8, 2009.

[101] C. Cohen-Tannoudji, J. Dupont-Roc, and G. Grynberg. Atom-Photon Interactions. John Wiley & Sons, Inc., New York, 1992.

[102] D. M. Brink and G. R. Satchler. Angular Momentum, 3rd Ed. Clarendon Press, Oxford, 1993.

[103] S. Appelt, G. Wäckerle, and M. Mehring. Deviation from berry's adiabatic geometric phase in a ^{131}Xe nuclear gyroscope. Phys. Rev. Lett., 72(25):3921–3924, 1994.

[104] E. Sjöqvist, X. X. Yi, and J. Âberg. Adiabatic geomtric phases in hygrogenlike atoms. Phys. Rev. A, 72:054101, 2005.

[105] S. Oh, Z. Huang, U. Preskin, and S. Kais. Entaglement, berry phases, and level crossings for the atomic breit-rabi hamiltonian. Phys. Rev. A, 78:062106, 2008.

[106] E.A. Hinds, C.E. Loving, and P.G.H. Sandars. Phys. Lett. B, 62:97, 1976.

[107] W.C. Griffith, M.D. Swallows, T.H. Loftus, M.V. Romalis, B.R. Heckel, and E.N. Fortson. Improved limit on the permanent electric dipole moment of ^{199}hg. Phys. Rev. Lett., 102:101601, 2009.

Appendix A

Sample MOLPRO input

If you put tomfoolery into a computer, nothing comes out of it except tomfoolery. But this tomfoolery, having passed through a very expensive machine, is somehow ennobled and no one dares criticize it.

–Pierre Gallois

The items which appear in *verbatim* are actually coding scripts. The dialog that is in between is for explanation as well as troubleshooting common errors.

The first thing to do is call the memory requirements. Often, one gets an error message along the lines of "not enough memory, require ### words and have ### words." If this is the case, just increase the memory. "Words" is related to bits, and is not the unit you need. Play around with it until the error message goes away.

```
memory,2500,m
gprint,orbital,civector;
```

The second line informs the program that you would like to have the orbitals and the ci-vector coefficients printed for every HF, MCSCF and MRCI calculation.

Next one must define the basis sets of interest. This is for ThF^+.

```
basis
```

```
 f=avtz;
 ecp,th,ecp60mwb;
 spdfg,th,ecp60mwb_seg;
end
```

This calls the aug-cc-pVTZ basis for F and the ECP60MWB effective core potential and basis set for Th. The "seg" refers to segmented and means this basis can be used for spin-orbit calculations. If the basis set is not known in MOLPRO, then one can import the basis by copying from the Stuttgart website [47] for heavy elements.

Now it is time to set the geometry

```
geometry
  f;
  th,f,r(i);
end
rlist=[1,2,3,4,5,6,7] bohr;
```

This geometry is in Z-matrix format. It says to place the Th atom from the F atom a distance $r(i)$ away, where $r(i)$ will be defined via a call to "rlist."

Now one is ready to calculate the meaty part. First, set the counter to zero, then start chugging away at steps. Go from the first element to the last in "rlist" in increments of 1. Define the "i$^{\text{th}}$" element of $r(i)$ as the "i$^{\text{th}}$" element of "rlist." I will break it up into the RHF-MCSCF and the the MRCI+SO sections.

```
i=0;
do ith=1,#rlist
   i=i+1
   r(i)=rlist(ith);
   {hf;start,atden;
     wf,38,1,0;}
```

```
{multi;frozen,2,1,1,0;closed,8,3,3,1;occ,11,4,4,2;
  wf,38,1,0;
  wf,38,1,2;wf,38,4,2;}
{multi;closed,8,3,3,1;occ,11,4,4,2;
  wf,38,1,0;
  wf,38,1,2;wf,38,4,2;}
{multi;closed,8,3,3,1;occ,12,5,5,2;
  wf,38,1,0;state,2;wf,38,4,0;
  wf,38,1,2;state,2;wf,38,4,2;
  wf,38,2,0;wf,38,3,0;
  wf,38,2,2;wf,38,3,2;}
{multi;closed,8,3,3,1;occ,13,6,6,2;
  wf,38,1,0;state,2;wf,38,4,0;
  wf,38,1,2;state,2;wf,38,4,2;
  wf,38,2,0;wf,38,3,0;
  wf,38,2,2;wf,38,3,2;}
{multi;closed,8,3,3,1;occ,13,6,6,2;
  wf,38,1,0;state,3;wf,38,4,0;
  wf,38,1,2;state,2;wf,38,4,2;state,2;
  wf,38,2,0;wf,38,3,0;
  wf,38,2,2;state,2;wf,38,3,2;state,2;}
{multi;closed,8,3,3,1;occ,13,6,6,2;
  wf,38,1,0;state,5;wf,38,4,0;state,3;
  wf,38,1,2;state,3;wf,38,4,2;state,3;
  wf,38,2,0;state,2;wf,38,3,0;state,2;
  wf,38,2,2;state,2;wf,38,3,2;state,2;}
{multi;closed,8,3,3,1;occ,13,6,6,2;maxiter,25;
```

```
  wf,38,1,0;state,5;wf,38,4,0;state,3
  wf,38,1,2;state,3;wf,38,4,2;state,3;
  wf,38,2,0;state,2;wf,38,3,0;state,2;
  wf,38,2,2;state,2;wf,38,3,2;state,2;}
```

Each subsequent step in the MCSCF (or "multi") is to gradually build wave functions from the ground up starting with a calculation on $^1\Sigma$ and $^3\Delta$, then adding progressively more spin multiplicities and spatial symmetries. The "wf,38,Sym,2*Spin" command lines are organized such that the pieces with degenerate spatial and spin multiplicities are next to each other. In the MRCI terms below, the energy values are stored in parameters. For brevity, I have only included one label, but one can save multiple. The save command stores the orbital to be used in a spin-orbit calculation later when the "ci;hlsmat,ecp..." command is entered. "ref" commands call the reference symmetries which are degenerate with the symmetry in the given MRCI calculation.

```
{ci;core,8,3,3,1;
  wf,38,1,0;state,5;ref,4;options,maxit=50;save,6010.2;}
esig(i)=Energy(1);
{ci;core,8,3,3,1;
  wf,38,1,2;state,3;ref,4;options,maxit=50;save,6110.2}
{ci;core,8,3,3,1;
  wf,38,4,2;state,3;ref,1;options,maxit=50;save,6210.2;}
{ci;core,8,3,3,1;
  wf,38,2,2;state,2;ref,3;options,maxit=50;save,6310.2}
{ci;core,8,3,3,1;
  wf,38,3,2;state,2;ref,2;options,maxit=50;save,6410.2;}
{ci;core,8,3,3,1;
  wf,38,2,0;state,2;ref,3;options,maxit=50;save,6510.2}
```

```
   {ci;core,8,3,3,1;
     wf,38,3,0;state,2;ref,2;options,maxit=50;save,6610.2;}
   {ci;core,8,3,3,1;
     wf,38,4,0;state,3;ref,1;options,maxit=50;save,6710.2}
   {ci;
     hlsmat,ecp,6010.2,6110.2,6210.2,6310.2,6410.2,6510.2,6610.2,6710.2;
     print,vls=0,hls=0}
   so1(i)=Energy(1);

   table,r,esig,so1,...
   digits,#,#,#,#...
   save,filename.txt,new;
enddo
```

The final command is to store the energies into a file named "filename.txt" and to rewrite the file after each loop. The line "digits..." tells how many digits after the decimal place to keep in each variable.

The common error messages that one finds are related to the "occ" and "closed" cards. Sometimes, through misunderstandings, a user might not give the appropriate number of occupied orbitals and the MCSCF will freak out because it cannot possibly perform the requested calculation. If this is the case, merely think logically and add to the occupied card. Add wisely because an increase in this number will greatly increase computational time. If the error message is ambiguous, and just seems to exit, it is likely that the "closed" space is such that only one, or possibly zero, electrons are left in the "active" space, defined as occ-closed. An MRCI calculation cannot do anything if there is only one, or zero, electron(s). This is because there is nothing to correlate.

This file would calculate all the states arising from the s^2, sd, and d^2 atomic

orbital configuration on the Th^{2+} core. Recall that this will only work near the bottom of the potential wells. The larger the value of $r(i)$, the more these states approach each other and the more likely tiny energy differences will cause severe problems in the calculation. Think smart, but more importantly, think efficient. I carried the calculation to a point of first failure and then stopped. These are the curves presented in Fig. 3.8 b.

Appendix B

Pure S appendix

In Sec. 4.3, there was a Hamiltonian of the form

$$H = \omega_L S_z - \omega_r(\cos(\theta_r)S_z - \sin(\theta_r)S_x), \tag{B.1}$$

which looks like

$$H = \begin{pmatrix} a_1 & c_1 & 0 & 0 & \dots \\ c_1 & a_2 & c_2 & 0 & \vdots \\ 0 & c_2 & \ddots & \ddots & c_{n-2} \\ \vdots & 0 & c_{n-2} & a_{n-1} & c_{n-1} \\ \dots & 0 & 0 & c_{n-1} & a_n. \end{pmatrix}, \tag{B.2}$$

In this system, not only is this matrix symmetric, it contains the following added symmetry: $a_1 = -a_n$, $a_2 = -a_{n-1}$, etc. Also, the coupling coefficients c_i follow a similar property: $c_1 = c_{n-1}$, etc. These properties are key to simplifying the eigenvalues of the tridiagonal matrix in this case.

Eigenvalues of an $n \times n$ tridiagonal matrix are given by the roots of the polynomial

p_n, defined recursively by

$$\begin{aligned} p_0(\lambda) &= 1, \\ p_1(\lambda) &= (a_1 - \lambda), \\ p_2(\lambda) &= (a_2 - \lambda)p_1(\lambda) - c_1^2 p_0(\lambda) \\ &\vdots \\ p_n(\lambda) &= (a_n - \lambda)p_{n-1}(\lambda) - c_{n-1}^2 p_{n-2}(\lambda). \end{aligned} \tag{B.3}$$

Here the constants are defined as

$$a_m = m(\omega_L - \cos(\theta_r)), \tag{B.4}$$

$$c_m \sim \begin{pmatrix} S & 1 & S \\ -m & q & m-q \end{pmatrix}. \tag{B.5}$$

Thus, the symmetry pops right out.

A simple example is the case of $S = 1/2$. The characteristic polynomial is

$$p_2(\lambda) = (\lambda - \frac{1}{2}a)(\lambda + \frac{1}{2}a) - \left(\frac{1}{2}b\right)^2 = (\lambda^2 - \frac{1}{4}(a^2 + b^2)) \tag{B.6}$$

where $a = (\omega_L - \omega_r \cos(\theta_r))$ and $b = \omega_r \sin(\theta_r)$. For the case of $S = 1$ a similar equation (after simplification)

$$\begin{aligned} p_3(\lambda) &= \lambda((\lambda - a)(\lambda + a) - 2\left(\frac{1}{\sqrt{2}}b\right)^2) \\ &= \lambda(\lambda^2 - (a^2 + b^2)) \end{aligned} \tag{B.7}$$

For integer values there is always a diagonal element that is 0. As is evident, this has the same form as (B.6) with the added piece of λ multiplying everything yielding an eigenvalue of 0. In addition, Eq. (B.7) is scaled by a factor of 4 from from Eq. (B.6), thus making the the eigenvalues a factor of 2 larger. This is because the value of m in (B.7) is twice as large as the value of m in (B.6).

We can generalize the characteristic polynomial to a very simple expression due to the added symmetries. It is given by

$$p_{2S+1} = \prod_{m=(m_{\min}\geq 0)}^{m_{\max}} (\lambda^{2(1-\delta_{m_{\min},0})} - m^2(a^2+b^2)). \tag{B.8}$$

The Kronecker δ-function in (B.8) is to insure that in the event $m_{\min} = 0$ there is only one eigenvalue $\lambda = 0$.